A New Approach to CNC Programming of Plunge Milling

Sherif Mahmoud Mohamed Abdelkhalek

A Thesis

In The Department

of

Mechanical and Industrial Engineering

Presented in Partial Fulfillment of the Requirements

For the Degree of Doctor of Philosophy "Mechanical Engineering" at

Concordia University

Montreal, Quebec, Canada

September, 2013

CONCORDIA UNIVERSITY

School of Graduate Studies

This is to certify that the thesis prepared

By: Sherif Mahmoud Mohamed Abdelkhalek

Entitled: A New Approach to CNC Programming of Plunge milling

and submitted in partial fulfillment of the requirements for the degree of

Doctor of Philosophy (Mechanical Engineering)

complies with the regulations of the University and meets the accepted standards with respect to originality and quality.

Signed by the final examining committee:

Dr. Olga Ormandjieva	Chair
Dr. Hsi-Yung (Steve) Feng	External Examiner
Dr. Wei-Ping Zhu	External to Program
Dr. Ali Akgunduz	Examiner
Dr. Sivakumar Narayanswamy	Examiner
Dr. Zezhong C. Chen	Thesis Supervisor

Approved by:

_____

Chair of Department or Graduate Program Director

_____ _____

Dean of Faculty

ABSTRACT

A New Approach to CNC Programming of Plunge Milling

Sherif Abdelkhalek, PhD.

Concordia University, 2013.

In current industrial applications many engineering parts are made of hard materials including dies, mold cavities and aerospace parts. Manufacturing these types of parts is classified as pocket milling. By using the regular machining methods, pocket milling takes a long time accompanied by high cost. Plunge milling, is a new machining strategy that has proven to have an excellent performance in the rough machining of hard materials. In plunge milling, the cutter is fed in the direction of the spindle axis, with the highest structural rigidity which showed a very interesting performance in removing the excess material rapidly in the rough operations. Mainly, according to the previous researchers, two directions are adopted to improve the efficiency of the plunge milling process. First, to reduce the cutting forces and increase chatter stability which attracts the majority of the researchers. Second, to optimize the tool path planning which has less attention.

Therefore, in the first part of the research, a new practical approach is established in optimized procedures to generate the tool paths for plunge milling of pockets, even for these with free-form boundaries and islands. This innovative approach is proposed as follows: (1) fill a pocket with minimum number of specified radii circles which are tangent to each other and/or the pocket boundary without overlapping by building an algorithm using the maximum hole degree (MHD) theory for solving the circle packing problem. (2) cover the areas left between the non-overlapped circles by the same used specified radii. Finally, solve the travelling sales man problem (TSP) for the circles with the same radii by

using the simulated annealing algorithm. According to the results, this approach significantly advances the tool path planning technique for pockets plunge milling.

In the second part of the research, a new algorithm is proposed to calculate the global solution for constraint polynomial functions by using subtractive clustering which makes the results more accurate and faster to be obtained. This part is extremely useful to calculate the depth of cut for each plunging place in case of having a polynomial surface as a bottom of the machined pocket with high accuracy, and less calculation time to avoid gauging between the tool and the bottom surface.

The polynomial function can be classified according to the number of variables. In the proposed research, the functions with one and two variables have more importance because they graphically represent curves and surfaces which are the cases under study. Since the polynomial function under study can be represented graphically according to the number of the variables, the change in the function's shape can be detected by the feature recognition. The feature recognition is done for the function's shape by calculating the surface or curve curvature at the data points. The main procedure is; (1) identifying the entire features of the objective function which are classified according to the curvature as convex, concave, plane, and hyperbolic, (2) applying the sub-clustering technique for convex and concave regions to find the approximated centers of these regions, and eventually, (3) the clusters' centers are calculated and used as initial points for local optimization technique which gives the local critical point for each region. The local minima are calculated, the global minimum is the minimum of the local minima.

DEDICATION

To my parents, my wife and my two kids:
Roaa and Eyad.

ACKNOWLEDGMENTS

I would like to express my sincere thankfulness and appreciation to my supervisor Dr. Chevy Chen for his guidance and support during the period of my PhD. work. His way of guidance developed my research experience and significantly improved my research and technical skills.

I greatly thank my parents and my wife for their support and patience. I also would like to show my sincere appreciation to my former and present fellows in the CAD/CAM laboratory (Maqsood Ahmed Khan, Shuangxui Xie, Mahmoud Rababah, Muhammad Wasif, Aqeel Ahmad, Liming Wang, Du Chun, Mohsen Habibi, Zaher Khattab, Yuansheng Zhou, Ka Ho Yu, and Ruibiao Song). The friendly environment in the laboratory they have created, in addition to the support I got from them, has encouraged me to pursue and improve my ideas for the research.

Table of contents

FIGURES

TABLES

Chapter 1

1.1 Introduction

CNC machining is considered as the core of manufacturing technology. The machining operation is generally divided into two main processes which are distinguished by the purpose and the cutting conditions; (1) roughing cuts, and (2) finishing cuts. Roughing cuts are used to remove large amounts of material from the starting work piece as rapidly as possible. This is done in order to produce a shape close to the desired form while leaving some extra material on the work piece for a subsequent finishing operation. Finishing cuts are used to complete the part and achieve the final dimension, tolerances, and surface finish. Roughing cuts are done at high feeds and cutting depths with low cutting speeds while finishing cuts are carried out at low feeds and cutting depths with high cutting speeds.

For several decades, researchers dedicated great attention to improve the finishing cuts seeking an increase in the machining efficiency while maintaining high machining quality. According to many studies and researches, roughing cuts, (rough machining) could take more than 60% of the total machining time, which attracted much academic and industrial attention. To increase the efficiency of rough machining, especially for hard materials, the emerging cutting strategy (plunge milling) was proposed as an effective solution. Pockets are great examples for the parts with the higher amount of material to be removed in the roughing step, which are widely used in the industry recently.

Optimization is the main tool to the improvement. Therefore the optimization will have an important role in our research. The optimization is used to decrease the total

machining time, also our own optimization technique will be used to improve the efficiency of the plunge milling process by calculating the accurate depth of cut.

1.1.1 Plunge milling

The plunge milling method is also known as the z-axis milling. In the plunge milling process, the feed movement of the cutter is along the axial direction and provides a combination between drilling and milling by using the bottom edge of the cutter [1], as shown in Fig. (1.1); where a_e is the radial cutting depth, and S is each step's distance along the side direction.

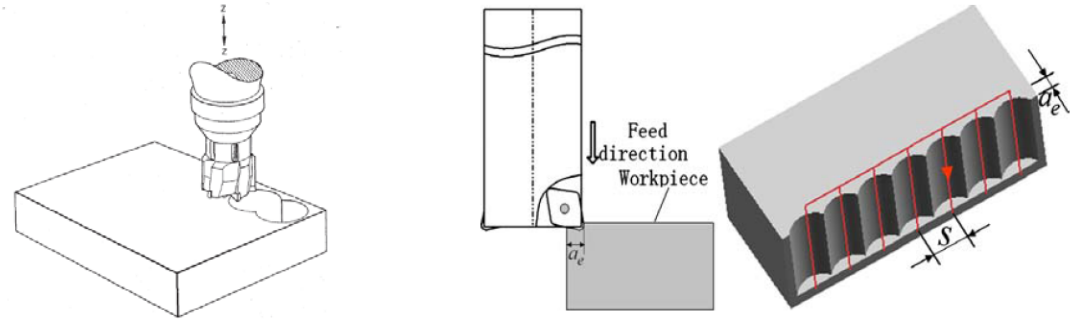

Figure (1. 1). Plunge milling.

There are three main types of the plunge milling process with different types of plungers depending on the process configuration; (1) hole making, (2) hole enlarging, and (3) intermittent plunge milling, as shown in Fig. (1.2)

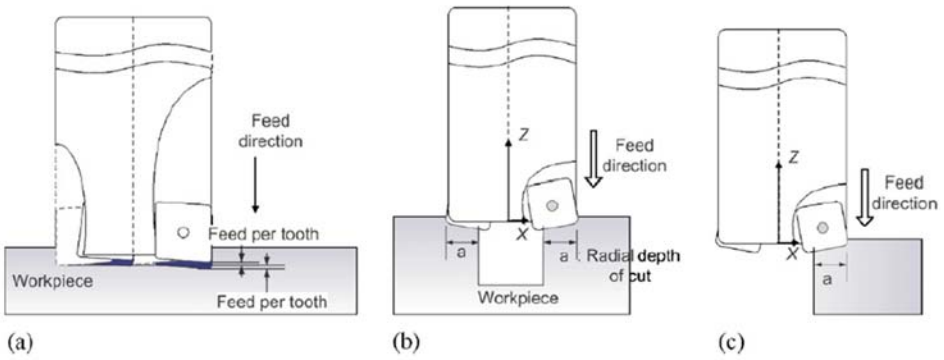

(a) Hole making, (b) hole enlarging, and (c) intermittent.

Figure (1. 2). Plunge milling processes.

Compared to side milling, plunge milling has the following advantages: (1) high axial rigidity for super alloy processing, (2) low requirement for radial force, reducing possibility for work piece distortion, and producing better surface smoothness, (3) protecting cutters from breaking, and (4) relatively stable, and small cutting force and vibrations. Because of the mentioned advantages, plunge milling is perfectly suitable for roughing the high metal removal rate parts like die mold cavities and, and parts related to aerospace industries. With the lower radial cutting forces, this process is perfect for thin wall roughing. Dies, molds cavities, thin wall parts … etc. are considered as pockets. Compared with side milling [2] the axial cutting force of plunge milling is larger, but the radial cutting force is smaller. Namely, the bearing capacity of the axial force is superior to the radial force of the cutter. This makes use of the anisotropic characteristics of the force bearded by the cutter. As for conditions of the large allowance removal for the materials that are difficult to cut as well as the large length of the cutter, a larger cutting feed parameter can be given in plunge milling which is suitable for machining pockets.

1.1.2 Pocket milling

Pocket milling is one of the most common operations in machining metal parts. Pocket milling is defined as removing all the material inside some arbitrary closed boundary of a work piece to a certain depth. Such a shape is frequently called a generalized pocket, as shown in Fig. (1.3). Pockets are classified among the parts which have the property of a large amount of the material has to be removed during the machining process. Dies, molds cavities, and thin wall parts can be considered as pockets with a sculptured bottom surface. As I will illustrate later in the literature review, the Plunge milling is noticed to be better for pocket roughing in comparison to side milling.

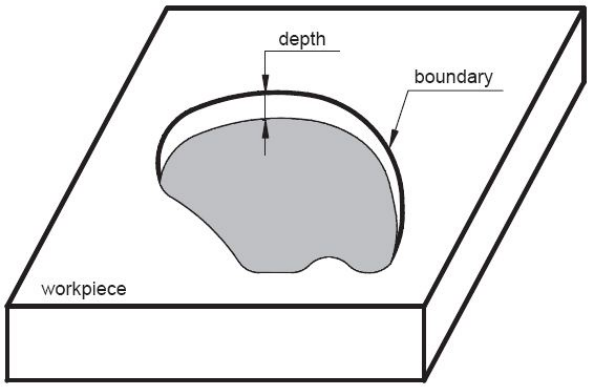

Figure (1. 3). Generalized pocket illustration.

1.1.3 Ploynomial functions global optimization

By definition, polynomial is an expression consisting of a finite length which is composed of variables and constants. The polynomial function may contain one or more variables. It can also be of a single degree which is specified as linear, or more (quadratic, cubic… n^{th}) degree. The remarkable ability of the polynomial functions in modeling, attract the attention of the optimization researchers. The industry is one of the important fields

which is affected by the polynomial functions' ability in modeling, specially modeling the surfaces and curves.

Because of the nature of the polynomial functions the global optimization is considered as one of the interesting challenges. Calculating the global optimal solution for a polynomial function is one of the great challenges in the optimization field. There are many methods for calculating the global optimum like the deterministic methods (Branch and bound, Cutting plane), the stochastic methods (Simulated annealing), the heuristics, and metaheuristics methods (Genetic algorithm, practical swarm optimization, and ant colony optimization). All of these methods have advantages and disadvantages; the main disadvantages are the long computational time, and the low accuracy of the results. So our objective is to establish a new approach to increase the accuracy and reduce the computational time.

1.2 Problem statement

The pocket machining operations aim to remove all the material inside a pre-defined boundary between two surfaces using minimal machining time. The only constraint specified by the part geometry is the boundary of the pocket. As all of the machining operations, the pocket machining is divided mainly into two steps, the rough machining step and the finish machining step. The rough machining of a pocket may take more than 60% of the machining time which is a considerable amount. In addition, if the part material is very hard or the pocket has a high depth, the roughing time will increase to more than 60% of the time. From the review, most of the authors adopted the plunge milling as the

most suitable process for the rough pocket machining because it has a high metal removal rate.

The other problem we will discuss in our research is to find the global optimization of the polynomial functions in accurate manner with less computational time. Our focus will be on the polynomial functions with one and two variables. These types of polynomial functions have many utilities in the industrial field since they can represent curves, and surfaces. Finding the accurate global optimum solution of the polynomial function will be very beneficial to improve the pocket plunge milling process.

In the approach, optimization of the tool path planning for the pocket plunge milling is adopted. Taking into consideration, more than one plunger with different standard sizes will be used, and different types of pocket boundary shapes will be applied. This work will be for pockets with polygon boundary, pockets with polygon boundary with island, and pockets with Free-form boundary.

Moreover, by solving the global optimization problem of the polynomial functions, the pockets with sculptured bottom surface represented by polynomial functions will be considered by calculating the proper depth of cut at each plunging place. This problem can be formulated as covering a 2D pocket area by specified overlapped circles, and calculating the accurate depth of cut for each plunging place to avoid gauging the bottom surface.

The problems can be listed as:

1. Using different sizes of standard plungers.
2. Filling the pocket area with the standard plungers in a decreasing order.
3. Plunging the pockets with Free-form boundary and island.

4. Calculating the accurate depth of cut at each plunging place to avoid gauging with sculptured bottom surface.

1.3 Research objectives

The main objective of this research is to establish two new approaches. The first approach is to generate the tool paths for plunge milling of pockets with free-form boundaries and islands, and the second approach is a global optimization technique to find the global solution of the polynomial functions with one, and two variables. The pockets with sculptured bottom surfaces represented by polynomial functions will be considered by integrating the two approaches. This research covers algorithms development, related theorems establishment, computer program implement, and empirical verification. The main features of the innovative integrated approach are (1) gouge-free plunging of pockets with free-form boundaries, islands and sculptured bottom surface, and (2) optimized tool paths for standard plungers that are available. This approach includes the following five algorithms:

1. Fill a pocket with minimum number of specified radii circles which are tangent to each other and/or the pocket boundary without causing any overlap by building an algorithm using the maximum hole degree (MHD) theory for solving the circle packing problem.
2. Cover the areas left between the non-overlapped circles by the same used specified radii through building an algorithm to solve the minimal enclosing circle problem.
3. Solve the travelling sales man problem (TSP) for the centers of the circles with the same radii.

4. Obtain the optimum tool path planning for the plunge milling of pockets with island and free-form boundary.
5. Optimize the depth of cut for each plunging place in case of sculptured bottom surface with polynomial function.

As a result, the final algorithm will be able to find the optimum plunging tool path for pockets with free form boundaries and islands as well as the ability of using any number of preselected tools with standard or modified diameters due to the re-sharpening process. In addition, it has the ability to calculate the accurate depth of cut at each plunging place for pockets with sculptured bottom surfaces represented by polynomial functions.

1.4 Dissertation organization

The remaining sections of this dissertation are organized as follows. Chapter 2 reviews the research that has been done on the plunge milling process, and the plunge milling tool path planning, in addition to a review on the circle packing technique used in our plunge milling approach. Furthermore, a discussion on the optimization techniques used for the constrained polynomial functions. Finally the chapter will be ended by highlighting the subtractive clustering method involved in our optimization technique.

Chapter 3 presents in details our approach for the polynomial function global optimization by using the subtractive clustering technique. Several case studies are used to verify the proposed approach, with a comparison between our approach and one of the famous global optimization techniques, the particle swarm optimization (PSO) technique.

Chapter 4 illustrates the pocket plunge milling tool path optimization algorithms, and different examples to different types of pockets with the results of applying our

approach. A comparison is made between our approach, and two other plunge milling methods. A comprehensive example at the end of the chapter to show the results of applying our both approach on a pocket with island both have free form boundary, and the pocket bottom surface following a polynomial function. Chapter 5 contains the summary of this work with the main points for the future work.

Chapter 2

Literature review

This chapter reviews three main concepts used in this integrated approach; first, the concept of plunge milling, then the concept of circle packing, and finally the global optimization of polynomial functions using the sub-clustering technique which is also reviewed at the end of this chapter

2.1 Plunge milling

Despite the importance of the plunge milling process, it has less attention given by the researchers in which a limited literature is found. Li, et al, (2000, [1]) developed an analytical cutting force model to predicted the resultant cutting forces during cutting the cylindrical parts by using multi-blade plungers. Their method depended mainly on the relationship between the instantaneous chip area and the local cutting forces at each individual blade of the plunger. Wakaoka, (2002, [2]) improved the accuracy and surface roughness of the deep vertical wall machining by using the plunge cutting instead of using the side milling and by using a long end mill. Eventually, they proved that the plunge cutting, (1) gave higher metal removal rate comparing to the side milling, (2) enabled using high cutting speeds with different materials like cast iron, and plain carbon steel, (3) increased the tool life. Ko, and Altintas, (2007, [3]) studied the dynamics and stability of the plunge milling operations by building models to predict the cutting forces, torque, kinematics of chip generation, and chatter stability in both time, and frequency domain

which enable them to find a map of chatter-free cutting conditions for the plunge milling process, this had an important role in the process planning.

Another time domain simulation model was developed by Damir and Elbestawi, (2010, [4]) to study the dynamics of the plunge milling process for the systems with rigid and flexible work piece. Their model predicted the cutting forces and system vibration as a function of work piece and tool dynamics, tool setting error, and tool kinematics and geometry. Al-Ahmad, et al, (2007, [5]) specified the characteristics of plunge milling operation and made a comparison between plunge and conventional milling based on the accuracy and efficiency point of views by taking into consideration the geometrical configuration, cutting strategy, cutting edge trajectory, power, and cutting force. By applying both operations on a simple deep cavity, they found that the plunge milling had higher metal removal rate and shorter cutting time with higher power consumption as shown in Fig. (2.1).

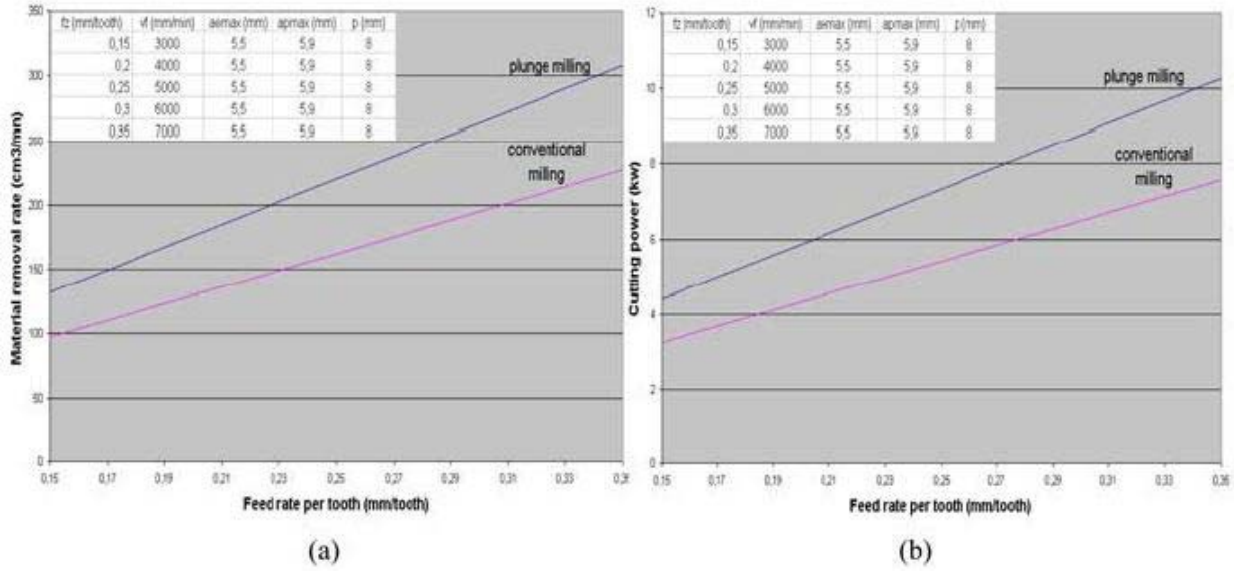

(a) (b)

(a) Metal removal rate (b) Cutting power.

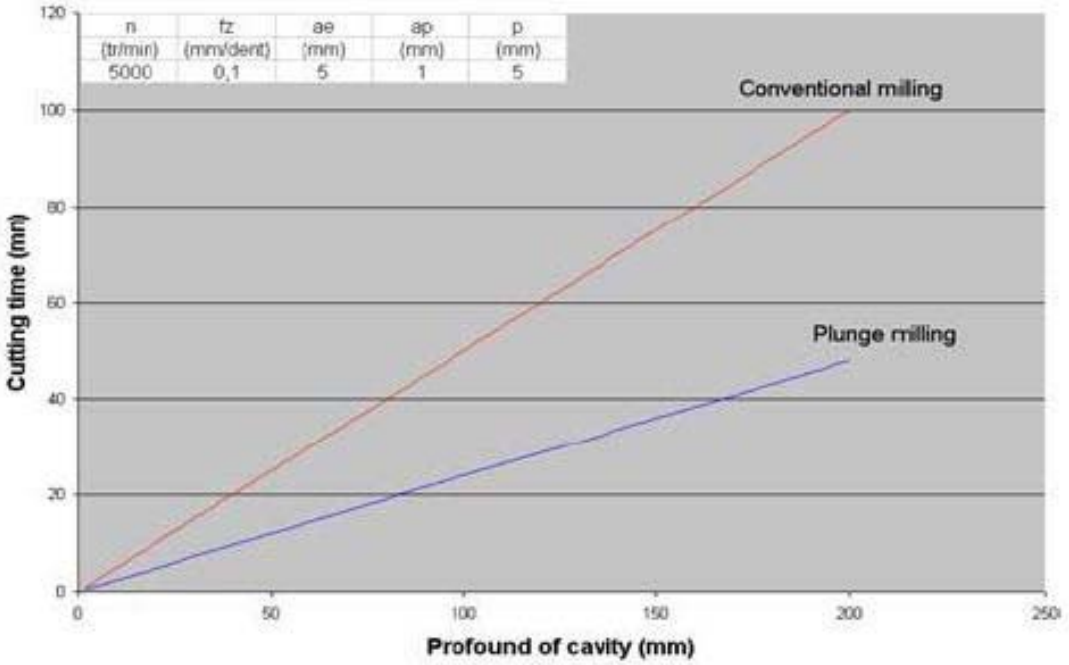

(c) Cutting time.

Figure (2. 1). Comparison between conventional and plunge milling [5].

Ren, et al, (2009, [6]) introduced the four axis plunge slot rough milling with high efficiency and low machining cost as the most efficient way for producing the open blisk's tunnels. They determined the rough milling region of open blisk's tunnel by generating the ruled enveloping surface of the blade's offset surface, and gave the algorithm of the tool path for four axis plunge milling. They used the ruled surface to approach the freeform surface. Their experiment showed that compared to the traditional side slot milling, the cutting force of four axis plunge milling was reduced by 60% as shown in Fig. (2.2), and the efficiency was increased to more than double.

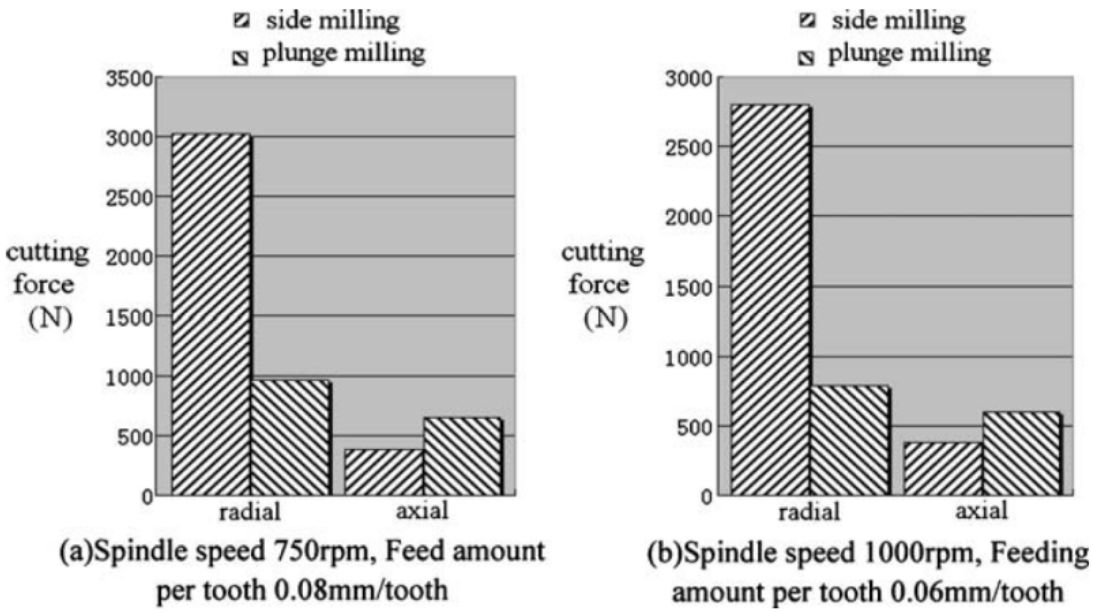

Figure (2. 2). Comparison of cutting forces between plunge milling and side milling under the condition of the same material cutting efficiency [6].

All the above mentioned researchers were interested in the cutting forces. Elmidany and Elkeran, (2006, [7]) were from the pioneers who were interested in the tool path planning of the plunge milling process. They proposed a new method called overlapped circles filling (Ocfill) as shown in Fig. (2.3), for optimizing the selection of plungers and toolpoint path generation. They fill a 2D area with a number of overlapped circles. The 2D area was expressed as the feature to be cut, and the circles were the plunging holes. Their results showed that the rough machining time was significantly reduced by value up to 28% when compared with the convintional methods existing in the commertial CAM softwares (MasterCAM). They used Voudouris' algorithm (GFLS) for optimizing Ocfill toolpoint path. The optimum path saved about 50% of the path length.

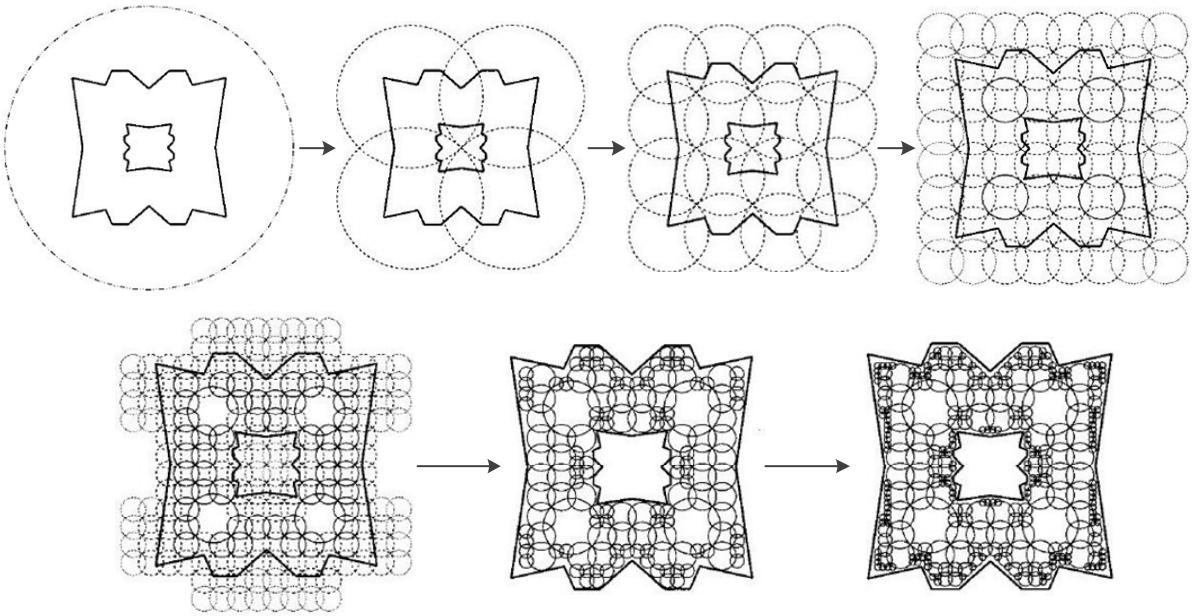

Figure (2. 3). Generation of Ocfill grid [7].

Another new algorithm was also proposed by Elmidany, (2006, [8]) which was to increase the area to be covered of the pocket. He mentioned that according to the pocket shape, there exists an optimal inclination angle for the filling direction. He calculated the optimal inclination angle of filling the plunged area to improve the percentage of area covered by the circles. He then used the geometry of the 2D area of the shape to be cut to estimate the optimal inclination angle of filling. He finally found that, the optimal inclination angle for filling of the plunged area was in the same direction as the longest width of the equivalent convex polygon of the boundary contour. He showed that the residual volume was minimized by comparing the proposed algorithm with his previous ocfill method [7] as shown in Fig. (2.4). The main concepts of his new algorithm are to

construct the equivalent convex polygon of the boundary contour and calculate the direction of the longest width of the equivalent convex polygon.

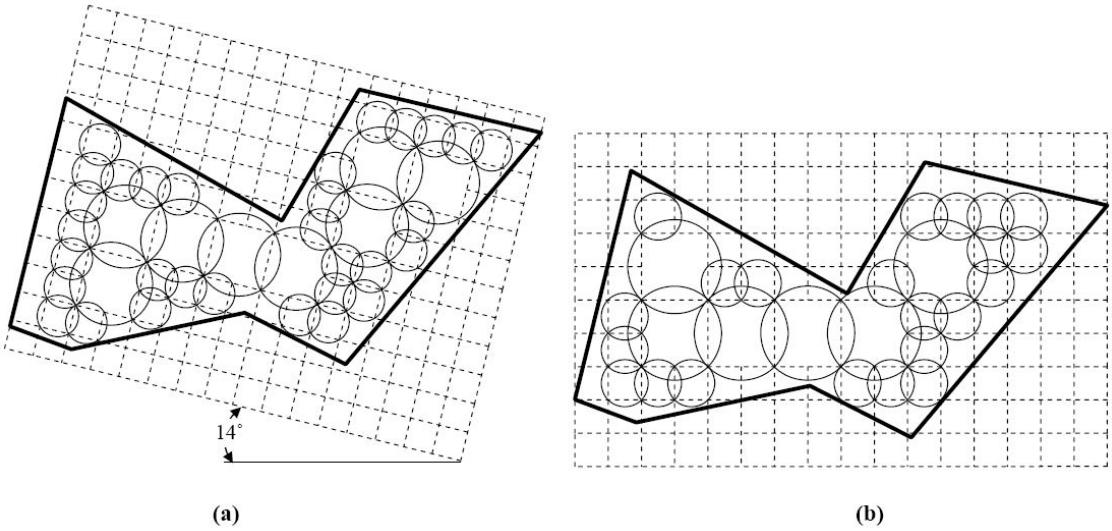

Figure (2. 4). Comparison of two methods (a) Modified Ocfill (b) Ocfill [8].

Wenfeng, et al, (2010 [9]), presented a new method of tool path planning for plunge milling based on achieving a constant scallop height by determining the proper interval between two adjacent cutter contact (CC) points (ΔL) as shown in Fig. (2.5). The results indicated that iso-scallop machining achieved the specified machining accuracy with fewer CL points than existed tool path generation approaches. Their proposed method offered an efficient solution for plunge milling tool path scheduling on pocket walls because the machining time was reduced while the quality of the machined surface was achieved properly.

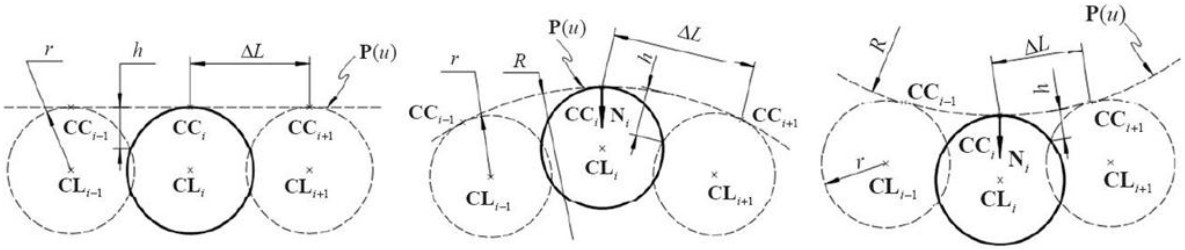

(a) Flat surface (b) Concave surface (c) Convex surface.

Figure (2. 5). The step distance according to different serfaces' shapes [9].

2.2 Circle packing

Based on our approach procedure, we would like to add an extra part to the literature about the available solutions for the well-known circle packing problem. Circles packing are configurations of circles with a specified pattern of tangency. At the very beginning it was studied by E. M. Andreev and Paul Koebe, after a while, circles packing went long unnoticed until William Thurston reintroduced them in a talk over 20 years ago. Circle packing hierarchy starts with a single circle, then a tangent circle is added to form a tangent pair, and then by adding another circle, a triple with interstice is obtained. A set of more than three circles is called "flower" which has many petals. When the circles totally fill the required area, it is called "packing" as shown in Fig. (2.6).

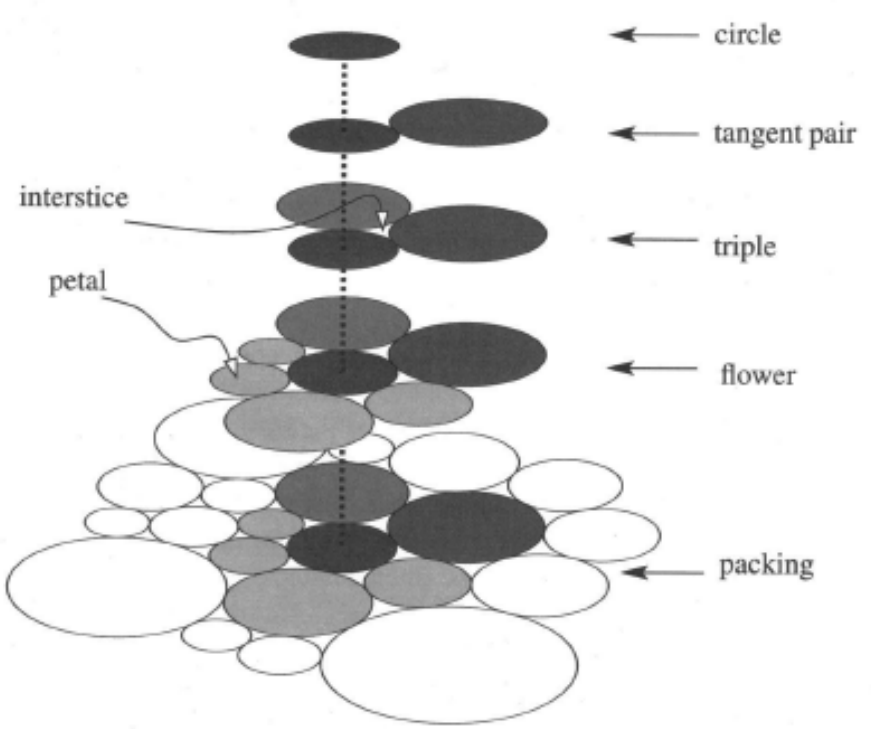

Figure (2. 6). Circle Packing Hierarchy.

The circle packing process has many applications in the industrial field; some of which are loading shipping containers with tubes, and cutting circular shapes out of rectangular metallic sheet [10]. Therefore, this attracted many researchers to find a proper way for packing circles in different shapes, based on the shape configuration and the type of application. To optimize the way for circle packing, several algorithms were applied by several groups, but most of the circle packing researchers applied what they called maximum hole degree (MHD) algorithm; especially those who work with packing unequal sized circles. Catillo, et al, (2005, [11]) represented several circle packing problems for the industrial applications, and some of the exact, and heuristic strategies are used to solve

these problems. They also presented illustrative numerical results through the use of generic global optimization software packages.

Huang, et al, (2006, [12]) proposed two new heuristics to pack unequal circles into a two-dimensional circular container and rectangular container [13] as shown in Fig. (2.7). The first algorithm, denoted by A1.0, was a basic heuristic for selecting the next circle to be placed according to the MHD rule. The second algorithm, denoted by A1.5, used a self-look ahead strategy to improve A1.0. Their experimental results showed that their approach had a good performance in terms of solution quality and computational time for packing unequal circles.

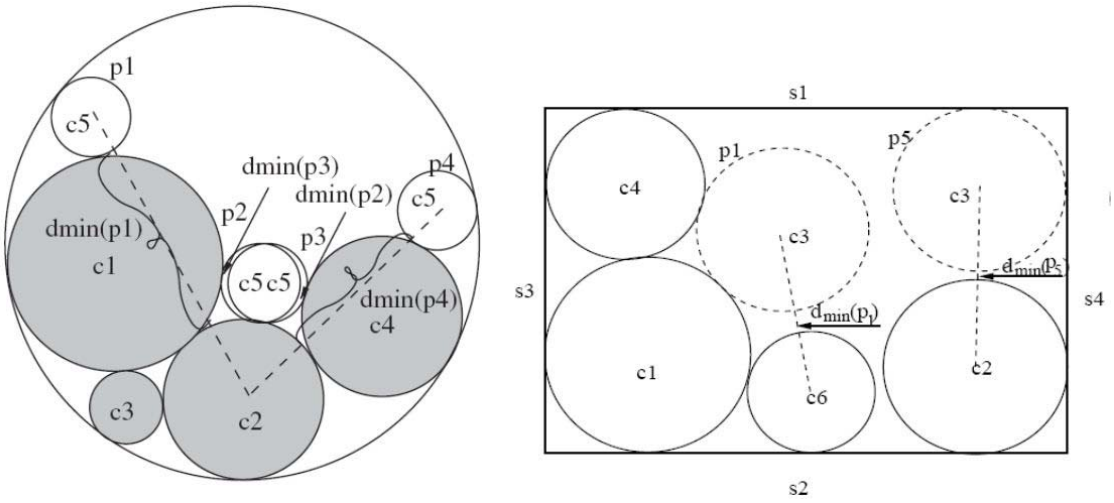

Figure (2. 7). Unequal circle packing for circular and rectangular containers using MHD method [12, 13].

Lu, et al, (2008, [14]) used the principle of maximum cave degree (MCD) for corner-occupying actions as shown in Fig. (2.8), which is the same principle used by Huang, et al, [12, 13], to solve the problem of packing equal or unequal circles into a larger circular container. The basic idea of their approach was to evaluate the benefit of a partial

configuration (where some circles have been packed and others remained outside) using the principle of maximum cave degree, and the improved Pruned-Enriched Rosenbluth method (PERM) strategy. Their computational results showed that the proposed approach produced high quality solutions within reasonable computational times.

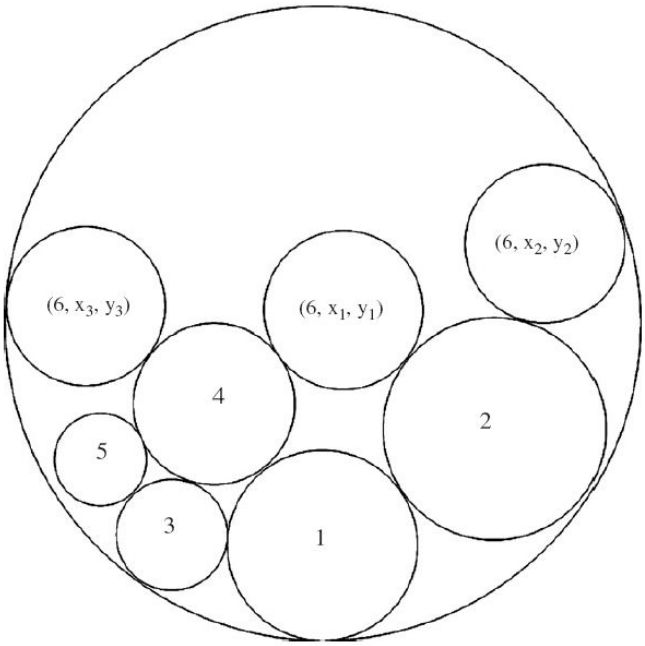

Figure (2. 8). The corner occupying action (COA) for single circle [14].

Kubach, et al, (2009, [15]) studied the strip packing problem (SPP) as well as the Knapsack Problem (KP). The SPP was used for the placement of a given finite set of circles of different sizes within a rectangular strip of fixed width which minimized the variable length of the strip. They solved the SPP problem by using MHD algorithm, and they applied in parallel manner a greedy algorithm to solve the KP problem for the initial configuration which enhanced the algorithms proposed by Huang, et al, [13]. The objective of Akeb, et al, (2009, [16]) was to solve some problems that were faced in the industry;

such as minimizing the holes which were used to pass the wires connecting the car's sensors with the display board taking into consideration that the size must be big enough to allow all wires to pass, avoid weakness of the car body, and other problems alike. They used the principle of MHD as shown in Fig. (2.9) to obtain the minimum circle radius and modify the selection of the next circle's radius by using the Beam Search (BS) algorithm.

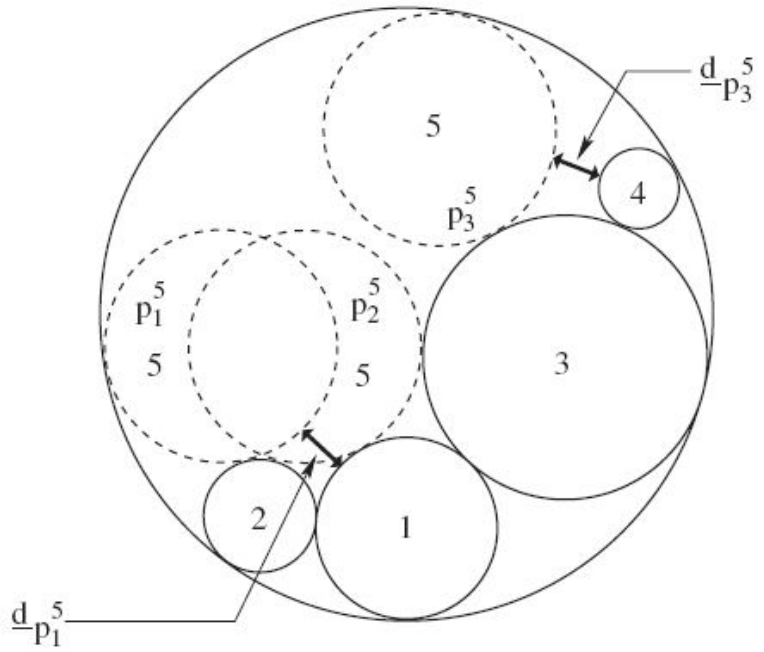

Figure (2. 9). Feasible distinct corner position of C5 [16].

Akeb, et al, (2011, [17]) discussed the circular open dimension problem (CODP) which is one of the circle packing family problems. They were given a strip of fixed width and unlimited length, as well as a finite set of n circular pieces of known radii. Their objective was to search for a global optimum length. They used the minimum local distance position (MLDP) algorithm for solving the CODP, which was equivalent to the MHD method as shown in Fig. (2.10).

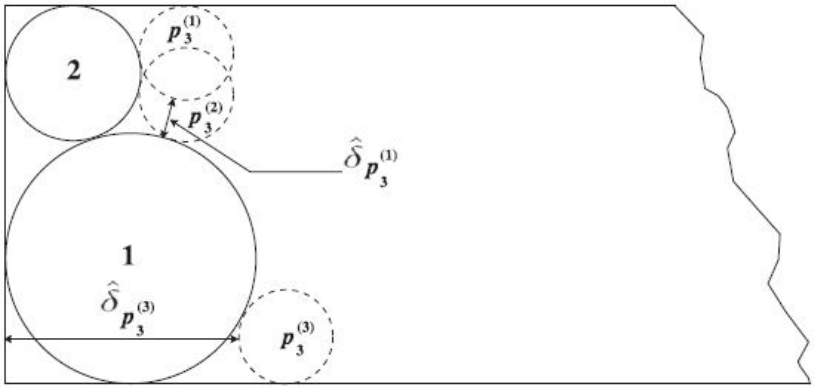

Figure (2. 10). Feasible distinct corner positions of C3 in the strip [17].

2.3 Global optimization of polynomial functions

Visweswaran, et al, (1991, [18]) proposed an algorithm to find the global optimum solution for one variable constrained and unconstrained polynomial function. Lasserre, (2001, [19]) transferred the real valued polynomial into a finite sequence of convex linear matrix inequality in order to find the global minimum of the unconstrained polynomial function. Hanzon, et al, (2003, [20]) worked on the general polynomial and they have built an approach to translate the original problem into a generalized eigenvalue problem to reach the global optimization solution. Nataraj, et al, (2007, [21]) presented an algorithm to calculate the global optimum solution for the unconstrained multivariate polynomial functions by applying a subdivision strategy. Also, Nataraj, et al, (2011, [22]) has proposed an algorithm to find the global optimum solution for constrained multivariable polynomial functions by using Bernstein coefficients approach.

2.4 Clustering techniques

Most of the clustering algorithms required the number of clusters' centers and their initial values. The Fuzzy C-Means and k-means algorithms are clear examples of these types of clustering algorithms. So the accuracy of the solution therefore depends mainly on the number of cluster centers and their initial values. The mountain method was presented by Yager, et al, (1994, [23]) as an efficient algorithm to solve the problem of finding the number of clusters through calculating the number and initial values of the cluster centers. This algorithm was initiated by gridding the data space and calculating a weight value for each grid point according to how close it is to the original data points. The grid point's weight increases by increasing the number of the close original data points. The highest weight value grid point will be selected as the first cluster center. Consequently since the first cluster center is located, the weight values of all grid points are reassigned depending on how far they are from the cluster center. The closer grid points have lower weight. The second cluster center is then chosen at the grid point with the highest remaining weight value. This process continues till the weight value of all grid points retract under a threshold. In this method, the computing time increases exponentially with the dimension of the problem because the mountain function must be calculated at each grid point. Therefore, a development has been achieved by Chiu, (1994, [24]) to the mountain method; given the name of subtractive clustering method. By using the data points directly as the candidates for cluster centers, instead of the grid points used in mountain method, the computational problem would be solved. The computation time became proportional to the problem size instead of the problem dimension. Bataineh, et al, (2011, [25]) made a comparison study for different models generated by using subtractive clustering algorithm

and others generated by using fuzzy c-means algorithm and they found that the models generated from subtractive clustering are usually more accurate than those generated using FCM algorithm. An algorithm is needed to generate accurate models using FCM while is not needed in the use of subtractive clustering. Also, they mentioned that FCM gives different results for different runs. Finally, there conclusion was that the subtractive algorithm produces consistent results.

Chapter 3

Polynomial function global optimization by using subtractive clustering technique

3.1 Introduction

Polynomial functions come in handy every day in which they have a lot of applications. People use them in the real world because of their ability to describe curves and surfaces of various types. For example, roller coaster designers may use polynomials to describe the curves in their rides. Combinations of polynomial functions are used in economics to do cost analyses. Polynomials have a great efficiency in modelling different situations in all types of fields like business' markets' modelling, in physics to describe the trajectory of projectiles, in industry to model physical phenomena or mainly for modeling the sculptured working surfaces, and curves, which we are interested in.

A new optimization technique is proposed in this chapter to calculate the global optimal solution for the constrained polynomial function. The main contribution of this technique is to find the global minimum or maximum with reduced the computing time, improved accuracy, and avoidance of sticking in the local minimum or maximum. Our focus will be on the one variable and two variables constrained polynomial functions because they represent curves and surfaces which are the most used in the industrial field. Since the one variable equation represents a curve and the two variables equation represents a surface, the problem can be transferred to a geometrical problem.

Our approach depends on recognizing the different features of the curves and surfaces represented by the constrained polynomial function which contain several local critical points (minima and maxima). These critical points are represented graphically as peak and valley points of the convex and concave features respectively. By knowing the local critical points; one of these points will be assigned as the global critical point. The feature recognition method divides the curve or surface into specified regions according to the curvature from convex, concave, plane, and saddle regions (for surfaces). Convex regions contain the local minima and concave regions contain the local maxima which can be calculated precisely by our algorithm.

The algorithm starts by patching the entity into many data points. The curvature at each data point will be calculated. The data points which have the same curvature nature will be grouped together into convex regions, concave regions, plane regions, and saddle regions. By clustering the planer projections of data points for each group to the enclosed clusters we can know the exact number of the clusters inside each region. By finding the center of each cluster, it will be the nearest point to the exact center point. The exact center point represents a peak point in case of concave region, and valley point in case of convex region. To calculate the exact center points, the clusters' center points will be used as initial points. Using close by points as initial points to find the exact points will make the search converge very fast. Using the initial local points in simple local optimizer leads to the exact local points very quickly. The minimum among the local minima will then be the global minimum. A comparison has been done on several case studies between the proposed algorithm and the practical swarm optimization (PSO) technique.

3.2 Geometric characterization of objective functions

The polynomial functions can be characterized according to the number of the variables to one and multi-variables. The polynomial function represents geometrically a curve in case of one variable function and a surface in case of two variables function. Consequently the curve and surface features describe the variation of the function. Recognizing these features guides to the peaks and valleys of the function. The optimization problem starts by assigning the objective function which is the polynomial function, and the constraints which are the inequalities bounded the working space.

3.2.1 One variable objective function

The objective function which contains one variable represents a curve. It can be written as

$$f(x) = \sum_{\alpha=1}^{n} c_\alpha x^\alpha \qquad c_\alpha \in R \tag{3.1}$$

$$f^* = \min_{x \in R} f(x) \tag{3.2.a}$$

Such that

$$a \le x \le b \tag{3.2.b}$$

The optimization process starts by patch the curve to several data points as shown in Fig. (3.1).

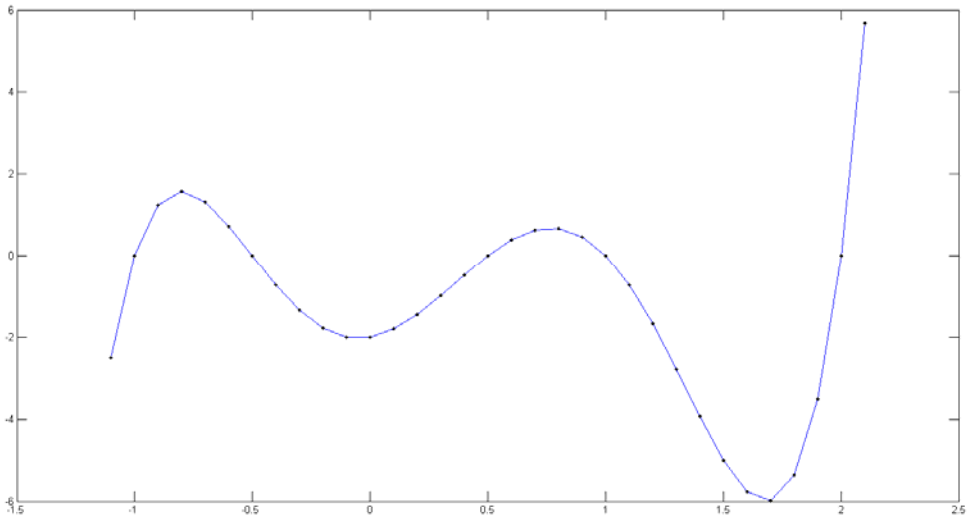

Figure (3. 1). Curve patching.

Then at each data point the local curvature is calculated by equation (3.3). The curvature value at each data point predicts the local geometry shape around this data point and classifies this point to the proper region by convex, concave, or plan according to table (3.1). The local curve curvature (k) calculations depend on the first and second derivatives of the polynomial function as shown in equation (3.3).

$$k = \frac{f''(x)}{\left(1+\left(f'(x)\right)^2\right)^{\frac{3}{2}}} \tag{3.3}$$

Table (3. 1). The Relation between the geometry shape and curve geometry features.

Curvature (k)	Local Shape
k = 0	Plane
k < 0	Concave
k > 0	Convex

3.2.2 Dual variables objective function

Dual variables objective function represents a surface. It can be written as

$$f(x,y)=\sum_{\beta}^{m}\sum_{\alpha=1}^{n}c_{\alpha}x^{\alpha}y^{\beta} \qquad c_{\alpha}\in R \tag{3.4}$$

$$f^{*}=\min_{(x,y)\in R} f(x,y) \tag{3.5.a}$$

Such that

$$\begin{aligned} a\le x\le b \\ c\le y\le d \end{aligned} \tag{3.5.b}$$

The optimization process starts with patch the surface to several data points Fig. (3.2).

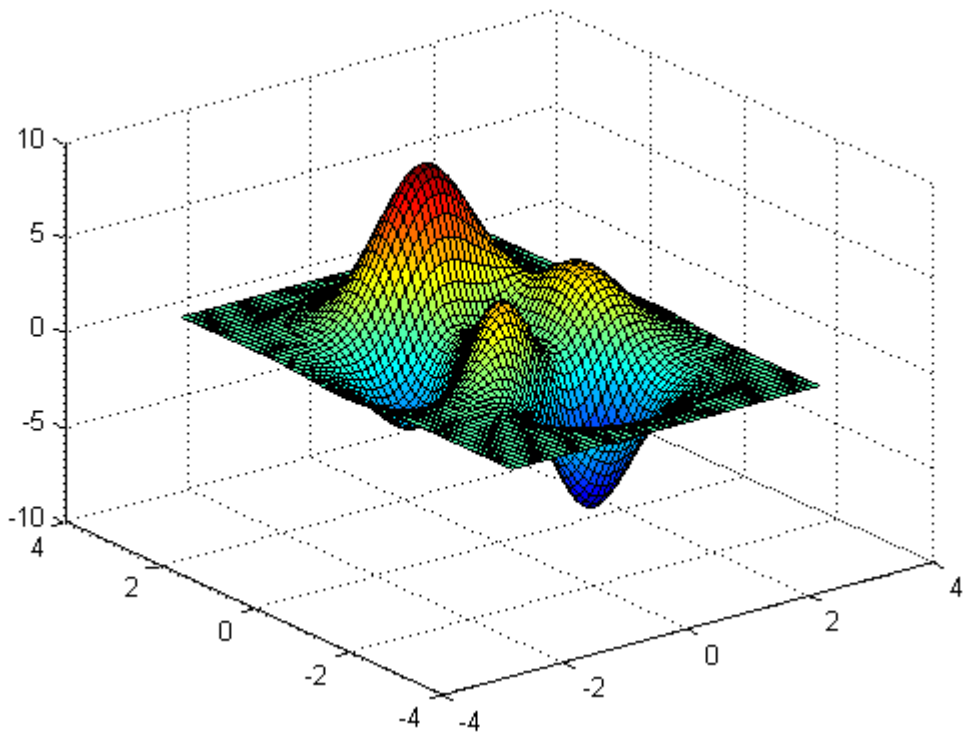

Figure (3. 2). Surface patching.

For calculating the curvature, surface is differed than the curve. In order to describe the surface from a geometric perspective, two critical surface curvatures must be calculated

at each data point: Gaussian curvature and mean curvature. These are enough to predict the local geometry shape around every data point. According to these curvatures, surface shape is categorised into four types: convex, concave, plane, and hyperbolic shape. All the points with the same shape are grouped. Gaussian curvature and mean curvature is calculated by using the first and second fundamental matrices coefficients of the surface. With the help of first and second fundamental matrices, Gaussian and mean curvatures can be calculated by using equations (3.6), (3.7). For Gaussian curvature (K):

$$\mathrm{K} = \frac{\mathrm{LN} - \mathrm{M}^2}{\mathrm{EG} - \mathrm{F}^2} \tag{3.6}$$

For Mean curvature, H:

$$\mathrm{H} = \frac{1}{2}\left(\frac{\mathrm{EN} - 2\mathrm{FM} + \mathrm{GL}}{\mathrm{EG} - \mathrm{F}^2}\right) \tag{3.7}$$

3.2.2.1 The First Fundamental Matrix of Surface

Usually, surfaces are represented by equations $Z = f(x, y)$ in which x and y are the planer coordinates, and **Z** is the position vector $[x, y, z]^{\mathrm{T}}$ of a point on the surface. The first fundamental matrix of the surface is given by

$$\mathbf{A} = \begin{bmatrix} \frac{\partial Z}{\partial x} \cdot \frac{\partial Z}{\partial x} & \frac{\partial Z}{\partial x} \cdot \frac{\partial Z}{\partial y} \\ \frac{\partial Z}{\partial y} \cdot \frac{\partial Z}{\partial x} & \frac{\partial Z}{\partial y} \cdot \frac{\partial Z}{\partial y} \end{bmatrix} = \begin{bmatrix} \mathrm{E} & \mathrm{F} \\ \mathrm{F} & \mathrm{G} \end{bmatrix} \tag{3.8}$$

According to Pythagorean theorem $ds^2 = dx^2 + dy^2$, Fig. (3.3).

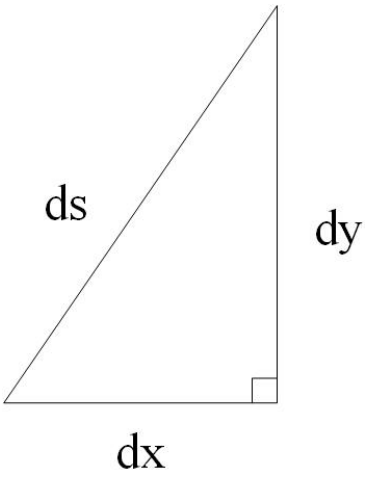

Figure (3. 3). Pythagorean theory.

Since the surface is wrapped, the modified Pythagorean theorem will be the first fundamental form as shown in Fig. (3.4). The first fundamental form is the expression for the arc length of the curve passing through any point on the curve:

$$ds^2 = Edx^2 + 2Fdxdy + Gdy^2 \tag{3.9.a}$$

since

$$E = \left(\frac{\partial z}{\partial x}\right)^2 \qquad F = \frac{\partial z}{\partial x}\cdot\frac{\partial z}{\partial y} \qquad G = \left(\frac{\partial z}{\partial y}\right)^2 \tag{3.9.b}$$

E, F, and G … The coefficients of the first fundamental form of the surface.

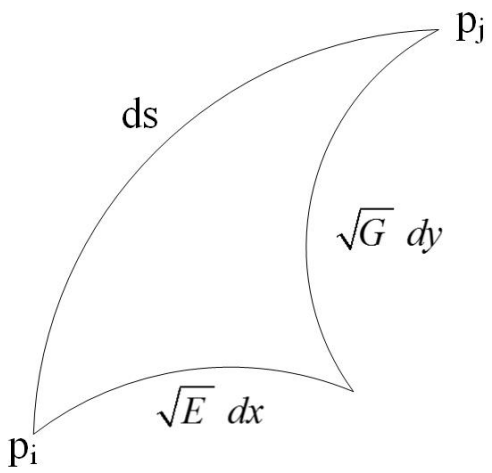

Figure (3. 4) Modified Pythagorean theory.

3.2.2.2 The Second Fundamental Matrix of Surface

Assuming the existence of the second order derivatives of the surface equations, the unit normal of a data point is obtained by $\mathbf{n} = \dfrac{\dfrac{\partial Z}{\partial x} \times \dfrac{\partial Z}{\partial y}}{\left| \dfrac{\partial Z}{\partial x} \times \dfrac{\partial Z}{\partial y} \right|}$ the second fundamental matrix is given by

$$\mathbf{B} = \begin{bmatrix} \mathbf{n} \cdot \dfrac{\partial^2 Z}{\partial x^2} & \mathbf{n} \cdot \dfrac{\partial^2 Z}{\partial x \, \partial y} \\ \mathbf{n} \cdot \dfrac{\partial^2 Z}{\partial y \, \partial x} & \mathbf{n} \cdot \dfrac{\partial^2 Z}{\partial y^2} \end{bmatrix} = \begin{bmatrix} \mathrm{L} & \mathrm{M} \\ \mathrm{M} & \mathrm{N} \end{bmatrix} \qquad (3.10.a)$$

since

$$L = n \cdot \frac{\partial^2 z}{\partial x^2} \qquad M = n \cdot \frac{\partial^2 z}{\partial x \, \partial y} \qquad N = n \cdot \frac{\partial^2 z}{\partial y^2} \qquad (3.10.b)$$

L, M, and N … The coefficients of the second fundamental form of the surface.

3.2.2.3 Surface Geometric Features

By considering the Gaussian and mean curvatures at each data point, the local geometric shape around the data point can be identified as shown in Fig. (3.5), the criteria are listed in table (3.2).

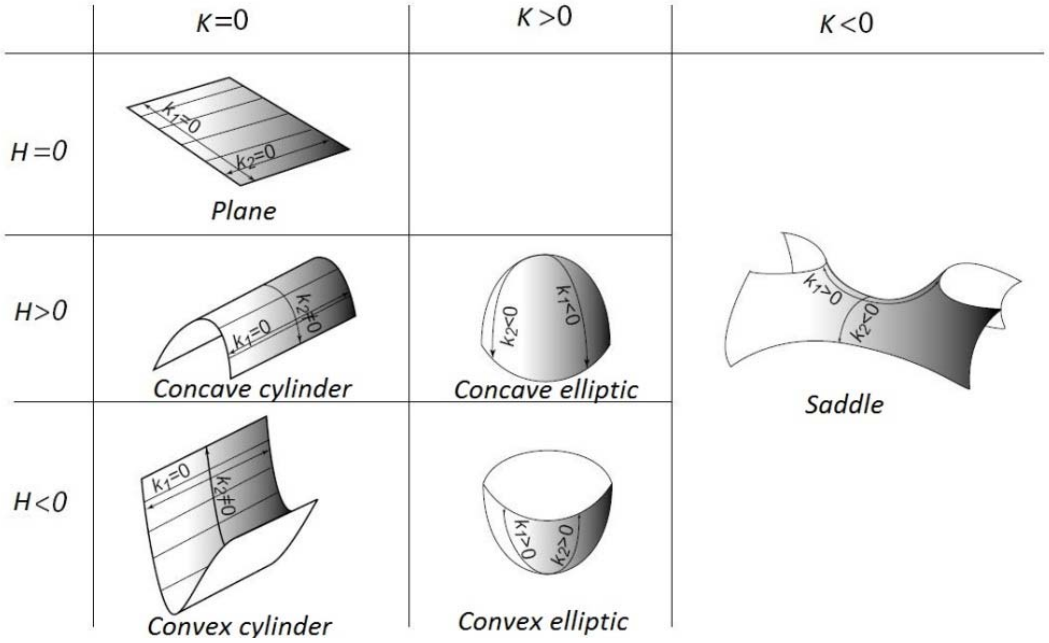

Figure (3. 5). Surface shapes according to Gaussian and mean curvature.

Table (3. 2). The Relation among the geometry shape and surface geometry features.

Gaussian Curvature (K)	Mean Curvature (H)	Point Feature	Local Shape
K = 0	H = 0	Parabolic	Plane
K = 0	H > 0	Parabolic	Concave Cylinder
K = 0	H < 0	Parabolic	Convex Cylinder
K > 0	H > 0	Elliptic	Concave Ellipse
K > 0	H < 0	Elliptic	Convex Ellipse
K < 0	H > 0 or H < 0	Hyperbolic	Saddle

3.3 Clustering technique

After recognizing the curvature at each data point for both the curve and the surface, the points which have the same curvature type will be grouped. The entity may contains one or more regions inside each group, for each region, it must contains one of the critical points. The next step is to then find the number of these regions inside each group, and the center of each region which represents one of the local critical points, for doing so the subtractive clustering technique is adopted. Clustering is the process of grouping a set of elements into the same group or cluster so that elements in the same group are to somehow similar or have common factor. According to the elements, distribution, and the objective of the clustering, different types of similarities are used to place elements into groups, where the similarity value controls how the clusters are shaped. Some examples of these types of similarities are distance, and intensity.

There are two main types of clustering; the hard clustering, and the soft clustering. In hard clustering, elements are divided into discrete clusters, where each element belongs to a single exact cluster. In soft clustering, the elements can have relationships with certain levels to more than one cluster, the relationships levels are attached to each element. The relationships levels for each element refer to how strong the bond is between the element and a particular cluster. Subtractive clustering is one of the processes to designate the relationships levels, consequently using these levels to assign the elements to one or more clusters.

3.3.1 Subtractive clustering method

Most of the clustering algorithms required the number of clusters' centers and their initial values. The Fuzzy C-Means and k-means algorithms are clear examples of these types of clustering algorithms. So the accuracy of the solution therefore depends mainly on the number of cluster centers and their initial values. Based on the literature review, we used the Subtractive Clustering Method to calculate the number of the clusters and the clusters' centers. The subtractive clustering method assumes that each data point is a potential cluster center. A data point with more neighboring data will have a higher opportunity to become a cluster center than points with fewer neighboring data. For subtractive clustering of a group of data points $\{x_1, x_2 \ldots x_n\}$; the method starts by considering each data point as a potential cluster center.

a. Initial potentials of the point set

At first, each data point is regarded as a potential cluster centre, and each cluster has only one data point as the centre itself. The potential of a data point, $\mathbf{x}_i$, is defined by

$$P_i = \sum_{j=1}^{n} e^{-\alpha \left\| \mathbf{x}_i - \mathbf{x}_j \right\|^2}, \ i = 1,2,...,n \qquad (3.11.a)$$

where

$$\alpha = \frac{4}{r_a^2} \qquad (3.11.b)$$

and r_a is a positive constant. The potential of a data point is a function of the distances between this point, and every other point. The shorter is the distance, the more contribution to the summation. For a data point in dense area, its potential is higher than that in sparse

area. Usually, the distance is in the metric of Euclidean norm that is the sum of the squares of the difference in each dimension. In order to consider the importance variation of dimensions, different weights are assigned to different dimensions. Therefore, the distance can be calculated by:

$$\left\| x_i - x_j \right\|^2 = w_1 \cdot s + w_2 \cdot \left(x_{i,3} - x_{j,3} \right)^2 + \ldots + w_{p-1} \cdot \left(x_{i,p-1} - x_{j,p-1} \right)^2 \tag{3.12}$$

The constant, r_a, is the radius defining the neighborhood of a data point: data points inside the circle produce significant potential for the centric data point, and data points outside exert little influence on the potential.

b. Choose the first cluster center and update the potentials

The data point with highest potential is selected as the first cluster center. The reason is that this point is closely surrounded by a maximum number of data points. The maximum potential P_{c_1} of the first cluster center $\mathbf{x}_{c_1}$ is:

$$\mathrm{P}_{c_1} = \max\left\{ \mathrm{P}_1, \mathrm{P}_2, \ldots, \mathrm{P}_n \right\} = \sum_{j=1}^{n} \mathrm{e}^{-\alpha \cdot \left\| \mathbf{x}_{c_1} - \mathbf{x}_j \right\|^2} \tag{3.13}$$

The potential of each data point is then revised by the formula

$$\mathrm{P}_i = \mathrm{P}_i - \mathrm{P}_{c_1} \mathrm{e}^{-\beta \cdot \left\| \mathbf{x}_{c_1} - \mathbf{x}_i \right\|^2}, \quad i = 1,2,\ldots,n \tag{3.14.a}$$

where

$$\beta = \frac{4}{r_b^2} \tag{3.14.b}$$

and r_b is a positive constant. The subtractive amount from the potential of each point is nonlinear, and inversely proportional to the distance between the point and the first cluster center. Therefore, the potentials of data points closer to the first cluster center are reduced

to a very small number, and the potential of the first cluster center becomes null at last. On the contrary, the point far away from the center has larger potential comparatively. The purpose of subtraction is to find the second cluster center farther away from the first one. The constant, r_b, is also a radius defining a circular region, and the point will have measurable reduction in potential, if contained in the region. Usually, r_b is set to be greater than r_a.

c. Choose the second cluster centre

Among the updated potentials of data points, the data point with the highest potential is selected as the second cluster center.

$$P_{c_2} = \max\{P_1, P_2, ..., P_n\} = \sum_{j=1}^{n} e^{-\alpha \left\| \mathbf{x}_{c_2} - \mathbf{x}_j \right\|^2} \tag{3.15}$$

Same as the previous step, part of the highest potential of the second cluster center is subtracted from the potential of every data point. In general, if the k^{th} cluster center is found, the potential modification is carried out using the formula

$$P_i = P_i - P_{c_k} e^{-\beta \left\| \mathbf{x}_{c_k} - \mathbf{x}_i \right\|^2}, \quad i = 1,2,...,n \tag{3.16}$$

This process will create a series of cluster centers, $\{ \mathbf{x}_{c_1}, \mathbf{x}_{c_2}, ..., \mathbf{x}_{c_k} \}$.

d. The criteria for accepting and rejecting cluster centers

If $P_{c_k} > \overline{\varepsilon} P_{c_1}$, the data point $\mathbf{x}_{c_k}$ will be accepted as a cluster center and continue. But if $P_{c_k} < \underline{\varepsilon} P_{c_1}$, the data point $\mathbf{x}_{c_k}$ will be rejected and the clustering process will be seized. The shortest distance among all the distances between $\mathbf{x}_{c_k}$ and cluster centers will be set as d_{min}. In case the stopping criteria was not satisfactory:

$$\frac{\mathrm{d}_{\min}}{r_a} + \frac{\mathrm{P}_{\mathrm{c_k}}}{\mathrm{P}_{\mathrm{c_1}}} \geq 1 \tag{3.17}$$

Again $\mathbf{x}_{c_k}$ will be accepted as the new cluster center, and the algorithm will continue, otherwise the new cluster center $\mathbf{x}_{c_k}$ will be rejected and the potential of $\mathbf{x}_{c_k}$ will be set as zero. This process will be repeated till the stopping criteria is satisfied. The two constants are set as, $\overline{\varepsilon} = 0.5$, and $\underline{\varepsilon} = 0.15$ .Through the subtractive process, the number of clusters, and their centers are found.

3.4 Optimization technique

The approach objective is to calculate the global optimum by finding all the available local minima. According to these objective, the optimization procedures are consist of three steps.

3.4.1 Patching

The first step starts with calculating several data points on the surface or the curve represented by the objective function. The selected data points have the same infinitesimal distances and areas between each other, this process is called patching. The selected data points will be the input points to our algorithm. By testing the curvature for each data point (Gaussian and main curvatures in case of the surface, and the local curvature in case of the curve) these points can be classified into different groups according to the curvature values at each point. These groups are convex, concave, plane, and saddle (in case of the surface) groups. According to the type of the optimization process, whether it is minimization or maximization, the working group will be assigned. The convex group will be the working group in case of minimization, and the concave group will be the working group in case of maximization.

3.4.2 Clustering

The working group data points will then be the input for the second step which is the clustering process. The subtractive clustering process is the candidate process to be applied in this algorithm because of the pre-mentioned advantages. Subtractive clustering process is looking for the clusters' centers of the input working group data points. According to the intensity distribution of the data points in the working group, the number of clusters' centers and their locations will be assigned. The clusters' center points are from the input data points. The main reason of applying the clustering process is to find the closest points to the real center points of the peaks or the valleys of the tested surface or curve which represented by the objective function, therefore the clusters centers are the closest points to the real center points of the peaks or the valleys. To find the real center points of the peaks or the valleys another step should be carried out.

3.4.3 Local optimization

The local optimization methods have some merits compared with the global optimization methods. The local optimization methods tend to converge very quickly whereas, global methods might take time. Also, the accuracy of the local optimization methods to discover the solution is much better than the accuracy of the global optimization methods, therefore the global optimization methods having many parameters must be tuned to improve the accuracy of finding the final solution. From everything mentioned above, it is concluded that; if the local optimization method is adapted to discover the global solution of multiple local minima and maxima functions it will be faster and more accurate.

Thereby we Quasi Newton method in our algorithm to ensures the high accuracy and low computational time. The Quasi-Newton method is one of the most famous algorithms for finding the local maxima or minima of the objective functions. Quasi-Newton method is based on Newton's method to find the stationary point of the objective function, where the gradient is 0. Newton's

method uses the first and second derivatives to find the stationary point staring from an initial point. The closer the initial point from the stationary point, the faster the solution is reached. By using the clusters centers that we obtain from the clustering algorithm as initial points for the Quasi-Newton method ensures a fast convergence in the optimization process. After calculating all the local optimum points, the global optimum point is one of them.

3.5 Applications

To verify the validity of our new approach, different case studies are tested. The cases are divided according to the number of variables; one variable and two variables objective functions. Different objective functions with different numbers of the local minima are used.

3.5.1 One variable objective function case studies

3.5.1.1 Case study I

In the first case study the objective function as shown in equation (3.18.a), with the constraint inequality equation (3.18.b). Fig. (3.6.a) shows the data points coming from gridding the objective function. By checking the data points, they are grouped into two groups as shown in Fig. (3.6.b).

$$f(x) = x^4 + 3x^3 - 9x^2 - 23x - 12 \tag{3.18.a}$$

Such that

$$-4.5 \geq x \geq 4.5 \tag{3.18.b}$$

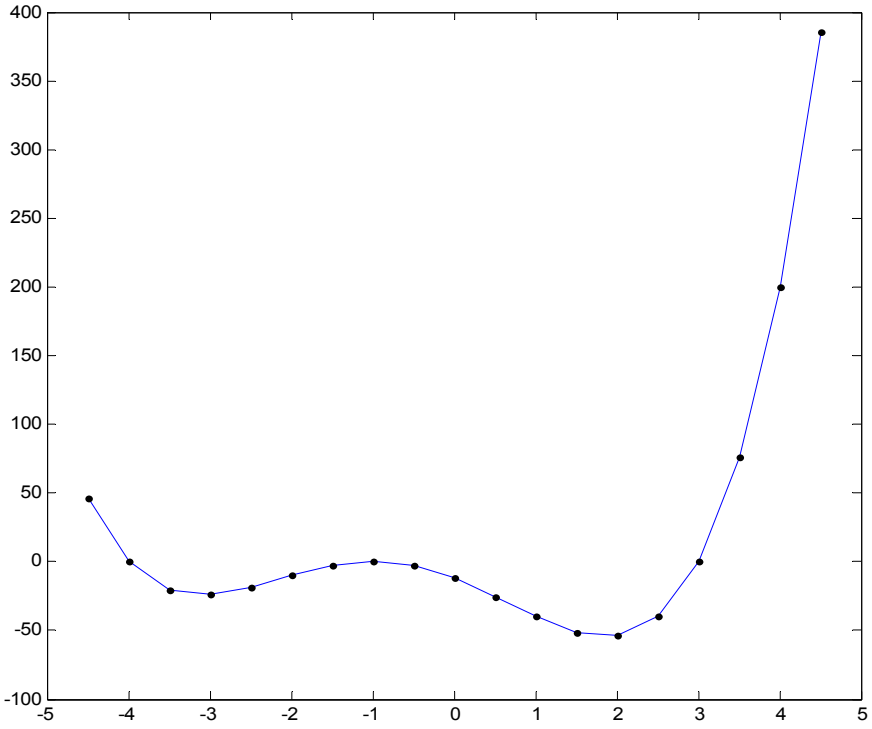

(a) First case study data points.

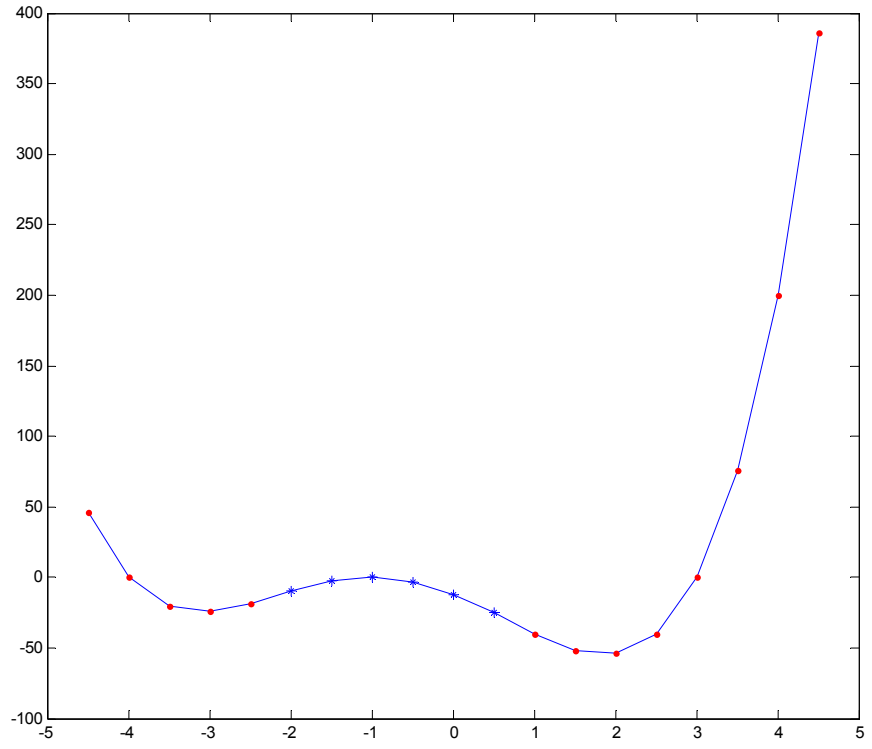

(b) Data points groups (Convex group " . ", Concave group " *)

For a minimization problem the convex group is selected. By applying the subtractive clustering technique the number of clusters with the clusters' centers are calculated as shown in Fig. (3.6.c). The clustering technique gives two clusters with two centers as shown in table (3.3).

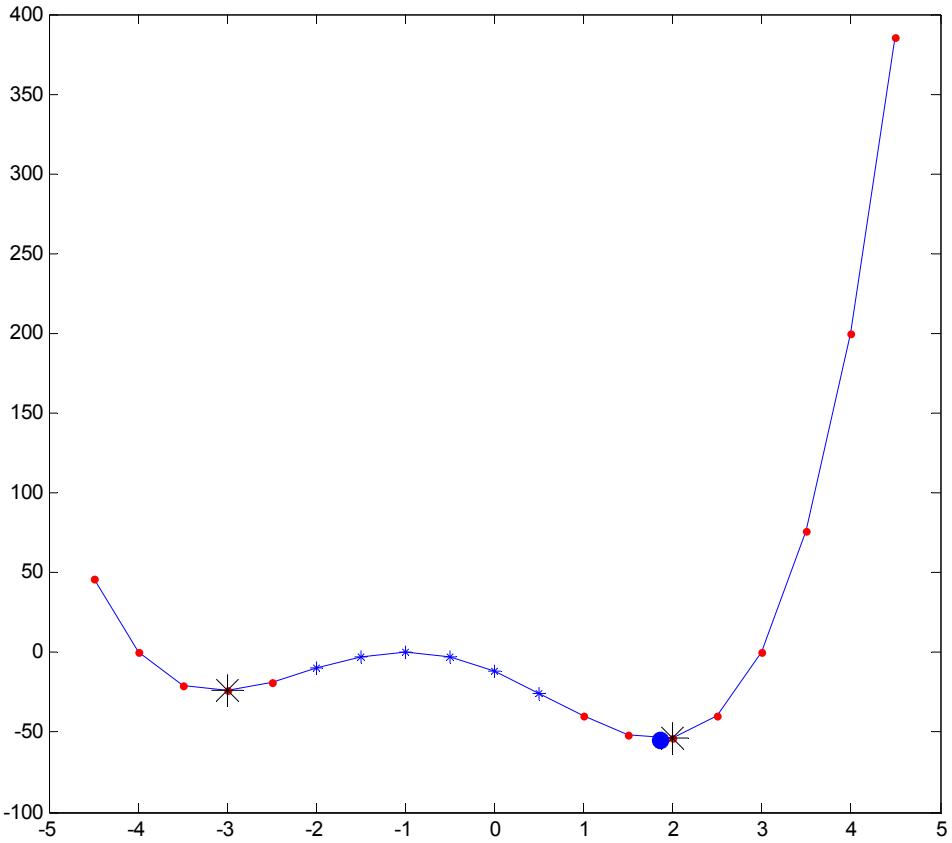

(c) The center point of each cluster "*", and the global minimum point "●".

Figure (3. 6). Curve first case study.

Table (3. 3). Case study I clusters centers.

	x	F(x)
1	-3	-24
2	2	-54

Using the clusters' centers as initial points in Quasi-Newton algorithm, the exact local minima is calculated as illustrated in table (3.4).

Table (3. 4). Case study I exact local minima.

	x	f(x)
1	-3.103	-24.211
2	1.853	-54.644

The smaller value of the f(x) represents the global minimum of the objective function as shown in table (3.4).

3.5.1.2 Case study II

$$f(x) = \frac{1}{8}x^6 + \frac{1}{4}x^5 - \frac{7}{8}x^4 - \frac{3}{2}x^3 - 2x^2 - 2x - 2 \qquad (3.19.a)$$

Such that

$$-2.5 \geq x \geq 2.5 \qquad (3.19.b)$$

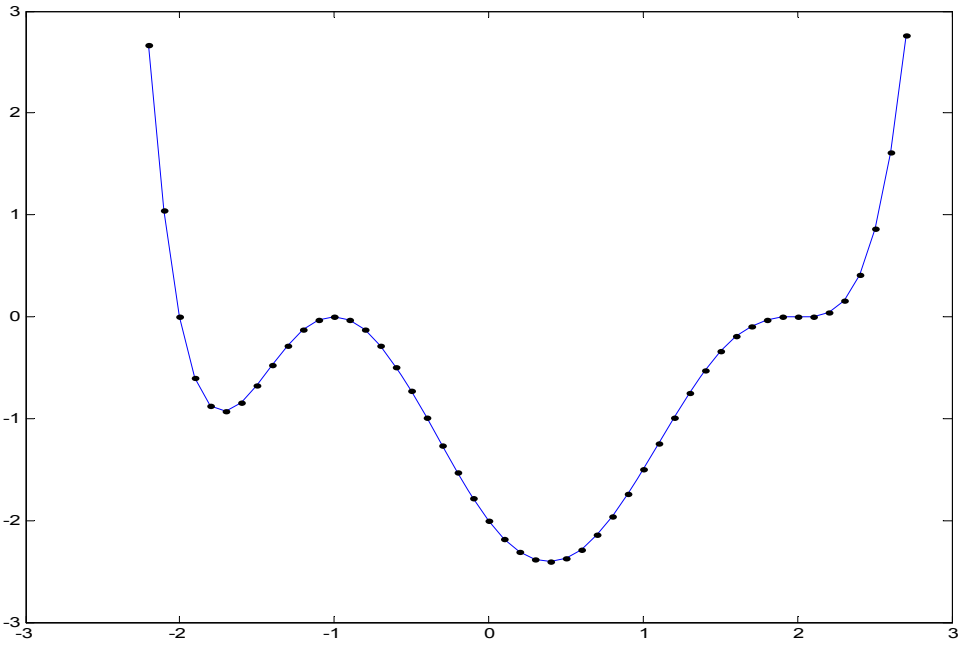

(a) Second case study data points.

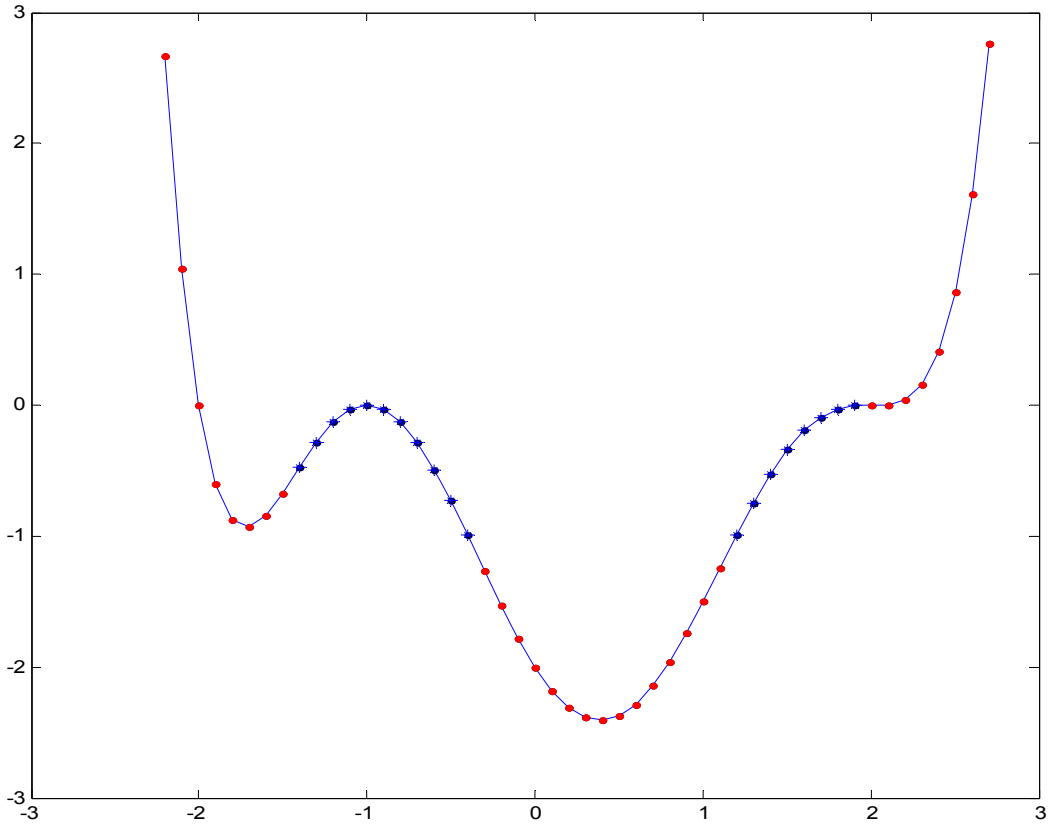

(b) Data points groups (Convex group " . ", Concave group " * ")

For a minimization problem the convex group is selected. By applying the subtractive clustering technique, the number of clusters with the clusters' centers are calculated as shown in Fig. (3.7.c). The clustering technique gives three clusters with three centers as shown in table (3.5).

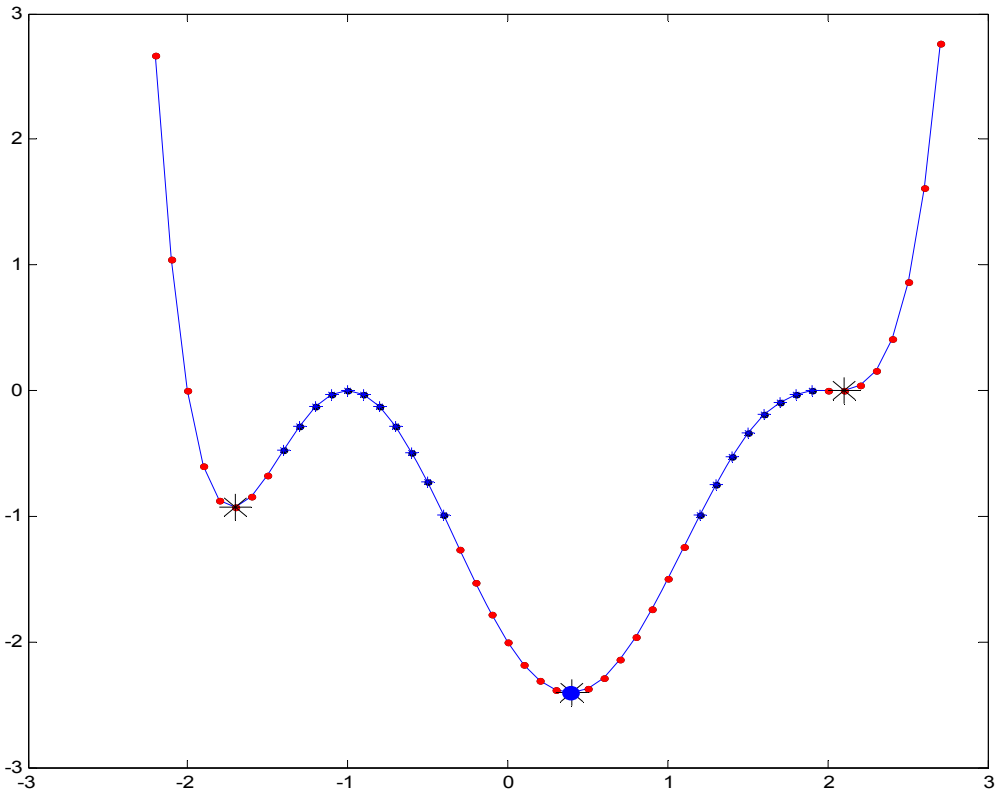

(c) The center point of each cluster "*", and the global minimum point "●".

Figure (3. 7). Curve second case study.

Table (3. 5). Case study II clusters centers.

	x	F(x)
1	0.4	-2.408
2	2.1	0.0049
3	-1.7	-0.931

Using the clusters' centers as initial points in Quasi-Newton algorithm, the exact local minima are calculated as illustrated in table (3.6).

Table (3. 6) Case study II exact local minima.

	x	f(x)
1	0.387	-2.409
2	2.07	0.003
3	-1.721	-0.934

The smaller value of the f(x) represents the global minimum of the objective function as shown in table (3.6).

3.5.1.3 Case study III

$$f(x) = 4x^5 - 8x^4 - 5x^3 + 10x^2 + x - 2 \tag{3.20.a}$$

Such that

$$-1.5 \geq x \geq 2.5 \tag{3.20.b}$$

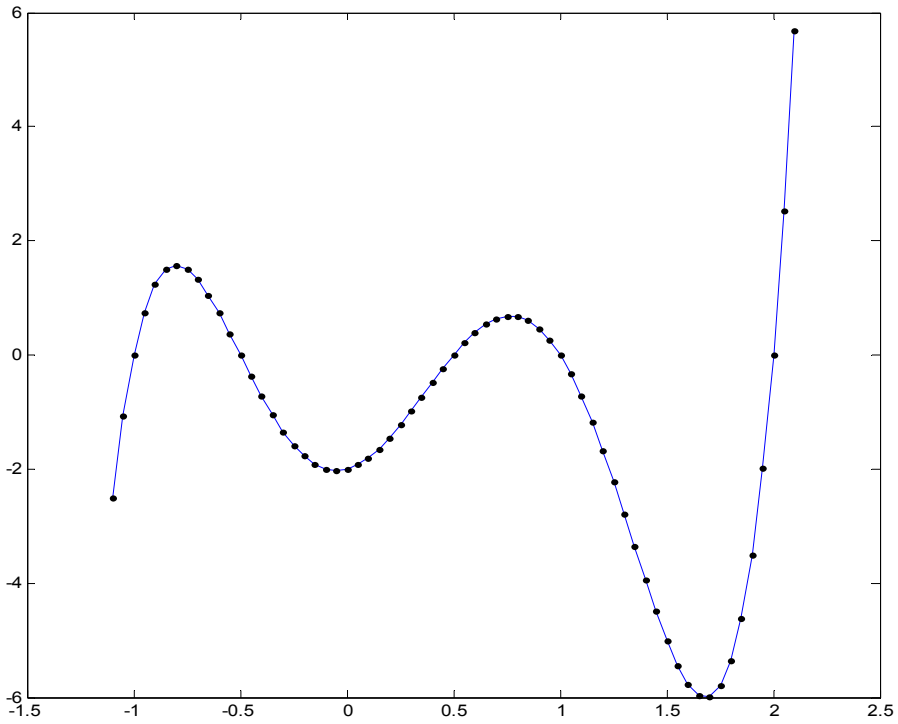

(a) Third case study data points.

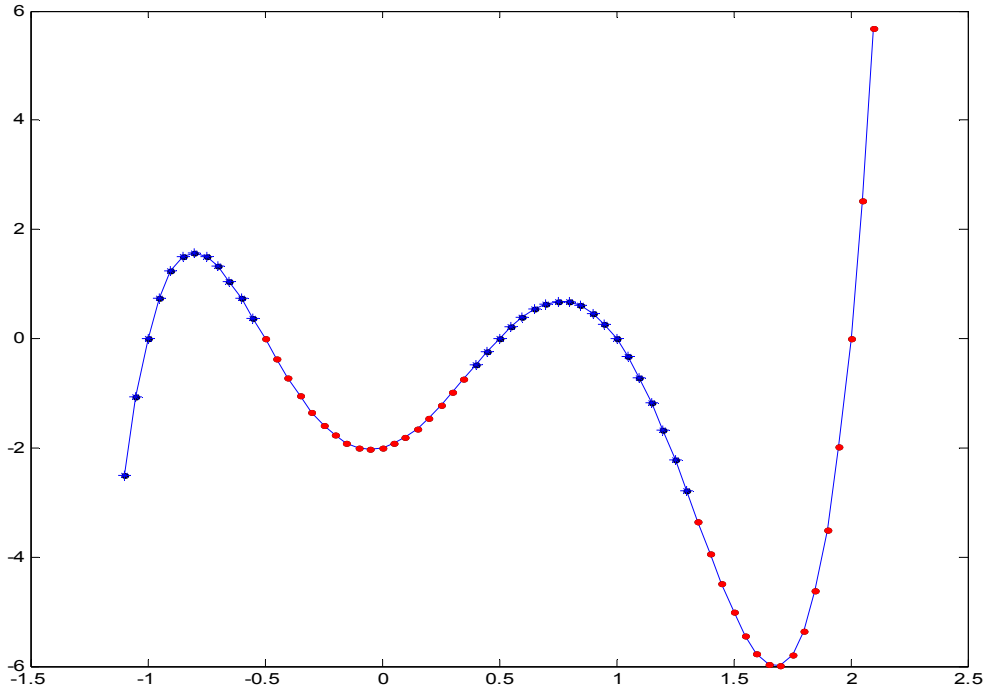

(b) Data points groups (Convex group " . ", Concave group " * ")

By applying the subtractive clustering technique to the convex group as a minimization problem, the number of clusters with the clusters' centers are calculated as shown in Fig. (3.8.c). The clustering technique, gives two clusters with two centers as shown in table (3.7).

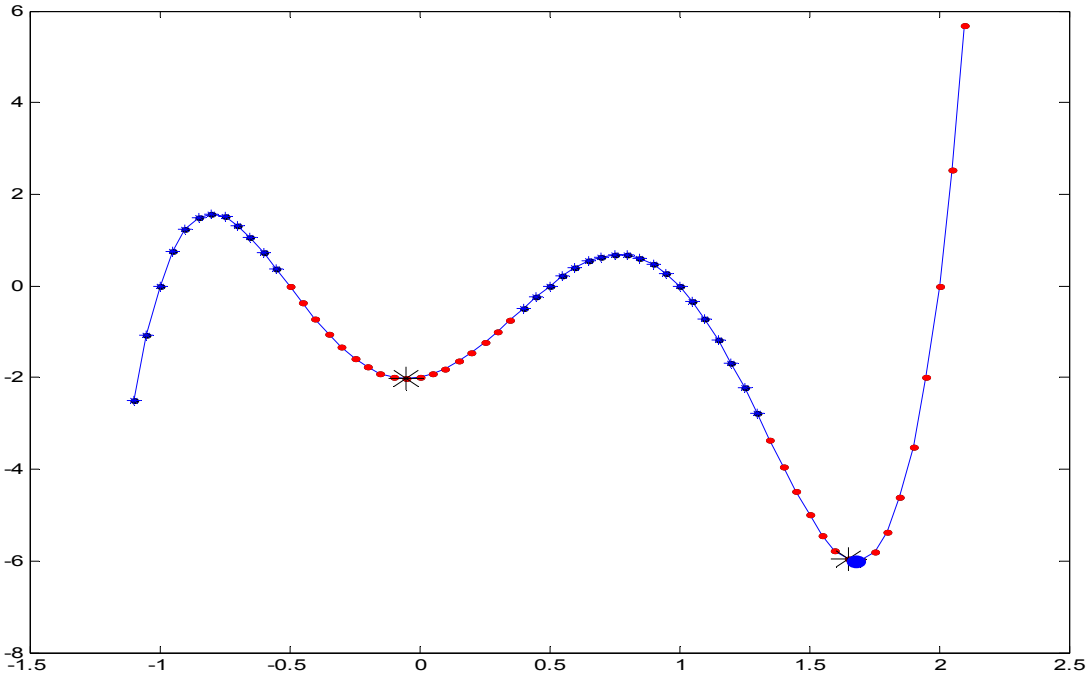

(c) The center point of each cluster "*", and the global minimum point "●".

Figure (3. 8). Curve third case study.

Table (3. 7). Case study III clusters centers.

	x	F(x)
1	-0.05	-2.024
2	1.65	-5.963

Using the clusters' centers as initial points in Quasi-Newton algorithm, the exact local minima are calculated as illustrated in table (3.8).

Table (3. 8). Case study III exact local minima.

	x	f(x)
1	-0.048	-2.024
2	1.681	-6.007

The smaller value of the f(x) represents the global minimum of the objective function as shown in table (3.8).

3.5.1.4 Case study IV

$$f(x) = x^8 - 4x^7 - x^6 + 12x^5 + 3x^4 - 4x^3 - 7x^2 - 20x - 12 \quad (3.21.a)$$

Such that

$$-1.5 \geq x \geq 3 \quad (3.21.b)$$

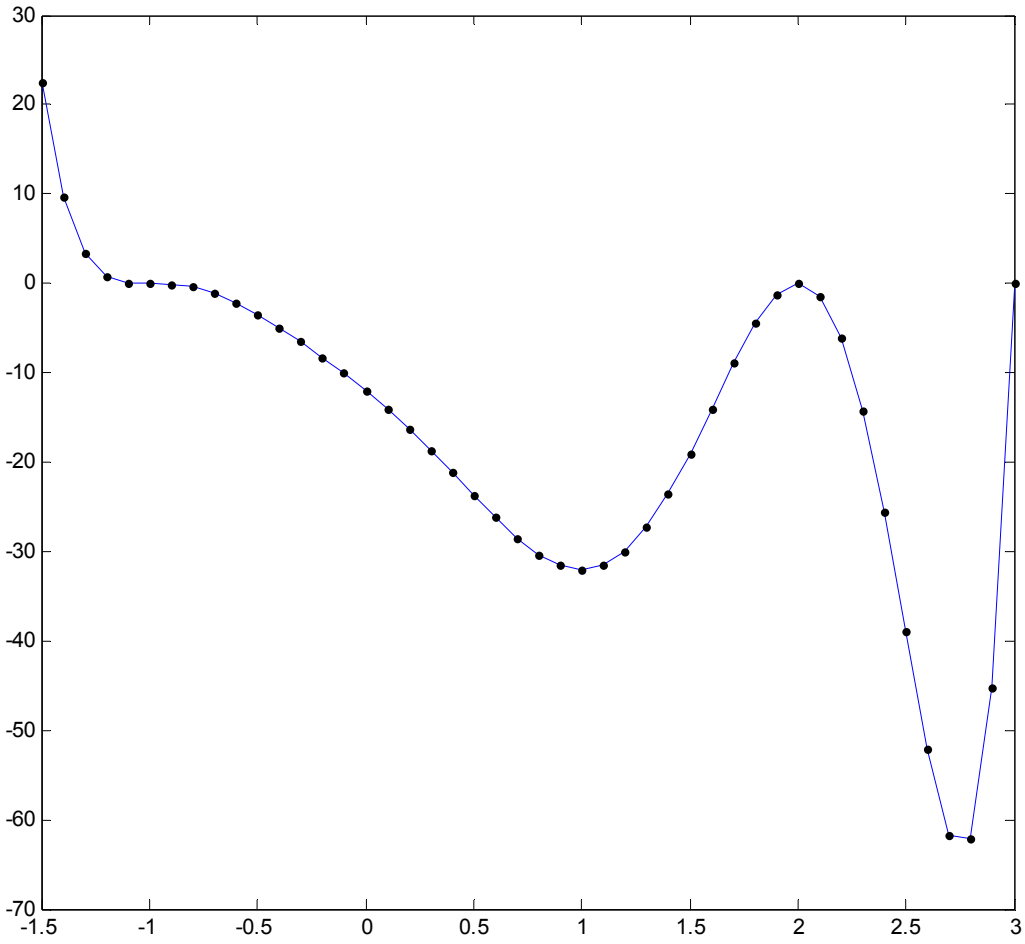

(a) Fourth case study data points.

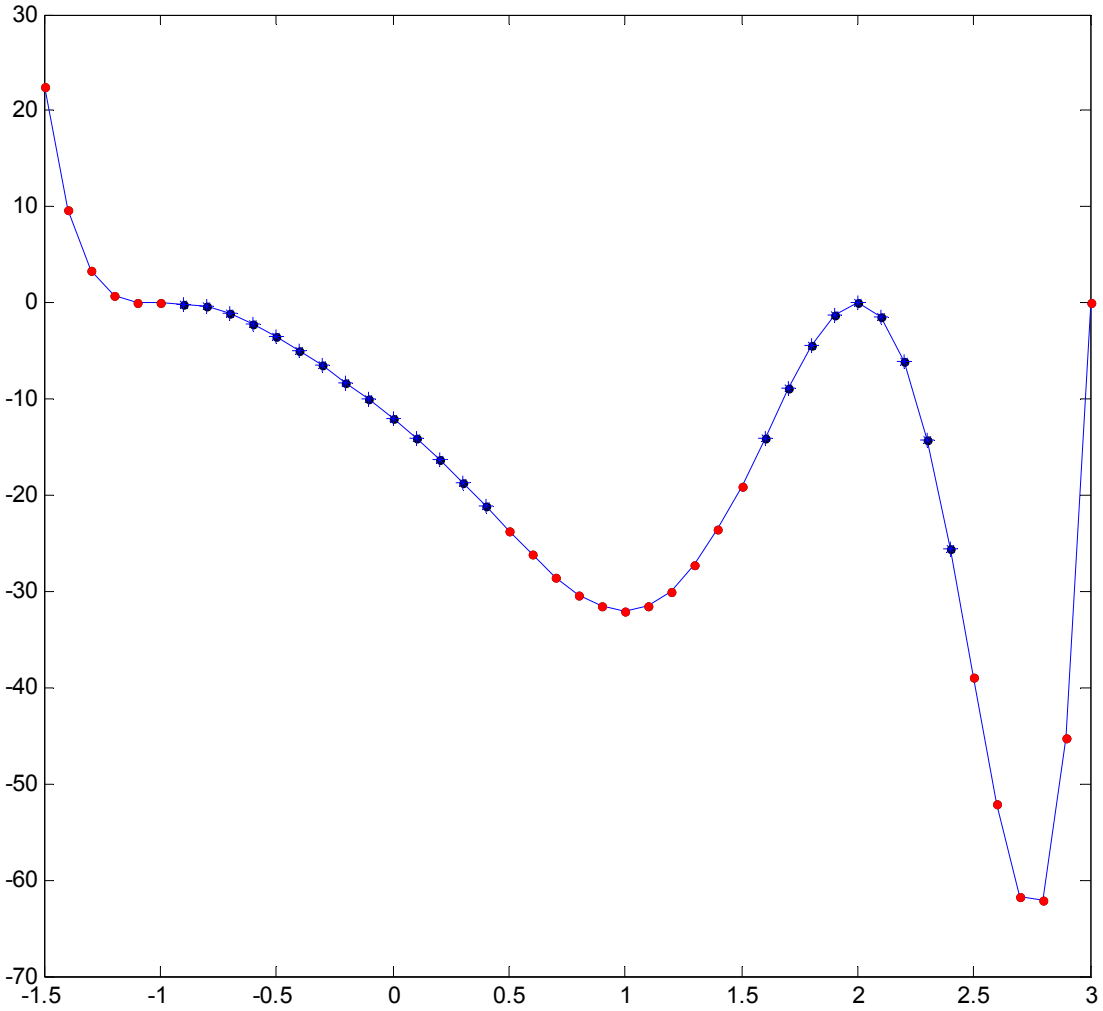

(b) Data points groups (Convex group " . ", Concave group " *")

To solve the minimization problem the convex group is selected. By applying the subtractive clustering technique, the number of clusters with the clusters' centers are calculated as shown in Fig. (3.9.c). The clustering technique gives three clusters with three centers as shown in table (3.9).

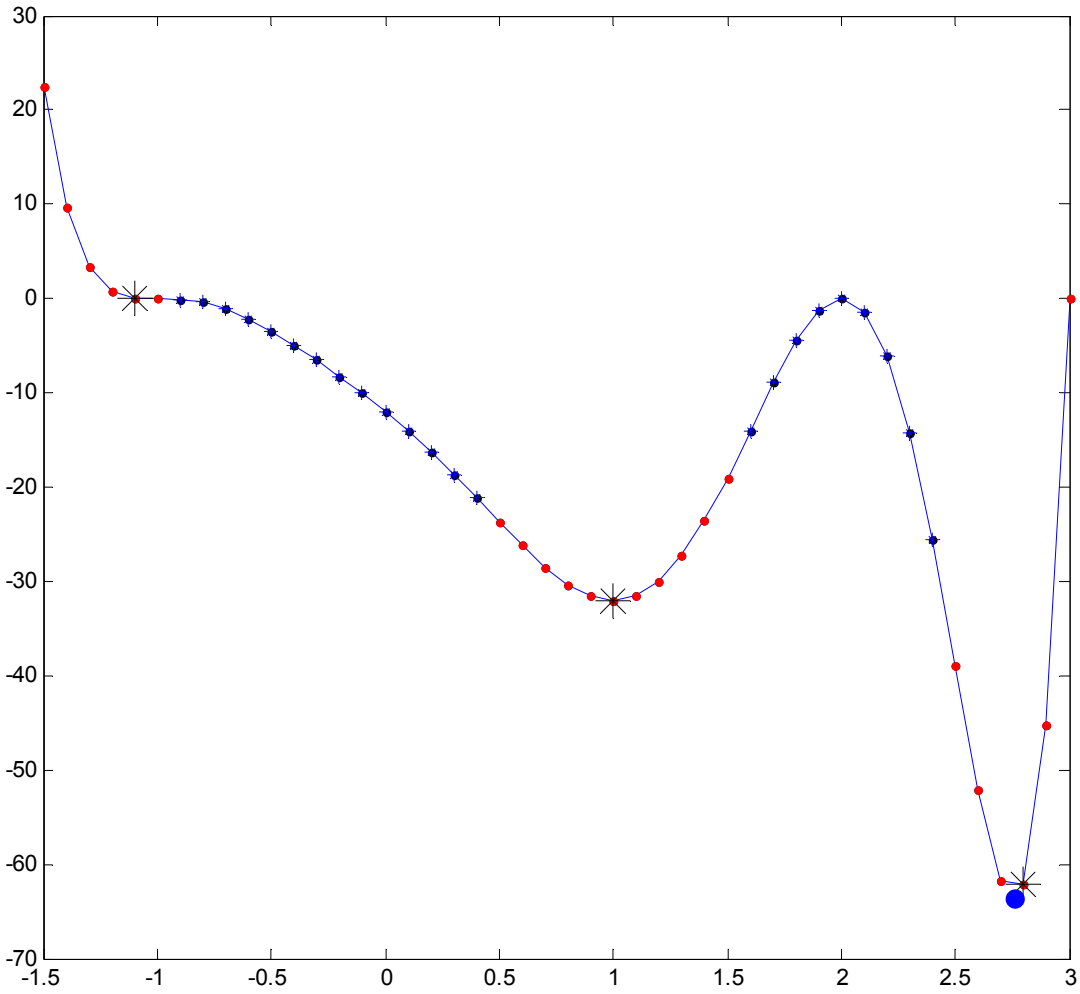

(c) The center point of each cluster "*", and the global minimum point "●".

Figure (3. 9). Curve fourth case study.

Table (3. 9). Case study IV clusters centers.

	x	F(x)
1	-1.1	0.087
2	1	-32
3	2.8	-62.089

Using the clusters' centers as initial points in Quasi-Newton algorithm, the exact local minima are calculated as illustrated in table (3.10).

Table (3. 10). Case study IV exact local minima.

	x	f(x)
1	-0.998	0.004
2	1	-32
3	2.755	-63.516

The smaller value of the f(x) represents the global minimum of the objective function as shown in table (3.10).

3.5.2 Two variables objective function case studies

3.5.2.1 Case study I

In the first case study, the objective function as shown in equation (3.22.a), and the working space constraints are the variables boundaries as inequality constraints. Fig. (3.10.a) shows the data points coming from gridding the objective function. By testing the data points' curvature, they are grouped into four groups as shown in Fig. (3.10.b).

$$f(x,y) = \frac{1}{3}xye^{\left((-2x^2-\frac{1}{2}y^2+\frac{1}{2}y)/1000\right)} \tag{3.22.a}$$

Such that

$$\begin{aligned} -100 \geq x \geq 100 \\ -100 \geq y \geq 100 \end{aligned} \tag{3.22.b}$$

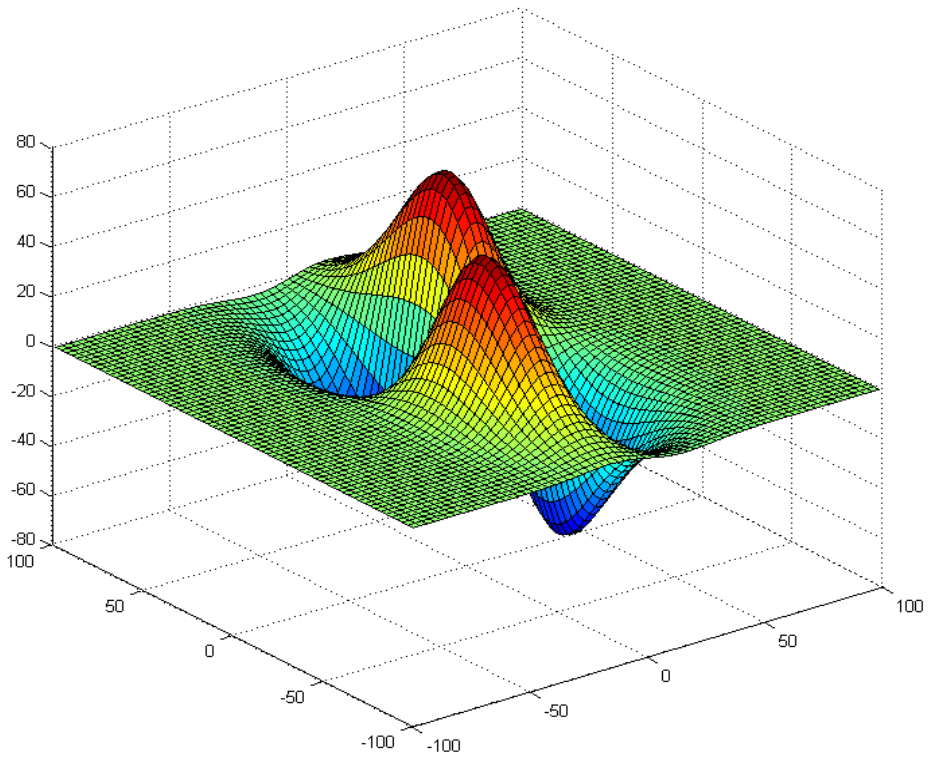

(a) First case study data points.

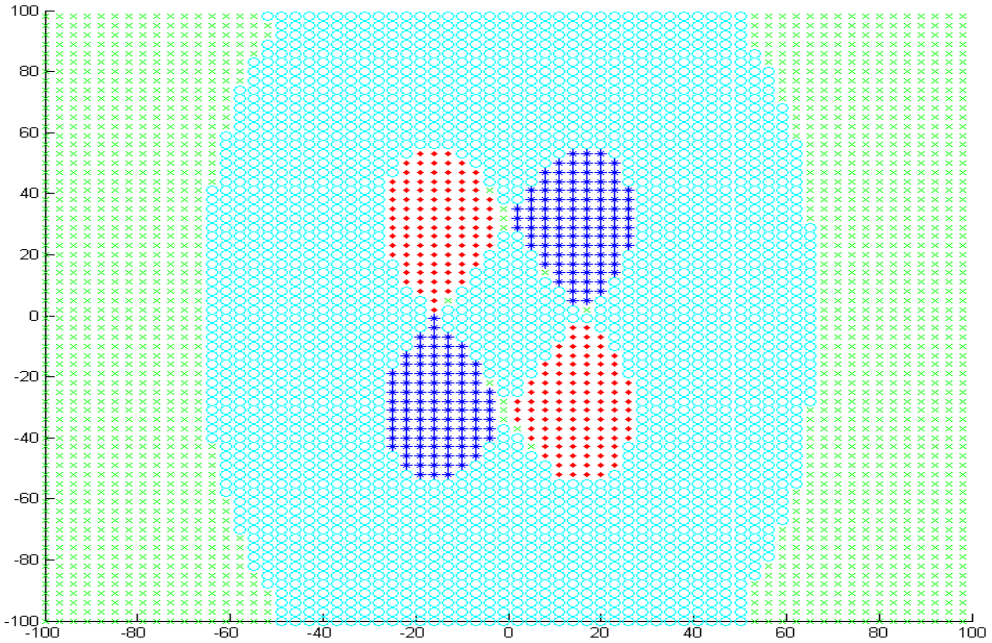

(b) Data points groups (Convex group " . ", Concave group " * ", hyperbolic group " o ", and plane group " x ").

For a minimization problem the convex group is selected. By applying the subtractive clustering technique, the number of clusters with the clusters' centers are calculated as shown in Fig. (3.10.c). The clustering technique gives two clusters with two centers as shown in table (3.11).

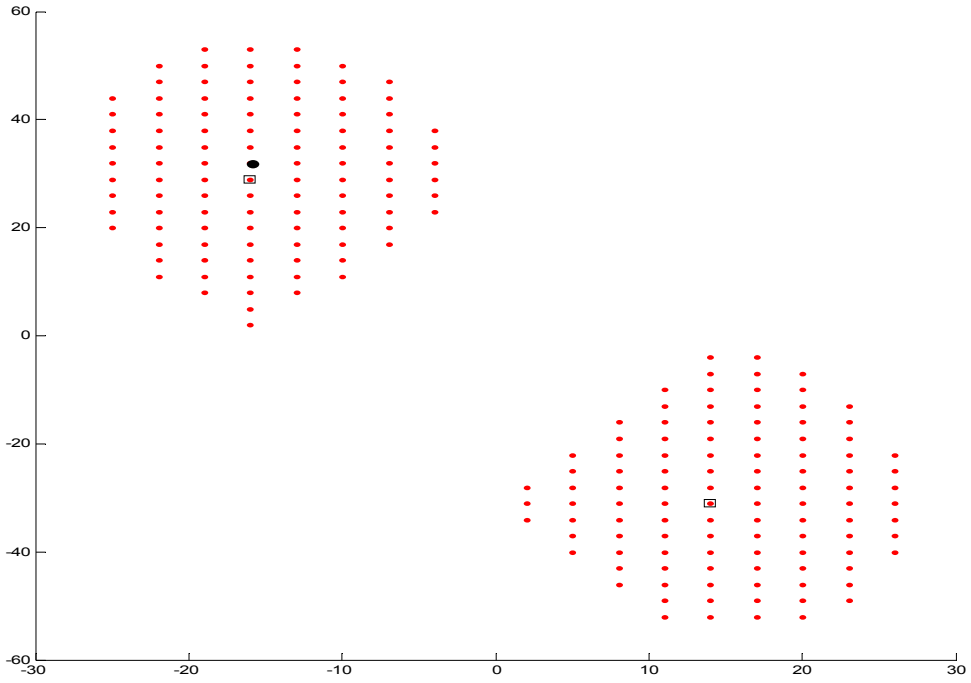

(c). Convex data points clusters with the clusters centers "□" and the global minimum point "●'

Figure (3. 10). Surface first case study.

Table (3. 11). Case study I clusters centers.

	x	y
1	14	-31
2	-16	29

Using the clusters centers as initial points in Quasi-Newton algorithm, the exact local minima are calculated as illustrated in table (3.12).

Table (3. 12). Case study I exact local minima.

	x	y	f(x,y)
1	15.8114	-31.8738	-62.3552
2	-15.8114	31.8738	-62.2943

The smaller value of the f(x,y) represents the global minimum of the objective function as shown in table (3.12).

3.5.2.2 Case study II

The objective function

$$f(x,y) = 3(1-x)^2 e^{-x^2-(y+1)^2} - (2x - 10x^3 - 10y^5)e^{-x^2-y^2} - 0.3e^{(-x-1)^2 y^2} \qquad (3.23.a)$$

Such that

$$\begin{aligned} -3.5 \geq x \geq 3.5 \\ -3.5 \geq y \geq 3.5 \end{aligned} \qquad (3.23.b)$$

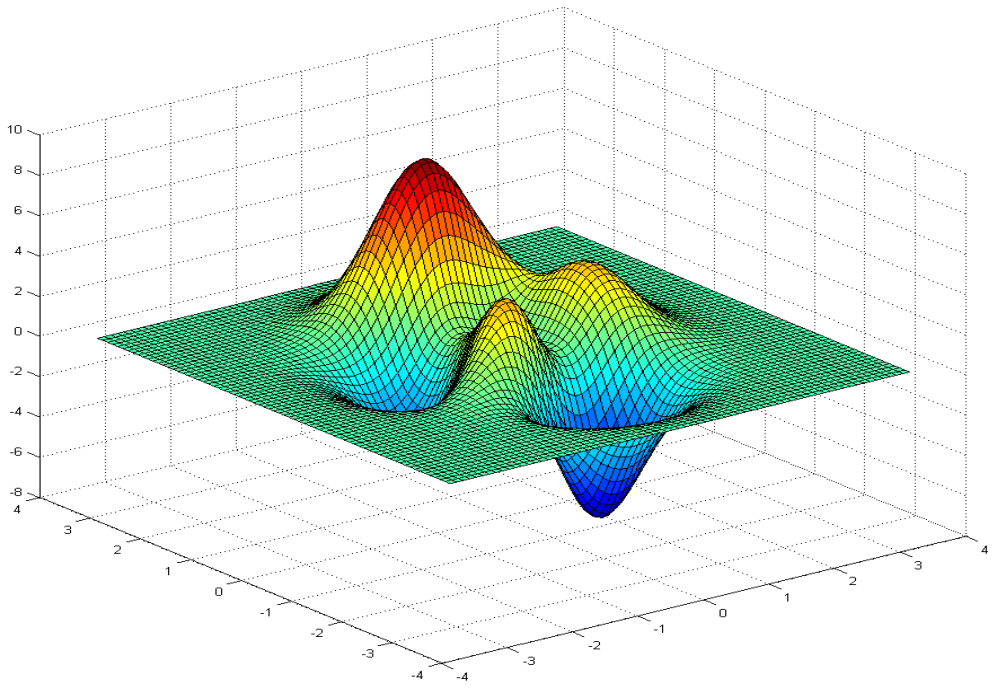

(a) Second case study data points.

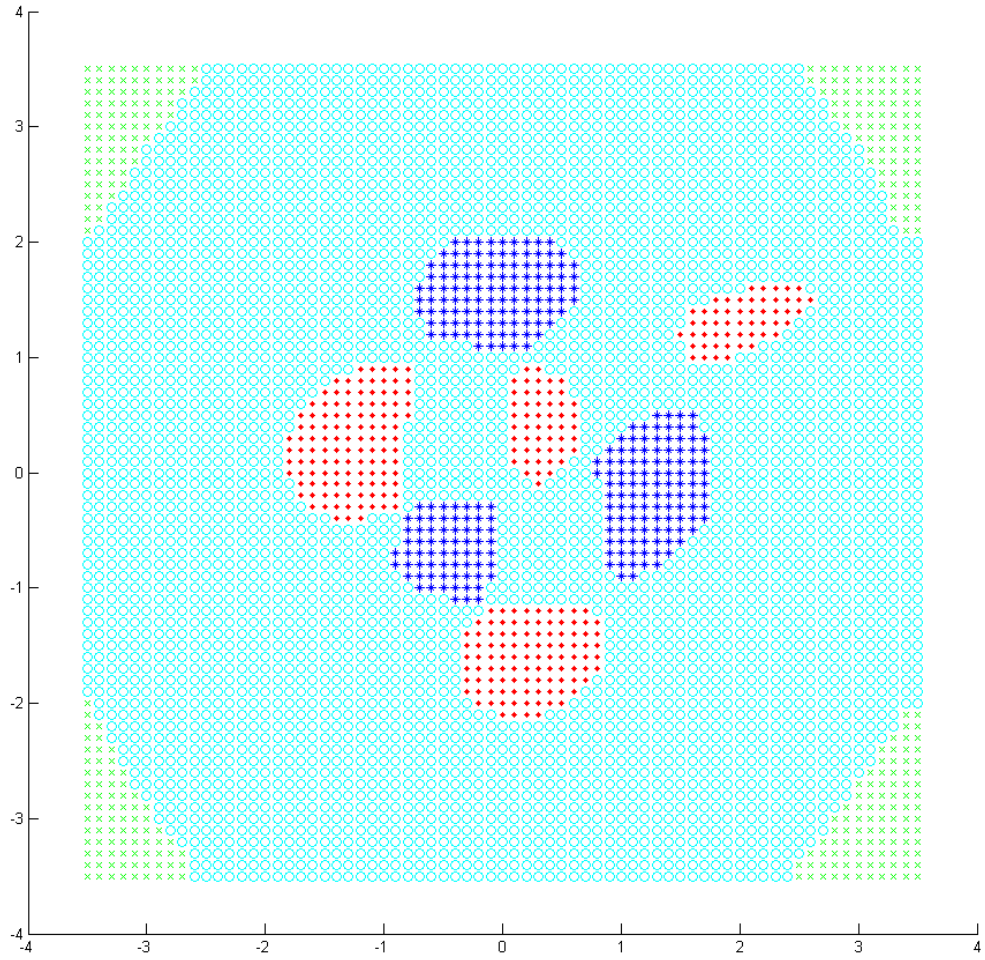

(b) Data points groups (Convex group " . ", Concave group " * ", hyperbolic group " o ", and plane group " x ").

For solving the minimization problem the convex group is selected. By applying the subtractive clustering technique, the number of clusters with the clusters' centers are calculated as shown in Fig. (3.11.c). The clustering technique gives four clusters with four centers as shown in table (3.13).

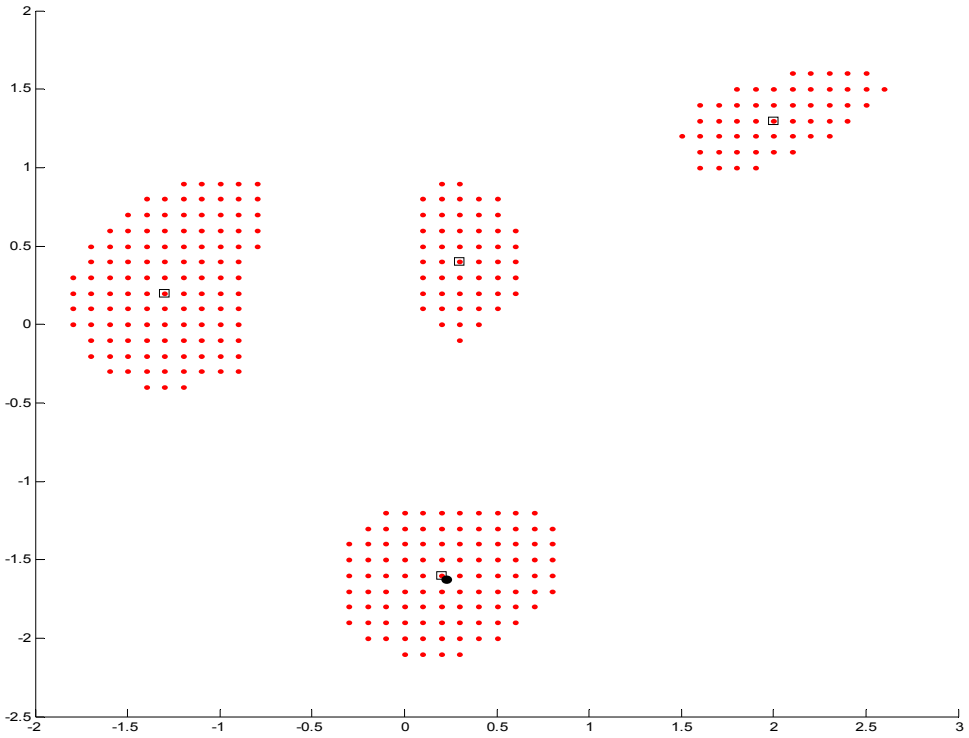

(c) Convex data points clusters "." with the clusters centers "□" and the global minimum point "●"

Figure (3. 11). Surface second case study.

Table (3. 13). Case study II clusters centers.

	x	y
1	0.2	-1.6
2	-1.3	0.2
3	2	1.3
4	0.3	0.4

Using the clusters' centers as initial points in Quasi-Newton algorithm, the exact local minima are calculated as illustrated in table (3.14).

Table (3. 14). Case study II exact local minima.

	x	y	f(x,y)
1	0.2283	-1.6255	-6.511
2	-1.3474	0.2045	-3.0498
3	4.1981	2.2898	0
4	0.2964	0.3202	-0.0649

The smaller value of the f(x,y) represents the global minimum of the objective function as shown in table (3.14).

3.5.2.3 Case study III

The objective function

$$f(x,y) = 4x^2 - 2x^4 + \frac{1}{3}x^6 + xy - 4y^2 + 4y^4 \qquad (3.24.a)$$

Such that

$$\begin{aligned} -2 \geq x \geq 2 \\ -1 \geq y \geq 1 \end{aligned} \qquad (3.24.b)$$

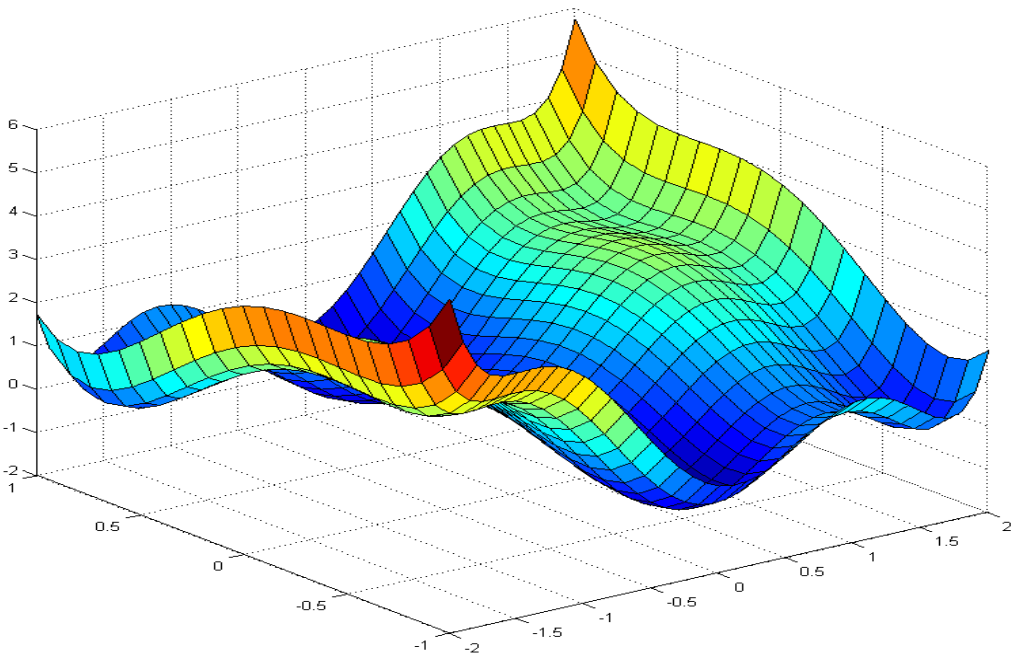

(a) Third case study data points.

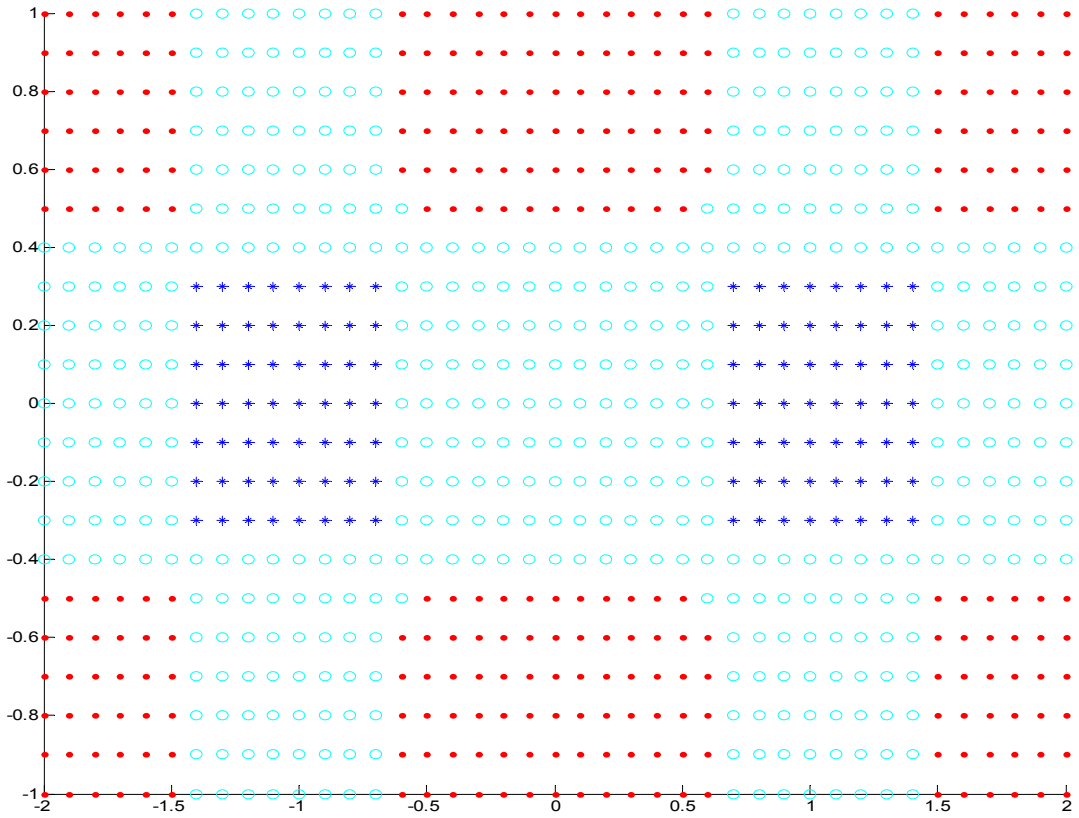

(b) Data points groups (Convex group " . ", Concave group " * ", hyperbolic group " o ", and plane group " x ").

To calculate the global minimum, the convex group is selected. By applying the subtractive clustering technique, the number of clusters with the clusters' centers are calculated as shown in Fig. (3.12.c). The clustering technique gives six clusters with six centers as shown in table (3.15).

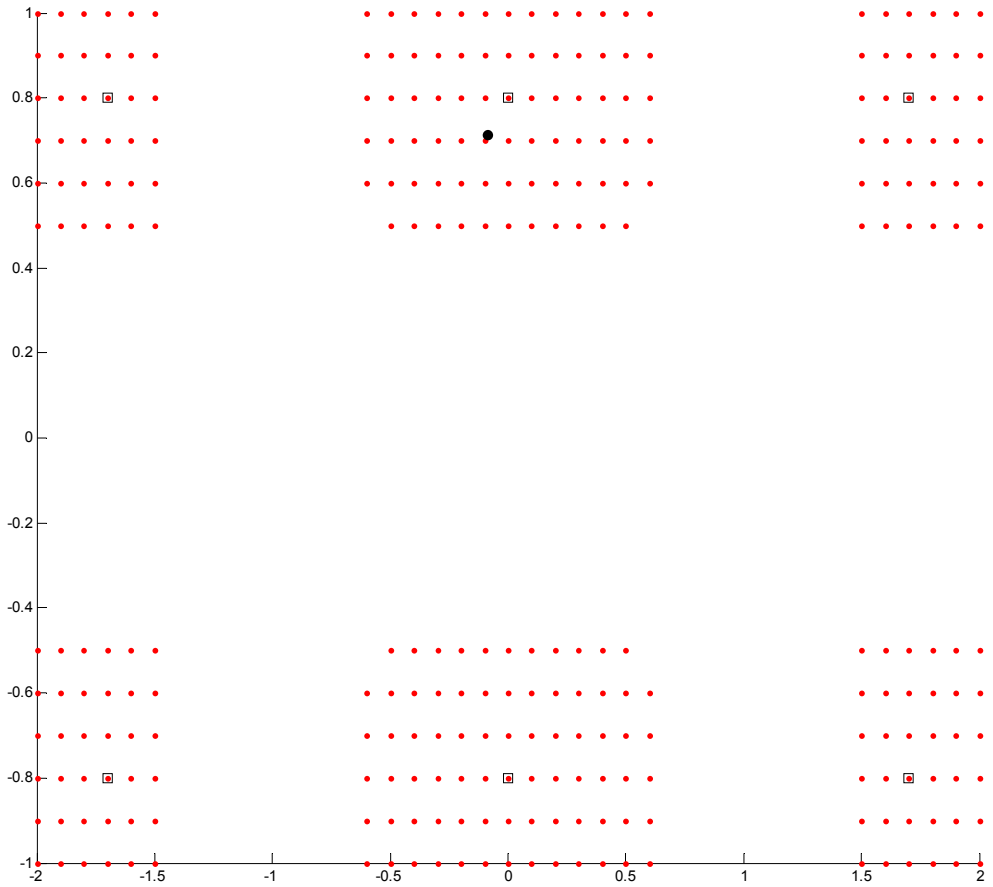

(c) Convex data points clusters "." with the clusters centers "□" and the global minimum point "●"

Figure (3. 12). Surface third case study.

Table (3. 15). Case study III clusters centers.

	x	y
1	0	0.8
2	0	-0.8
3	1.7	0.8
4	-1.7	0.8
5	1.7	-0.8
6	-1.7	-0.8

Using the clusters' centers as initial points in Quasi-Newton algorithm the exact local minima are calculated as illustrated in table (3.16).

Table (3. 16). Case study III exact local minima.

	x	y	f(x,y)
1	-0.089	0.712	-1.031
2	-0.089	-0.712	-0.903
3	1.703	0.796	-0.215
4	-1.703	0.796	-0.215
5	1.703	-0.796	-0.215
6	-1.703	-0.796	-0.215

The smaller value of the f(x,y) represents the global minimum of the objective function as shown in table (3.16).

3.5.2.4 Case study IV

The objective function

$$f(x,y) = 5\sin(\frac{\pi x}{30})\sin(\frac{\pi y}{30})e^{\frac{x}{30}} \tag{3.25.a}$$

Such that

$$\begin{aligned} -60 \geq x \geq 60 \\ -60 \geq y \geq 60 \end{aligned} \tag{3.25.b}$$

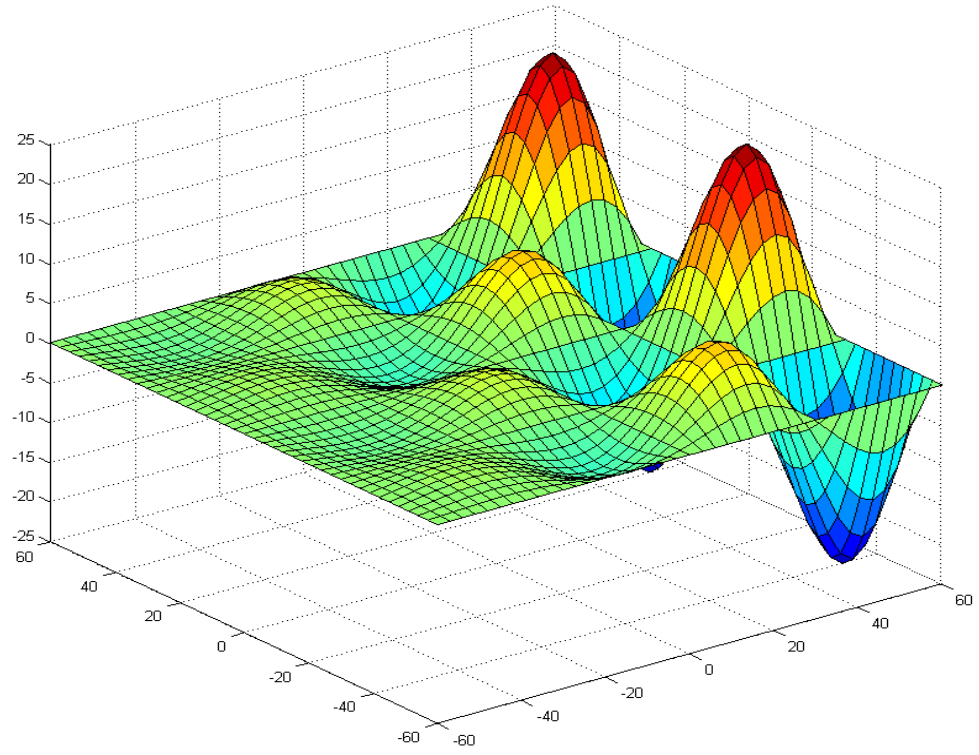

(a) Fourth case study data points.

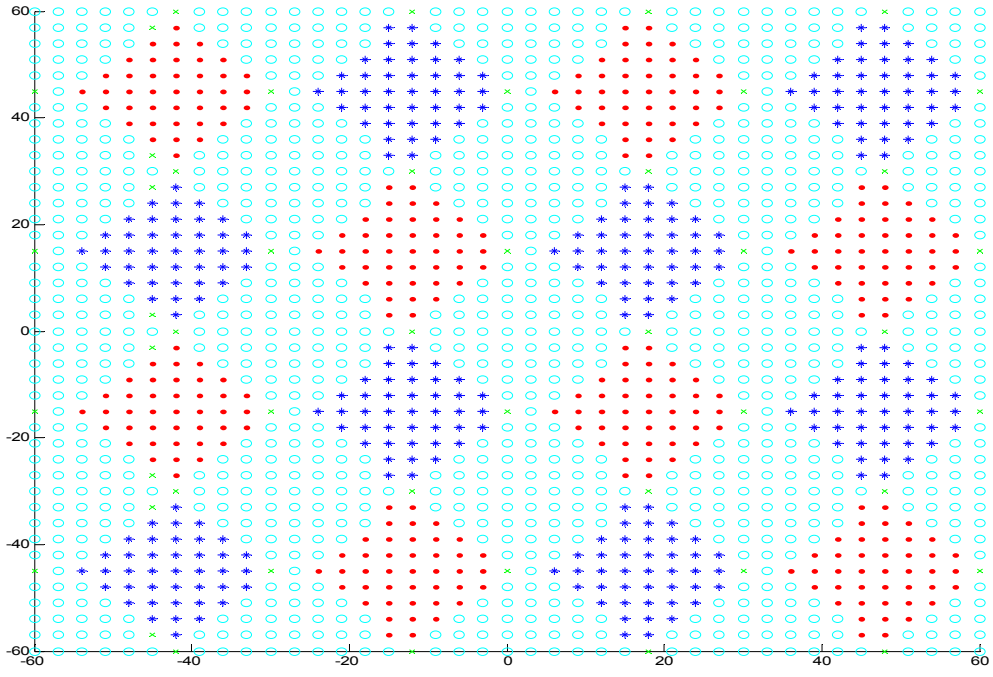

(b) Data points groups (Convex group " . ", Concave group " * ", hyperbolic group " o ", and plane group " x ").

Similar to the previous case studies, for solving the minimization problem the convex group is selected. By applying the subtractive clustering technique, the number of clusters with the clusters' centers are calculated as shown in Fig. (3.13.c). The clustering technique gives eight clusters with eight centers as shown in table (3.17).

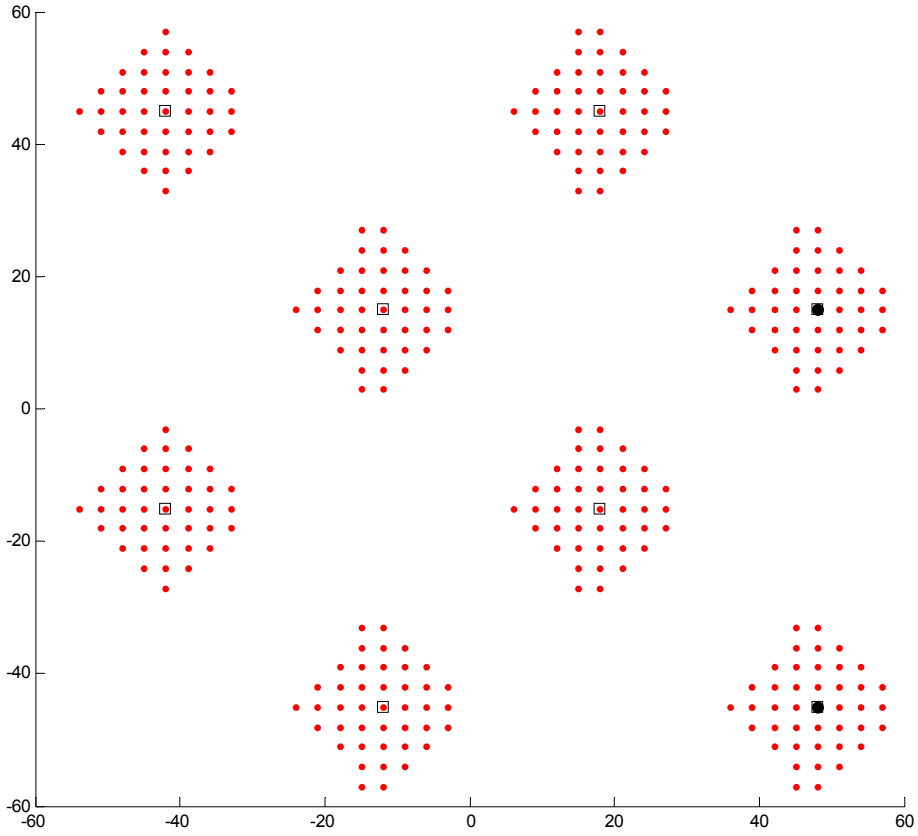

(c) Convex data points clusters "." with the clusters centers "□" and the global minimum point "●"

Figure (3. 13). Surface fourth case study.

Table (3. 17). Case study III clusters centers.

	x	y
1	18	-15
2	-12	15
3	18	45
4	-12	-45
5	48	15
6	48	-45
7	-42	-15
8	-42	45

Using the clusters' centers as initial points in Quasi-Newton algorithm, the exact local minima are calculated as illustrated in table (3.18).

Table (3. 18). Case study III exact local minima.

	x	y	f(x,y)
1	17.942	-14.99	-8.664
2	-12.057	14.99	-3.187
3	17.942	44.99	-8.664
4	-12.057	-44.99	-3.187
5	47.942	14.99	-23.553
6	47.942	-44.99	-23.553
7	-42.057	-14.99	-1.172
8	-42.057	44.99	-1.172

The smaller value of the f(x,y) represents the global minimum of the objective function. In this case, the algorithm gives two locations for the same value global minimum which cannot be detected by any other algorithms.

3.5.3 Comparison between our approach and PSO

The pre-mentioned case studies are solved by using the particle swarm optimization (PSO) algorithm in order to make a comparison with the results obtained by using our approach, as shown in table (3.19).

Table (3. 19). Comparison between our approach and PSO

One variable objective functions									
	The new approach				PSO				
	x	-	f(x)	Time (sec)	x	-	f(x)	Time (sec)	Time saved
1	1.853	-	-54.644	1.012	1.853	-	-54.644	2.023	50 %
2	0.387	-	-2.409	0.987	0.387	-	-2.409	1.619	39 %
3	1.681	-	-6.007	1.186	0	-	0	0.88	-
4	2.755	-	-63.516	1.278	2.755	-	-63.516	2.697	52.6 %
Two variables objective functions									
	x	y	f(x,y)	Time (sec)	x	y	f(x,y)	Time (sec)	Time saved
1	-15.8114	31.8738	-62.2943	1.1447	-6	6	-11.001	0.784	-
2	0.2283	-1.6255	-6.511	1.2415	0.2828	-1.5784	-6.499	3.8226	67.5 %
3	-0.089	0.712	-1.031	1.2376	0.089	-0.7127	-1.031	2.8393	56.4 %
4	47.942	14.99	-23.553	1.2654	6	-6	-2.1099	0.829	-

From the table (3.19), it is clear that by using the new approach there is a time saving of about 50 %. Also, in some cases, the PSO algorithm gets stuck in local minimum. In the PSO algorithm, each run leads to a different solution.

3.6 Conclusion

A new global optimization algorithm is proposed to solve polynomial functions of one, or two variables by using the subtractive clustering technique. The new proposed

algorithm proves to be successful in finding the global solution for polynomial functions with one, or two variables. The results obtained from comparing the new approach with the particle swarm optimization algorithm on several case studies showed that the new approach is faster by about two times, with a very good repeatability, and has a great capability to avoid getting stuck in the local minimum.

Chapter 4

Plunge milling tool path optimization

4.1 Introduction

From the literature review; it is found that the proper cutting forces and tool path planning are important elements to improve the efficiency of the plunge milling process. Therefore our focus will be on improving the efficiency of plunge milling process by maximizing the removed material using the least number of plunging points. This will strongly reduce the total machining time, in addition to optimizing each tool path by solving the travelling salesman problem (TSP) through the use of the simulated annealing optimization technique while taking into consideration a very important aspect which is the tool availability.

In this chapter, the 2D pocket with polygon boundary area is covered with specified radii circles in two steps. (1) Fill the pocket with the minimum number of specified radii circles which are tangent to each other and/or the pocket boundary without overlapping by building an algorithm using the maximum hole degree (MHD) theory for solving the circle packing problem. (2) Cover the areas left between the non-overlapped circles by using the same specified radii. After obtaining the circle loci, the circles are grouped according to the radii. The tool path for each group is optimized by solving the travelling salesman problem (TSP) using the simulated annealing (SA) technique. By the end of this chapter,

the model will be applied on a free-form pocket boundary with an island, and sculptured surface bottom.

4.2 Circle packing mathematical model

From geometry point of view, circle packing is the circles arrangement study (equal or different sizes) on a given plain surface such that no overlapping occurs, and all circles touch each other. According to literature, the maximum hole degree method is one of the most used methods for packing non-overlapped circles inside a specified boundary. Therefore, the maximum hole degree method is adopted in our work.

The mathematical model consists mainly of two algorithms. (1) Algorithm for filling a pocket with non-overlapping circles of specified radii by applying the maximum hole degree method to solve the non-overlapped circle packing problem. (2) Algorithm for covering the gaps between the non-overlapped circles coming from the first algorithm to maintain the complete covering of the surface area with the same specified radii circles.

4.2.1 Maximum hole degree theory

Inspired from human experience in packing, the benefits of placing an object at different positions in a container are different. This can be represented by a Chinese proverb; “Gold corner, silver side, and grass middle”. It means that for packing places inside a container the corner positions possess higher values than those at the side while the side positions possess higher values than those in the middle. From the previous discussion, for each position of the circle to be placed, there is a parameter represents the benefit of this position to the hole packing configuration. This parameter is called the hole

degree, in which corners have the highest hole degree which is called corner placement. Therefore, placing circles at corner positions leads to better packing configuration. The word corner is not just the region between two of the container's boundaries but also the region formed by two circles already placed inside the container, or a circle and any of the container boundaries. With regard to applying this theory on the practical case studies, an algorithm is built.

4.2.2 Algorithm to fill a pocket with tangent circles of specified radii

The packing problem is concerned with how to pack objects with a given shape, and size, into a bounded space without overlap. Filling the pocket area with circles of specified radii has been done in several steps according to the flow chart Fig. (4.1). The main procedure is filling the pocket with the specified circles in decreasing order, where they are tangent to the existing circles and/or the pocket polygon. These steps are repeated until there is no more space is available for any of the specified circles. The decreasing order is used with regard to the plunging application. Using the bigger diameters as much as we can reduces the number of plunging places which by rule reduces the machining time.

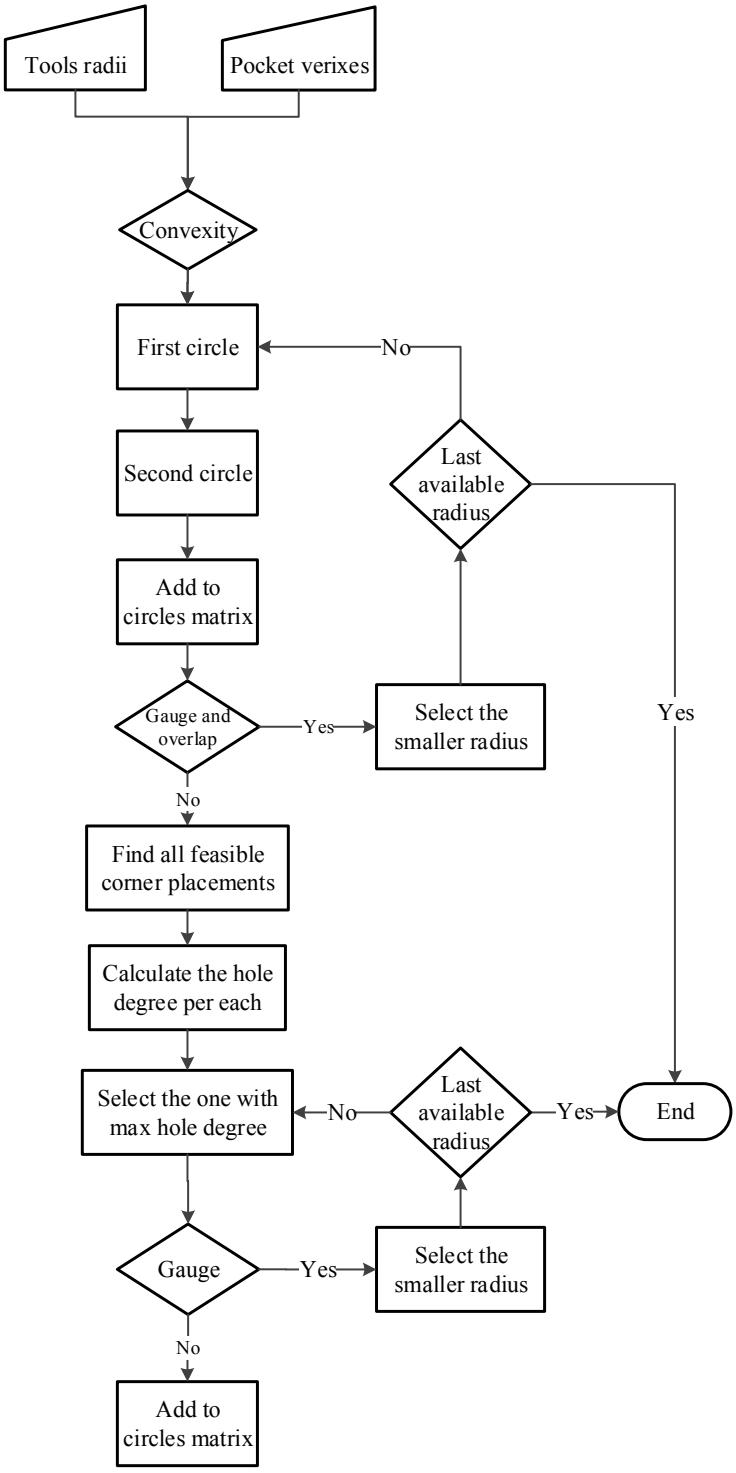

Figure (4. 1). First algorithm flow chart

4.2.2.1 Check convexity of the polygon corners

The polygon corners must be checked to know whether they are convex or concave. The convex corner is one of the candidate corner placements. The given is a polygon with its vertices ordered in a counter clock wise manner. The polygon vertices are $p_i\,(i=1,2,\ldots,n)$ as shown in Fig. (4.2). For any two edges $\overrightarrow{p_ip_{i+1}}, \overrightarrow{p_{i+1}p_{i+2}}$ since they are in xy plane, the cross product of the two edges gives the value and direction of the perpendicular in the z coordinate according to the right hand rule as shown in Fig. (4.2).

$$\overrightarrow{p_ip_{i+1}} \times \overrightarrow{p_{i+1}p_{i+2}} = \begin{cases} +z \rightarrow \text{Convex at } p_{i+1} \text{ corner} \\ -z \rightarrow \text{Concave at } p_{i+1} \text{ corner} \end{cases} \tag{4.1}$$

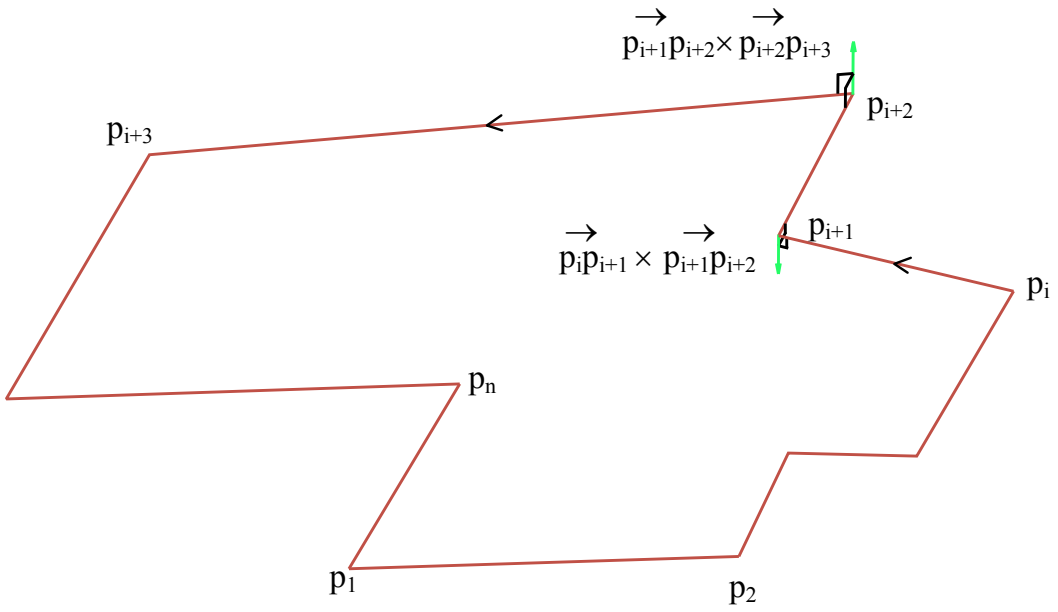

Figure (4. 2). Convexity check.

4.2.2.2 Check boundaries gauging

Gauging is not allowed in this algorithm. So, the current circle is checked for intersection with the polygon, if the intersection exists, the plunger will gauge the part. A

polygon with vertices p_i (i = 1, 2… n) and a circle with center O and radius R are shown in Fig. (4.3). The coordinates of $p_i = \begin{bmatrix} x_i \\ y_i \end{bmatrix}$, and the coordinates of $O = \begin{bmatrix} O_x \\ O_y \end{bmatrix}$. In general, the parametric equation of $\overrightarrow{p_i p_{i+1}}$ will be:

$$p(u) = \overrightarrow{p_i p_{i+1}} = p_i + u(p_{i+1} - p_i) \tag{4.2}$$

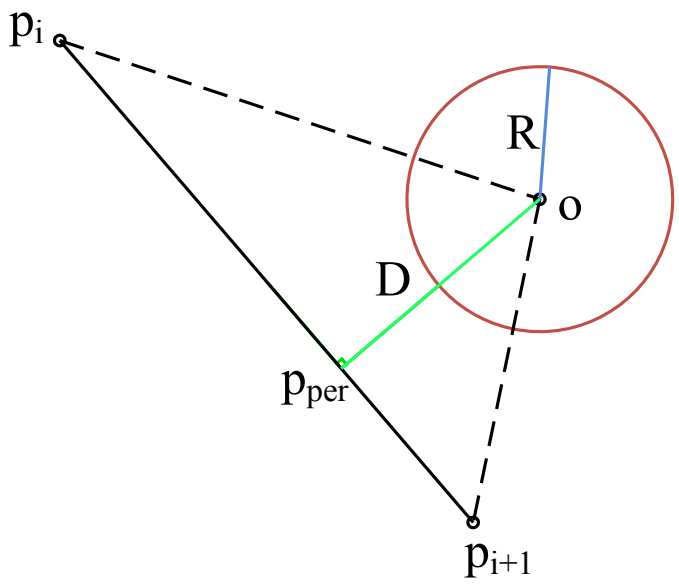

Figure (4. 3). Boundaries gauge check.

$$\overrightarrow{p_{per} O} \times \overrightarrow{p_i p_{i+1}} = 0 \tag{4.3}$$

Substituting in (4.3) with (4.2)

$$(O - p_{per}) \cdot (p_{i+1} - p_i) = 0 \tag{4.4}$$

$$\because p_{per} = p_i + u(p_{i+1} - p_i) \tag{4.5}$$

$$[O - p_i - u(p_{i+1} - p_i)] \cdot (p_{i+1} - p_i) = 0 \tag{4.6}$$

$$\left[\left(O-p_i\right)-u\left(p_{i+1}-p_i\right)\right]\cdot\left(p_{i+1}-p_i\right)=0 \tag{4.7}$$

$$\left(O-p_i\right)\cdot\left(p_{i+1}-p_i\right)-u\left(p_{i+1}-p_i\right)\cdot\left(p_{i+1}-p_i\right)=0 \tag{4.8}$$

$$\left(O-p_i\right)\cdot\left(p_{i+1}-p_i\right)-u\left|\overrightarrow{p_{i+1}-p_i}\right|^2=0 \tag{4.9}$$

The u value corresponding to the point p_{per} can be calculated as:

$$u_{per}=\frac{\left(o_x-x_1\right)\left(x_2-x_1\right)+\left(o_y-y_1\right)\left(y_2-y_1\right)}{\left|\overrightarrow{p_2-p_1}\right|^2} \tag{4.10}$$

$$x_{p_{per}}=x_1+u_{per}\left(x_2-x_1\right) \tag{4.11}$$

$$y_{p_{per}}=y_1+u_{per}\left(y_2-y_1\right) \tag{4.12}$$

The perpendicular distance from the center to $\overrightarrow{p_i p_{i+1}}$

$$D=\left|\overrightarrow{p_{per}O}\right| \tag{4.13}$$

Then gauging V_G depends on (u, D)

$$V_G=\begin{cases}0 & \left\{u\in[0,1], D>R\right\}\\ 1 & \left\{u\in[0,1], D<R\right\}\end{cases} \tag{4.14}$$

In some cases (concave corners) the perpendicular distance is less than the circle's radius but there is no gauging as shown in Fig. (4.4). The general form will then be:

$$V_G = \begin{cases} 0 & \{u \in [0,1], D > R\} \\ 1 & \{u \in [0,1], D < R\} \\ 0 & \{u \notin [0,1], |\overrightarrow{Op_i}| > R \text{ and } |\overrightarrow{Op_{i+1}}| > R\} \\ 1 & \{u \notin [0,1], |\overrightarrow{Op_i}| < R \text{ or } |\overrightarrow{Op_{i+1}}| < R\} \end{cases} \quad (4.15)$$

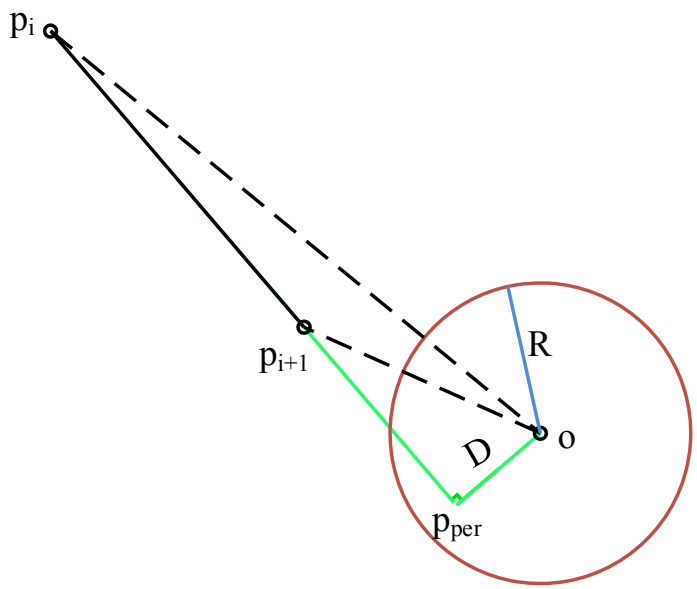

Figure (4. 4). General case.

4.2.2.3 Check circles overlap

The current circle is checked for intersection with any other circle inside the polygon. For two circles with centers O_1, O_2 and radii R_1, R_2, the center distance (D) must be checked as shown in Fig. (4.5)

$$D = |\overrightarrow{O_1O_2}| \quad (4.16)$$

Then intersection V_{int} depends on the value of (D)

$$V_{int} = \begin{cases} 0 & D > R_1 + R_2 \\ 1 & D < R_1 + R_2 \end{cases} \quad (4.17)$$

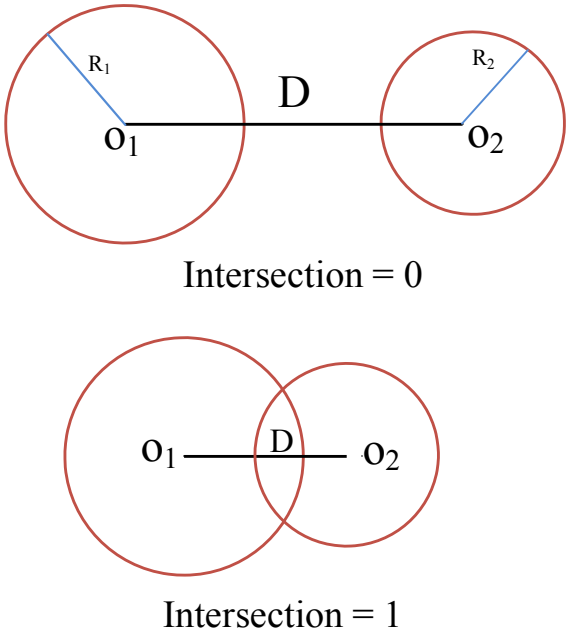

Figure (4. 5). Circles overlapping check.

4.2.2.4 Calculate the corner placements

According to the previous researches in circle packing, the corners are the best places to be packed because they give a very close packing arrangement which enable more items to be packed. The corner placement can be defined as a placement p_{cpj} of a given circle j with center point coordinates x_j , y_j , and radius r_j , is considered feasible if the circle lies completely inside the polygon (no gauging with the boundaries). A feasible placement is called a corner placement if the circle touches two items at least (i.e. two polygon edges, edge and circle or two other circles). The available corner placements to the next circle will be calculated in two cases: Case A: The current circle is tangent to one or more of the polygon edges, as shown in Fig. (4.6). Case B: The current circle is tangent to one or more of the existing circles inside the polygon, as shown in Fig. (4.7). In both cases it is given:

(1) Polygon with its vertices. (2) Circle with its location inside the polygon and its radius. (3) The radii of the circles to be packed.

Case (A)**:**

To calculate the available corner placement center (p_{cp}) in case of the current circle being tangent to one or more of the polygon sides, the polygon with its vertices are p_i (i = 1, 2… n) and a circle with center O and radius R, as shown in Fig. (4.6).

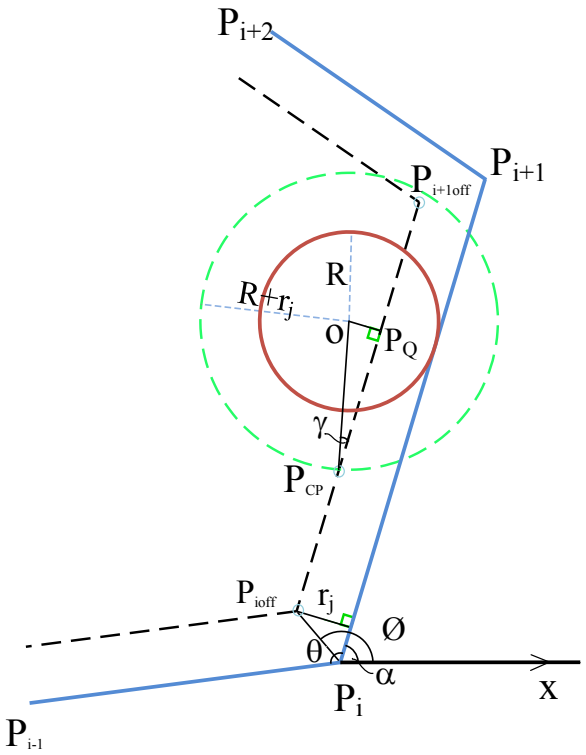

Figure (4. 6). Corner placements for a circle tangent to a boundary.

The coordinates of $p_i = \begin{bmatrix} x_i \\ y_i \end{bmatrix}$, and the coordinates of $O = \begin{bmatrix} O_x \\ O_y \end{bmatrix}$. The next circle will be with center $C = \begin{bmatrix} x_j \\ y_j \end{bmatrix}$, and radius r_j. In general, vector $\overrightarrow{p_i p_{i+1}}$ will be taken as an example. Two steps are required to calculate (p_{cp}):

(1) Calculate the offset points (p_{ioff}, p_{i+1off}) of the start and end points p_i , p_{i+1} inside the polygon:

a. Calculate the angle (θ) between $\overrightarrow{p_i p_{i+1}}$, and $\overrightarrow{p_{i-1} p_i}$

$$\overrightarrow{p_{i-1} p_i} \cdot \overrightarrow{p_i p_{i+1}} = \left|\overrightarrow{p_{i-1} p_i}\right| \left|\overrightarrow{p_i p_{i+1}}\right| \cos\theta \tag{4.18}$$

$$\theta = \cos^{-1}\left(\frac{\overrightarrow{p_{i-1} p_i} \cdot \overrightarrow{p_i p_{i+1}}}{\left|\overrightarrow{p_{i-1} p_i}\right| \left|\overrightarrow{p_i p_{i+1}}\right|} \right) \tag{4.19}$$

b. Calculate the angle (α) between $\overrightarrow{p_i p_{i+1}}$ and positive x-axis

$$x_{i+1} = x_i + \left|\overrightarrow{p_i p_{i+1}}\right| \cos\alpha \qquad 0 < \alpha < 2\pi \tag{4.20}$$

$$y_{i+1} = y_i + \left|\overrightarrow{p_i p_{i+1}}\right| \sin\alpha \tag{4.21}$$

$$\alpha = \cos^{-1}\left(\frac{x_{i+1} - x_i}{\left|\overrightarrow{p_i p_{i+1}}\right|} \right) \tag{4.22}$$

The offset point of (p_i) w.r.t the next circle with radius r_j will be (p_{ioff})

The polar angle of $\overrightarrow{p_i p_{ioff}} = \varnothing$

$$\varnothing = \alpha + \frac{\theta}{2} \tag{4.23}$$

$$\left|\overrightarrow{p_i p_{ioff}}\right| = \frac{r_j}{\sin\frac{\theta}{2}} \tag{4.24}$$

$$x_{ioff} = x_i + \left|\overrightarrow{p_i p_{ioff}}\right| \cos\varnothing \tag{4.25}$$

$$y_{ioff} = y_i + \left|\overrightarrow{p_i p_{ioff}}\right| \sin\varnothing \tag{4.26}$$

2. Calculate the corner placement center point w.r.t the radius of the next circle (r_j):

After offsetting the line $\overrightarrow{p_i p_{i+1}}$ by the value r_j inside the polygon, we get the line $\overrightarrow{p_{ioff} p_{i+1off}}$. By offsetting the circle with center O and radius R in order to have same center and radius equal to ($R+r_j$). The corner placement center points will be the intersection points between the offset circle and the line $\overrightarrow{p_{ioff} p_{i+1off}}$. To calculate the intersection points the equation $\overrightarrow{p_{ioff} p_{i+1off}}$ will be

$$Q = \overrightarrow{p_{ioff} p_{i+1off}} = p_{ioff} + v\left(p_{i+1off} - p_{ioff}\right) \qquad 0 < v < 1 \tag{4.27}$$

The dot product of the line $\overrightarrow{p_Q O}$, and $\overrightarrow{p_{ioff} p_{i+1off}}$ which are perpendicular to each other at $p_Q = 0$.

$$\left(O - Q\right)\cdot\left(p_{i+1off} - p_{ioff}\right) = 0 \tag{4.28}$$

Plugging equation (4.27) in (4.28):

$$\left[O - p_{ioff} - v\left(p_{i+1off} - p_{ioff}\right)\right]\left(p_{i+1off} - p_{ioff}\right) = 0 \tag{4.29}$$

The (v) value corresponding to the point (p_Q) can be calculated as:

$$v = \frac{(o_x - x_{iof})(x_{i+1off} - x_{ioff}) + (o_y - y_{ioff})(y_{i+1off} - y_{ioff})}{\left|\overrightarrow{p_{i+1off} - p_{ioff}}\right|^2} \tag{4.30}$$

$$x_Q = x_{ioff} + v(x_{i+1off} - x_{ioff}) \tag{4.31}$$

$$y_Q = y_{ioff} + v(y_{i+1off} - y_{ioff}) \tag{4.32}$$

and,

$$d = \left|\overrightarrow{p_Q O}\right| \tag{4.33}$$

For the triangle Δ O p_Q p_{cp}:

$$\left|\overrightarrow{p_{cp} O}\right| = R + r_j \tag{4.34}$$

$$x_Q = x_{cp} + \left|\overrightarrow{p_{cp} O}\right| .\cos\gamma.\cos\alpha \tag{4.35}$$

$$x_{cp} = x_Q - \left|\overrightarrow{p_{cp} O}\right| .\cos\gamma.\cos\alpha \tag{4.17}$$

$$y_Q = y_{cp} + \left|\overrightarrow{p_{cp} O}\right| .\cos\gamma.\ \sin\alpha \tag{4.37}$$

$$y_{cp} = y_Q - \left|\overrightarrow{p_{cp} O}\right| .\cos\gamma.\ \sin\alpha \tag{4.38}$$

γ … The angle between $\overrightarrow{p_{cp} O}$, and $\overrightarrow{p_{cp} p_Q}$.

Case (B):

To calculate the available corner placements in case of two circles are tangent to each other, as shown in Fig. (4.7). Two circles with centers (O_i, O_{i+1}) and radii (R_{i+1}, R_i) and center. The coordinates of $O_i = \begin{bmatrix} O_{xi} \\ O_{yi} \end{bmatrix}$, and the coordinates of $O_{i+1} = \begin{bmatrix} O_{xi+1} \\ O_{yi+1} \end{bmatrix}$. The next circle will be with center $p_{cp} = \begin{bmatrix} x_j \\ y_j \end{bmatrix}$ and radius r_j. To calculate the coordinates of the point p_{cp}:

1. Get the offset circle from the first circle by the value of r_j, the resultant circle will be with the same center O_i and radius $= R_i + r_j$.
2. Get the offset circle from the second circle by the value of r_j, the resultant circle will have the same center O_{i+1} and radius $= R_{i+1} + r_j$.
3. The intersection points between the resultant two offset circles will be the available corner placements centers to the next circle which can be calculated as follow:

   i. Get the cosine value of the angle θ between $\overrightarrow{O_iO_{i+1}}$ and $\overrightarrow{O_ip_{cp}}$:

$$\left|\overrightarrow{O_iO_{i+1}}\right| = R_i + R_{i+1} \tag{4.39}$$

$$\left|\overrightarrow{O_{i+1}p_{cp}}\right| = R_{i+1} + r_j \tag{4.40}$$

$$\left|\overrightarrow{p_{cp}O_i}\right| = r_j + R_i \tag{4.41}$$

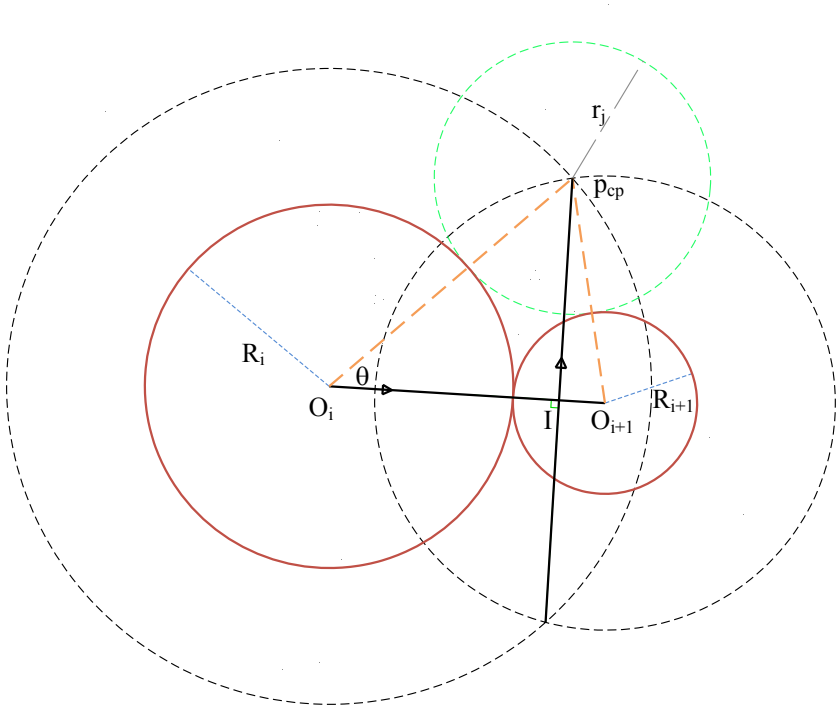

Figure (4. 7). Corner placements with other circles.

$$\cos\theta = \frac{\left|\overrightarrow{O_iO_{i+1}}\right|^2 + \left|\overrightarrow{O_ip_{cp}}\right|^2 - \left|\overrightarrow{p_{cp}O_{i+1}}\right|^2}{2\left|\overrightarrow{O_iO_{i+1}}\right|\left|\overrightarrow{O_ip_{cp}}\right|} \tag{4.42}$$

ii. Calculate the unit vector for line $\overrightarrow{O_iO_{i+1}}$ denoted by $\hat{U}$

$$\hat{U} = \frac{O_{i+1} - O_i}{\left|\overrightarrow{O_iO_{i+1}}\right|} \tag{4.43}$$

$$\hat{U} = \begin{bmatrix} U_x \\ U_y \end{bmatrix} \tag{4.44}$$

Calculate $\overrightarrow{O_iI}$

$$\left|\overrightarrow{O_iI}\right| = \left|\overrightarrow{O_ip_{cp}}\right| \cdot \cos\theta \tag{4.45}$$

From Fig. (4.7)

$$\left|\overrightarrow{O_i p_{cp}}\right| = \left(r_j + R_i\right) \tag{4.46}$$

$$\left|\overrightarrow{O_i I}\right| = \left(r_j + R_i\right) \cdot \cos\theta \tag{4.47}$$

$$\overrightarrow{O_i I} = \hat{U} \cdot \left(r_j + R_i\right) \cdot \cos\theta \tag{4.48}$$

iii. Calculate the unit perpendicular vector for line $\overrightarrow{O_i O_{i+1}}$:

$$\hat{U}_{per} = \begin{bmatrix} U_y \\ -U_x \end{bmatrix} \tag{4.49}$$

iv. Calculate the vector $\overrightarrow{Ip_{cp}}$

$$\left|\overrightarrow{Ip_{cp}}\right| = \left|\overrightarrow{O_i p_{cp}}\right| \cdot \sin\theta \tag{4.50}$$

$$\left|\overrightarrow{Ip_{cp}}\right| = \left(r_j + R_i\right) \cdot \sqrt{1 - \cos\theta^2} \tag{4.51}$$

$$\overrightarrow{Ip_{cp}} = \hat{U}_{per} \cdot \left(r_j + R_i\right) \cdot \sqrt{1 - \cos\theta^2} \tag{4.52}$$

$\therefore$ The intersection point p_{cp} can be calculated

$$p_{cp} = O_i + \overrightarrow{O_i I} + \overrightarrow{Ip_{cp}} \tag{4.53}$$

$$p_{cp} = O_i + U\left(r_j + R_i\right)\cos\theta + U_{per}\left(r_j + R_i\right)\sqrt{1 - \cos\theta^2} \tag{4.54}$$

4.2.2.5 Corner placements feasibility check

The corner placement is said to be feasible if it exists inside the polygon, and the circle with the center of this corner placement must at least touch two items inside the

polygon without intersection with any other item. To check the feasibility for the corner placement, two tests must be applied:

(a) Inside-polygon check.

(b) Circles intersection check. Given:

1. For each tangent circle and boundary there exist two corner placements.

2. For each two tangent circles there exist two corner placements.

According to the definition of the corner placement a tangency must occur between the next circle and two items inside the polygon (two circles, circle and boundary, or two boundaries).

a. The first check, inside-polygon check:

If the corner placement center is inside the polygon this means that the whole next circle will be inside the polygon according to the tangency condition. To check the corner placement center $C_j = \begin{bmatrix} x_j \\ y_j \end{bmatrix}$, if inside the polygon or not, the next steps are applied:

1. Obtain the points with the largest x-coordinate (x_{max}) and lowest x-coordinate (x_{min}) values among the polygon vertices.
2. Establish a horizontal line with a start, and an end points as:

$$\text{Start point } p_s = \begin{bmatrix} x_{min} \\ y_j \end{bmatrix}, \text{ End point } p_e = \begin{bmatrix} x_{max} \\ y_j \end{bmatrix}$$

The line equation is

$$L = p_s + u_l (p_e - p_s) \tag{4.55}$$

The horizontal line will intersect with some of the polygon boundaries.

3. Get the intersection points with the polygon boundaries $\left(p_{int} = \begin{bmatrix} x_{int} \\ y_j \end{bmatrix}, \text{int} = 1, 2, \ldots, k \right)$

k … the number of polygon boundaries.

4. The polygon boundaries general formula is

$$P = p_i + u\left(p_{i+1} - p_i\right) \tag{4.56}$$

At the intersection points the boundary line equation, and the horizontal line equation are equal

$$p_i + u\left(p_{i+1} - p_i\right) = p_s + u_l\left(p_e - p_s\right) \tag{4.57}$$

$$x_i + u\left(x_{i+1} - x_i\right) = x_{min} + u_l\left(x_{max} - x_{min}\right) \tag{4.58}$$

$$y_i + u\left(y_{i+1} - y_i\right) = y_j + u_l\left(y_j - y_j\right) \tag{4.59}$$

From (4.59):

$$u = \frac{y_j - y_i}{y_{i+1} - y_i} \tag{4.60}$$

If $u \in [0,1]$, Sub with (4.60) in (4.56)

$$p_{int} = p_i + u\left(p_{i+1} - p_i\right) \tag{4.61}$$

Since all the points have the same y_j coordinate

$$x_{int} = x_i + u\left(x_{i+1} - x_i\right) \tag{4.62}$$

If $u \notin [0,1]$, there is no intersection between this boundary and the horizontal line.

5. After obtaining all values of $x_{int}\,(int = 1,2,\ldots,k)$:

By excluding the points which have coordinates $\begin{bmatrix} x_{int} \\ y_j \end{bmatrix} = \begin{bmatrix} x_i \\ y_i \end{bmatrix}$. For the rest of x_{int} the value of C_{in} will indicate if the circle is inside or outside the polygon according to the number of intersection points with the polygon boundaries to the right and the left of the tested point (n_r, n_l)

$$C_{in} = \begin{cases} 1, (n_r, n_l) \in \{2n+1\} \\ 0, (n_r, n_l) \in \{2n\} \end{cases} \quad n = 0,1,2,... \tag{4.63}$$

$n_r \ldots$ Number of points with $x_{int} > x_j$ (to the right of the tested point)

$n_l \ldots$ Number of points with $x_{int} < x_j$ (to the left of the tested point)

Examples are illustrated in Fig. (4.8).

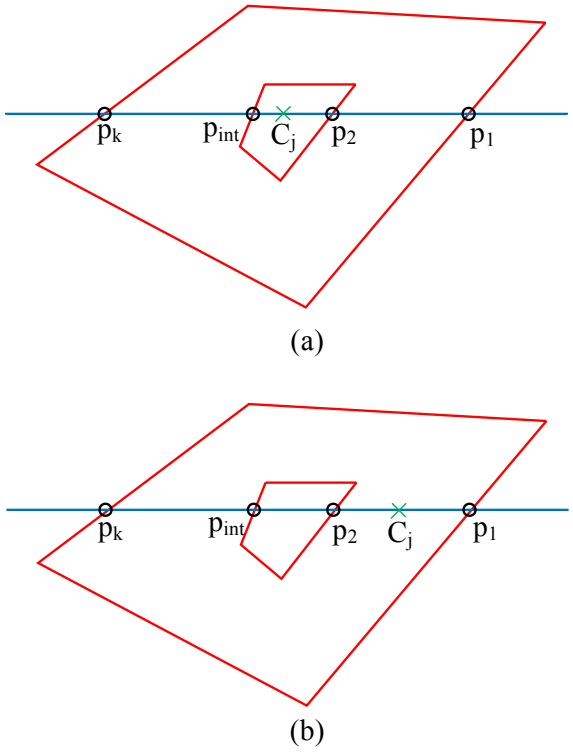

Figure (4. 8). Check point inside a polygon.

b. The second check, circle overlaps check:

In this algorithm the intersection between circles or a circle encloses by another circle is not allowed as shown in Fig. (4.9). Therefore the center of the corner placement must be checked to avoid overlap between the next circle and any of the already existing circles inside the polygon. To start the check, the distances between the center of the corner placement and the other circle centers D must be calculated:

$$D = \left|\overline{C_j O_i}\right| \tag{4.64}$$

To be sure that the intersection will not occur, the comparison between D and the value of $\left(R_i + r_j\right)$ gives the value of V_{int} which indicates the intersection

$$V_{int} = \begin{cases} 1 & D < \left(R_i + r_j\right) \\ 0 & D > \left(R_i + r_j\right) \end{cases} \tag{4.65}$$

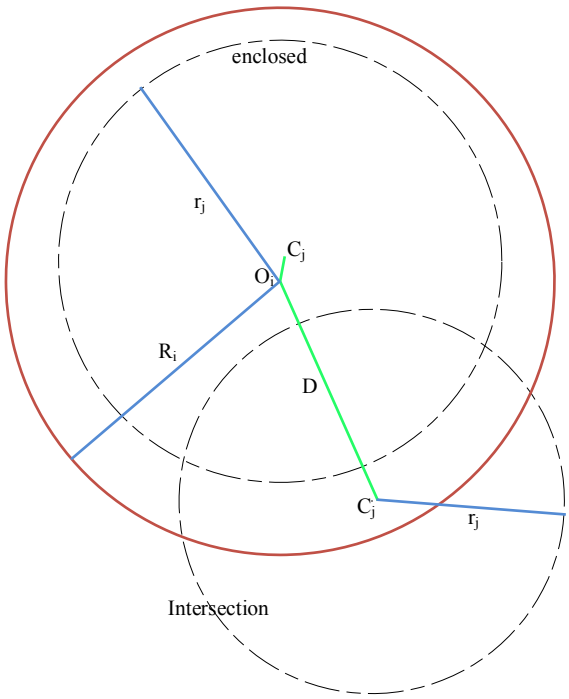

Figure (4. 9). Circles overlap check.

4.2.2.6 Max hole degree

Filling a pocket with circles of specified radii which are tangent to each other or to the pocket boundary without overlapping is based on three important concepts: (1) Corner placement. (2) Hole degree. (3) Maximum hole degree (MHD) rule. The hole degree of a corner placement indicates how close the given circle is to the other circles inside the polygon (and to the polygon boundaries). The higher the hole degree of the corner placement, the higher will be the density of the circles. Therefore, the maximum hole degree rule indicates that for a given set of possible corner placements, the placement with the maximum hole degree should be selected as the next one.

The last step is to calculate the main parameters to get the maximum holed degree value for the tested corner placement:

i. The corner placement center is pre-calculated.

ii. Hole degree (HD) of a corner placement, which can be calculated using the following steps:

1. Calculate the perpendicular distances between the corner placement center, and the pocket boundaries which will not be tangent to the coming circle at point p_B, as shown in Fig. (4.10).

$$d_{i,s_k} == \sqrt{\left(x_i - p_{Bx}\right)^2 + \left(y_i - p_{By}\right)^2} - r_i \tag{4.66}$$

2. Calculate the distances between the corner placement center, and the existing circles which will not be tangent to the coming circle, as shown in Fig. (4.10).

$$d_{i,j} = \sqrt{\left(x_i - x_j\right)^2 + \left(y_i - y_j\right)^2} - r_i - r_j \tag{4.67}$$

3. The hole degree denoted by λ can be calculate by the formula

$$\lambda = \left(1 - \frac{d_{min}}{r_i}\right) \tag{4.68}$$

d_{min}…The minimum value among all $\left(d_{i,j}, d_{i,s_k}\right)$

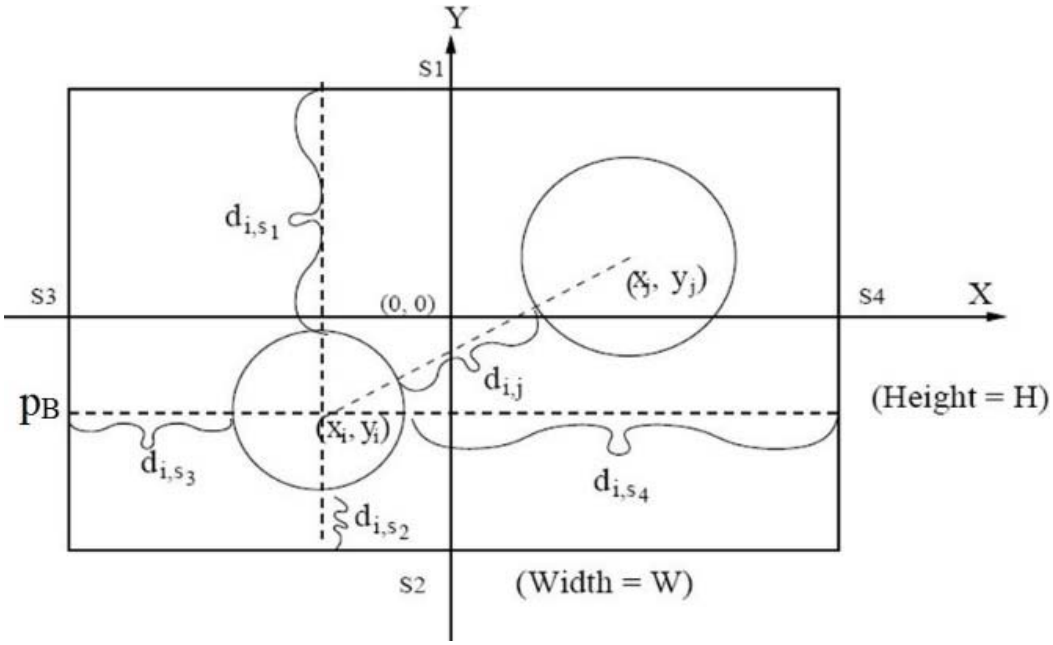

Figure (4. 10). Hole degree of a corner placement.

iii. Max hole degree (MHD) of a corner placement:

Intuitively, since the next circle should be placed as close as possible to the circles already existing inside the polygon, a packing procedure should select the corner placement having the maximum hole degree to put the next circle into the polygon. The priority is to the circle of a higher diameter should be taken into consideration.

4.2.2.7 Applications

Two case studies are illustrated for concave and convex polygons Fig. (4.11), and Fig. (4.12) by using three circles with specified radii (20, 15, 10).

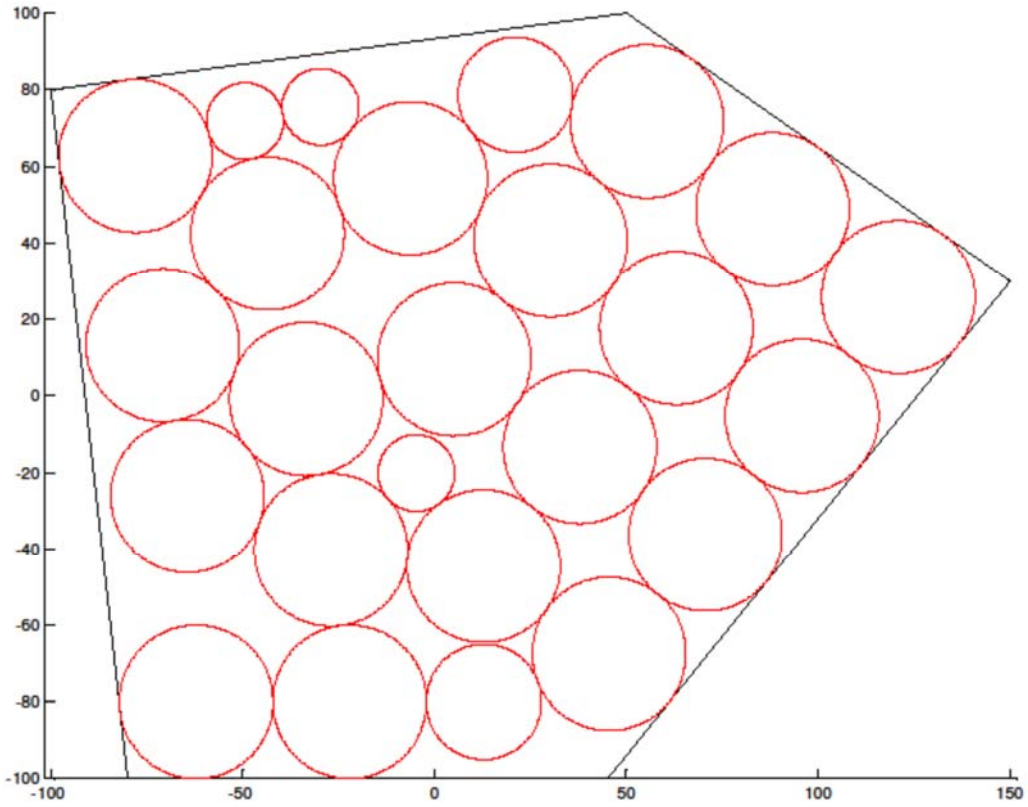

Figure (4. 11). First case study for convex polygon.

Table (4. 1). First case study results.

Circle size	R_1=20 mm	R_2=15 mm	R_3=10 mm	Covered area
No. of circles	20	2	3	75.57 %

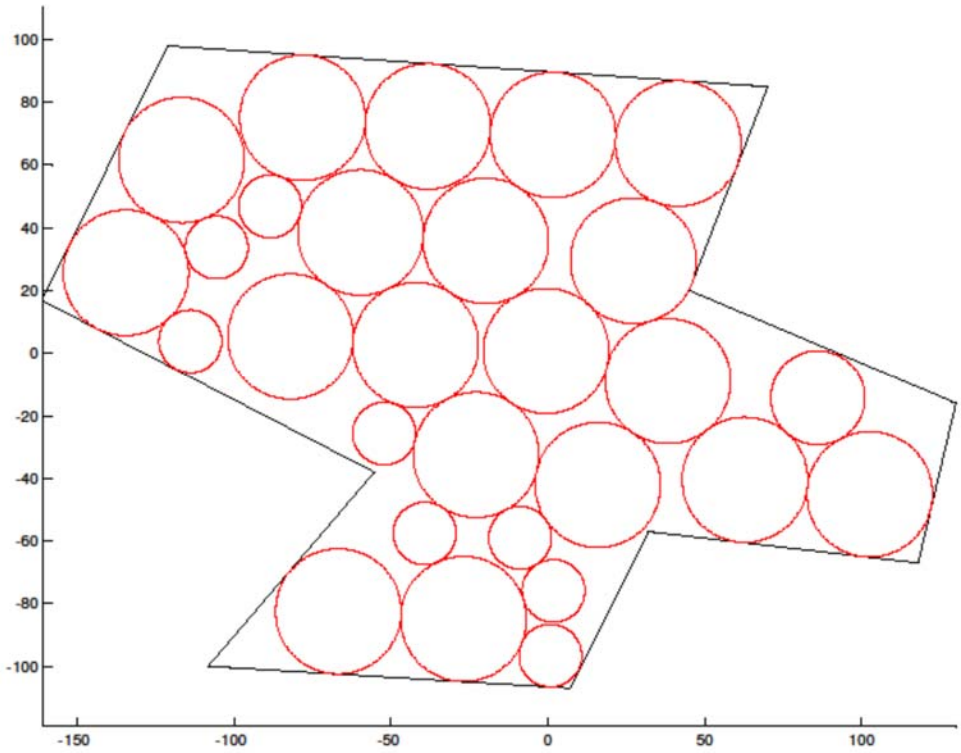

Figure (4. 12). Second case study for polygon with some concave corners.

Table (4. 2). Second case study results.

Circle size	R_1=20 mm	R_2=15 mm	R_3=10 mm	Covered area
No. of circles	19	1	8	75.53 %

4.2.3 Algorithm to cover the gaps between the non-overlapped with the minimum number of specified radii circles

For pocket machining, it is not allowed to have a material left at the middle of the pocket after the machining process. Applying the circle packing algorithm will cover the polygon area by non-overlapped circles which will leave a non-covered area between these circles. Therefore, another algorithm is proposed to cover the areas between the circles.

The input data is the non-overlapping circles radii and centers positions, the specified circles radii, and the pocket vertices as shown in the flowchart Fig. (4.13).

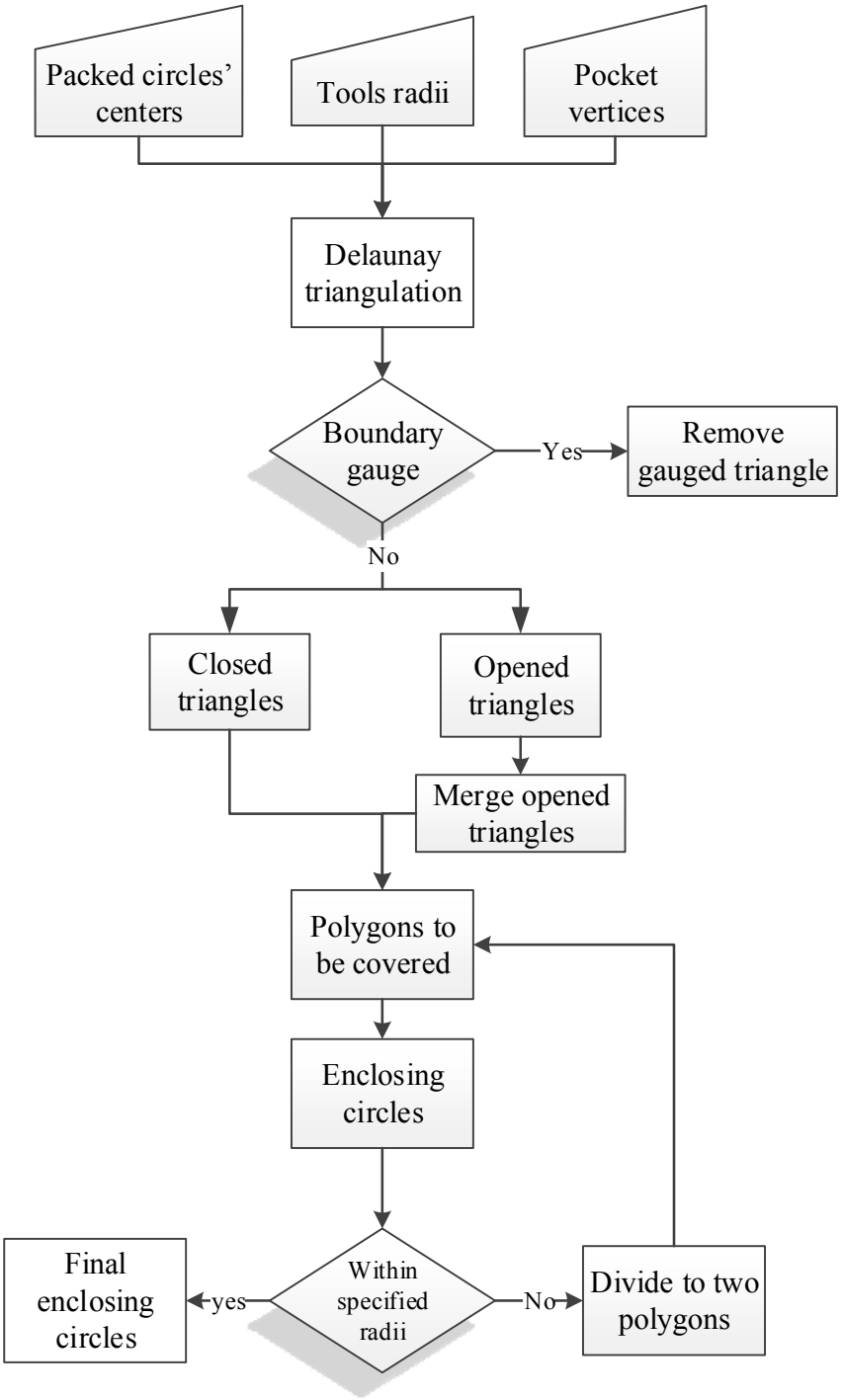

Figure (4. 13). Second algorithm flow chart

4.2.3.1 Assign the non-covered area

The non-covered area is a free area between at least three tangent circles or more. To assign the area, the smallest polygon surrounding this area is found for less calculating time. By using the centers loci, and the radii of the non-overlapped circles the steps to find the polygon are as follow:

i. The Delaunay triangulation is applied on the centers of the non-overlapping circles

Triangulation of the center points of the non-overlapping circles gives an initial description of the non-covered area. The good triangulation is the one giving triangles close to being equiangular, which is known as MaxMin angle criterion. A triangulation that is optimal in the sense of the MaxMin angle criterion and which is defined on the convex hull of a point set is called a Delaunay triangulation.

Properties of Delaunay triangulation:

1. The outer boundary must be convex hull Fig. (4.14).

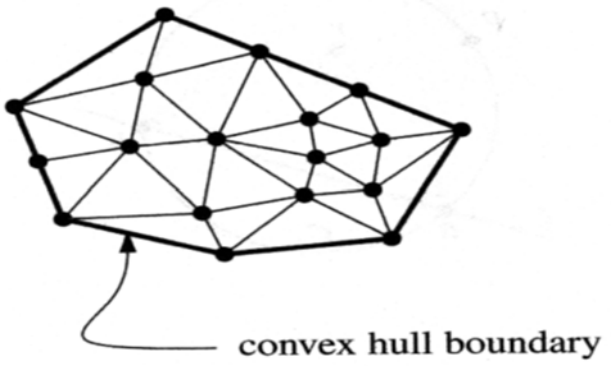

Figure (4. 14). Convex hull boundary for Delaunay triangulation.

2. A circle circumscribing any Delaunay triangle does not contain any other points in its interior. In other words, three points $p_i, p_j, p_k \in P$ are vertices of the same triangle iff the circle through p_i, p_j, p_k contains no other points of P in its interior Fig. (4.15).

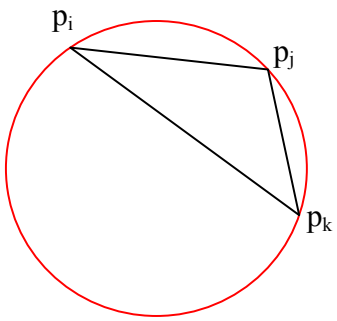

Figure (4. 15). Delaunay triangle.

3. MaxMin angle criterion is applied (Lawson's local optimization procedure 'LOP'). The Delaunay triangulation maximizes the minimum angle. Compared to any other triangulation of the points, the smallest angle in the Delaunay triangulation Fig. (4.16.b) is at least as large as the smallest angle in any other Fig. (4.16.a).

$$\min_{1 \le i \le 6} \alpha_i < \min_{1 \le i \le 6} \alpha_i' \qquad (4.69)$$

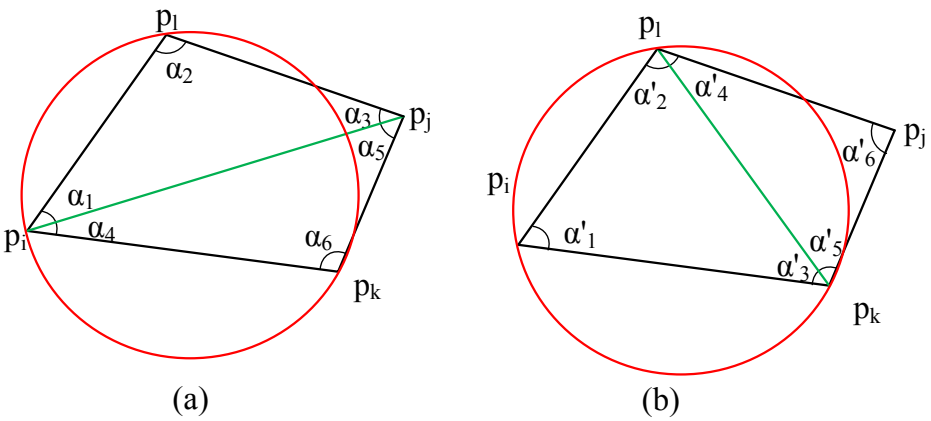

Figure (4. 16). Edge flip to find max min angle.

4. For a set of points P, the Delany triangulation data output,

$$N_{tri} = 2n - 2 - k \tag{4.70}$$

$$N_{ed} = 3n - 3 - k \tag{4.71}$$

N_{tri} … number of triangles.

N_{ed} … number of edges.

n … number of points in set P.

k … number of points on convex hull boundary of P.

ii. Classify the triangles

In order to form the polygon containing the free area between a set of tangent circles, two principles must be considered:

(1) Closed triangle which L = R1+ R2 Fig. (4.17.a).

(2) Opened triangle which L > R1+ R2 Fig. (4.17.b).

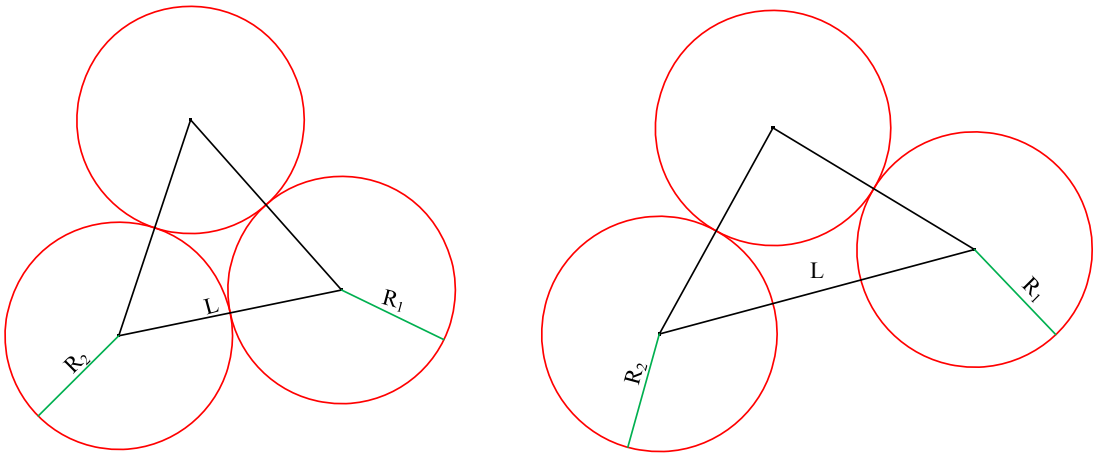

(a) Closed triangle (b) Opened triangle.

Figure (4. 17). Difference between triangles.

iii. Form the enclosing polygons

The single triangle contains the free area between three tangent circles, but for the open triangle, it has a shared link with one or two other open triangles. So the open triangles with a shared open edge Fig. (4.18.a) must be merged to obtain a closed polygon which contains the free area between a set of tangent circles Fig. (4.18.b).

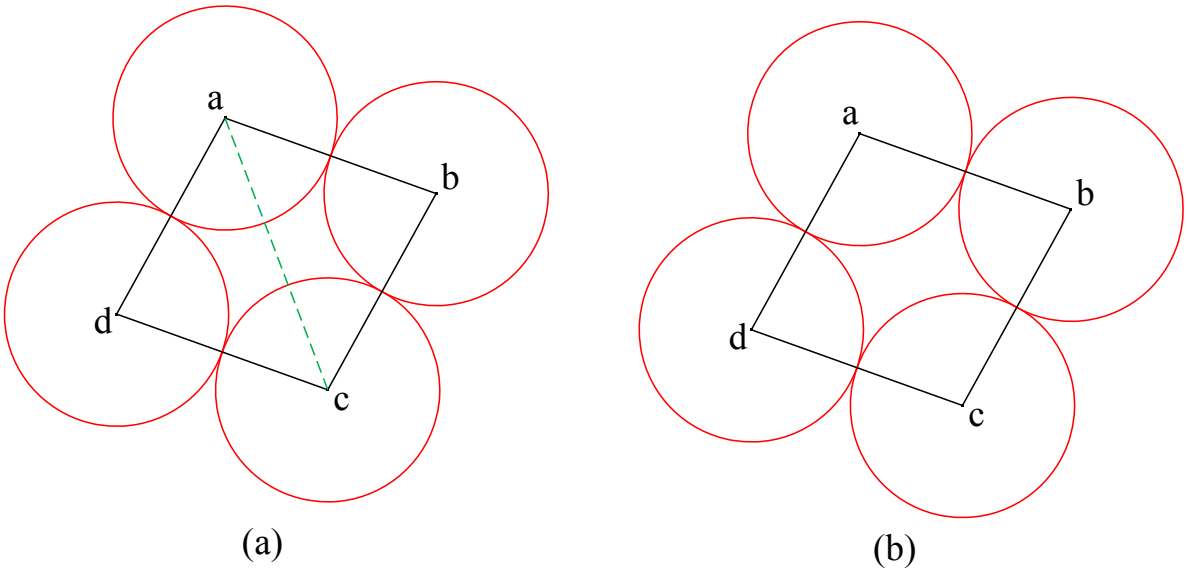

Figure (4. 18). Merging the open triangles with the shared open edge.

To get the smaller polygon which surrounds the same free area, the tangent points for the set of tangent circles are connected Fig. (4.19). For a tangent point $p \in \overline{ab}$ the coordinates are calculated:

$$u=R_1/(R_1+R_2) \tag{4.72}$$

$$p_x=a_x+u(b_x-a_x) \tag{4.73}$$

$$p_y = a_y + u(b_y - a_y) \tag{4.74}$$

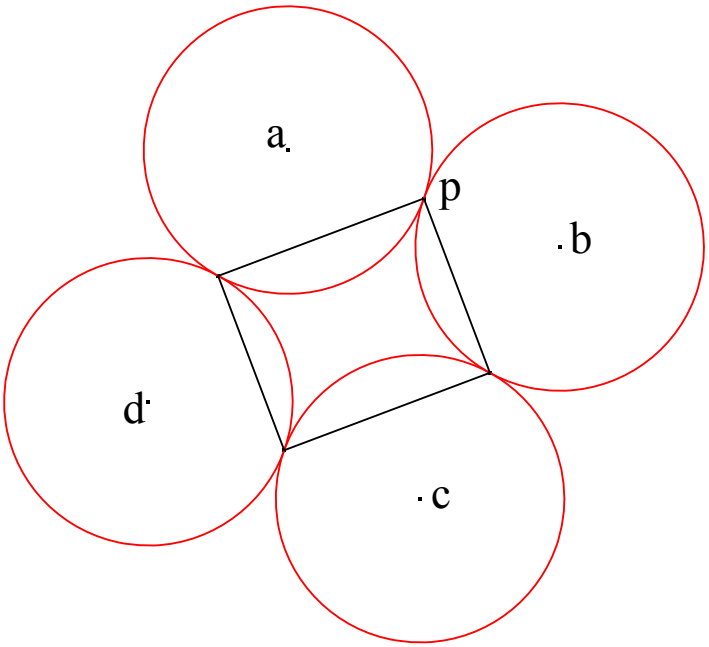

Figure (4. 19). Smaller polygon connect the tangent points.

4.2.3.2 Calculate the enclosing circle

The next step is to find out the data of the circles (radius and center point) which cover the polygons coming from the previous step. The circle data can be calculated by using the tangent points (ab, bc, cd, da) of the set of the tangent circles Fig. (4.20). Let $x_{max} = \max(ab_x, bc_x, cd_x, da_x)$, $x_{min} = \min(ab_x, bc_x, cd_x, da_x)$, $y_{max} = \max(ab_y, bc_y, cd_y, da_y)$, and $y_{min} = \min(ab_y, bc_y, cd_y, da_y)$:

$$cen_x = (x_{max} - x_{min})/2 \tag{4.75}$$

$$cen_y = (y_{max} - y_{min})/2 \tag{4.76}$$

$$R=\sqrt{(x_{max}-cen_x)^2+(y_{max}-cen_y)^2} \quad (4.77)$$

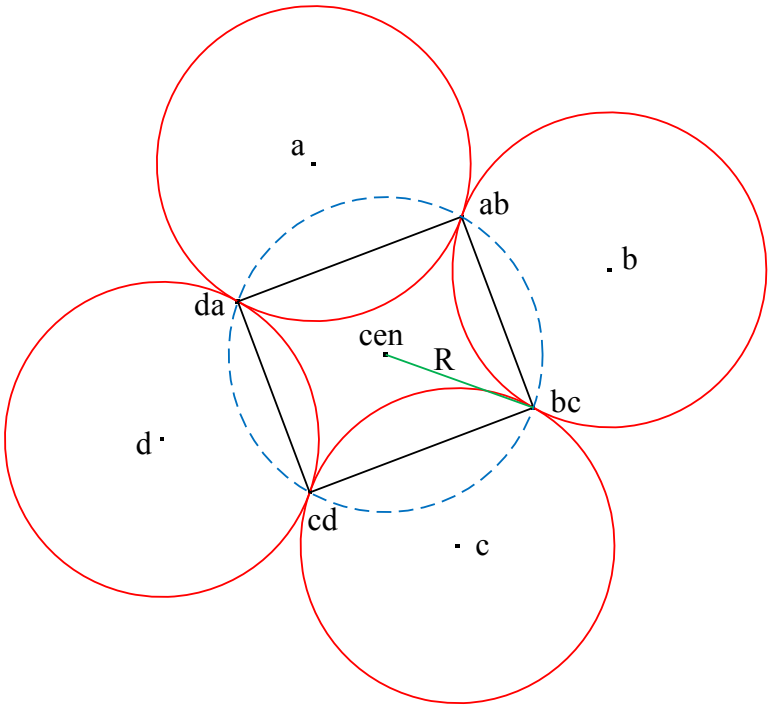

Figure (4. 20). Circle enclosing the polygon.

The circle radius is readjusted to the closest bigger value between the specified radii. If the radius of the enclosing circle is bigger than the maximum radius of the specified radii, the polygon is divided and the enclosing is done again till the covering radii are within the values of the specified radii.

4.2.3.3 Applications

By applying the second algorithm on the first, and second case studies Fig. (4.21), and Fig. (4.22).

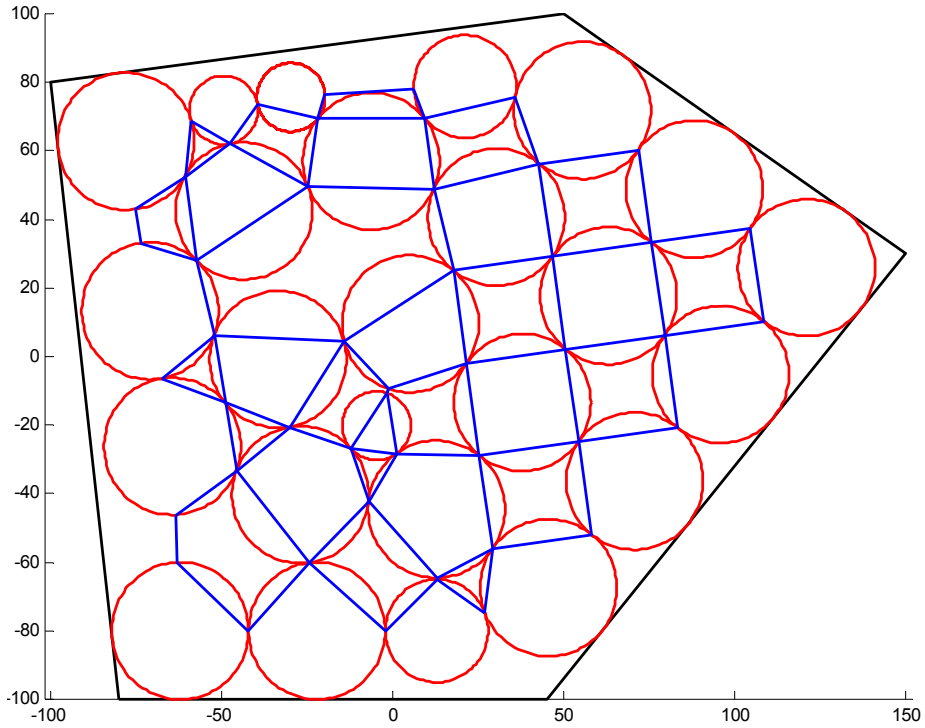

(a) Assign the non-covered area.

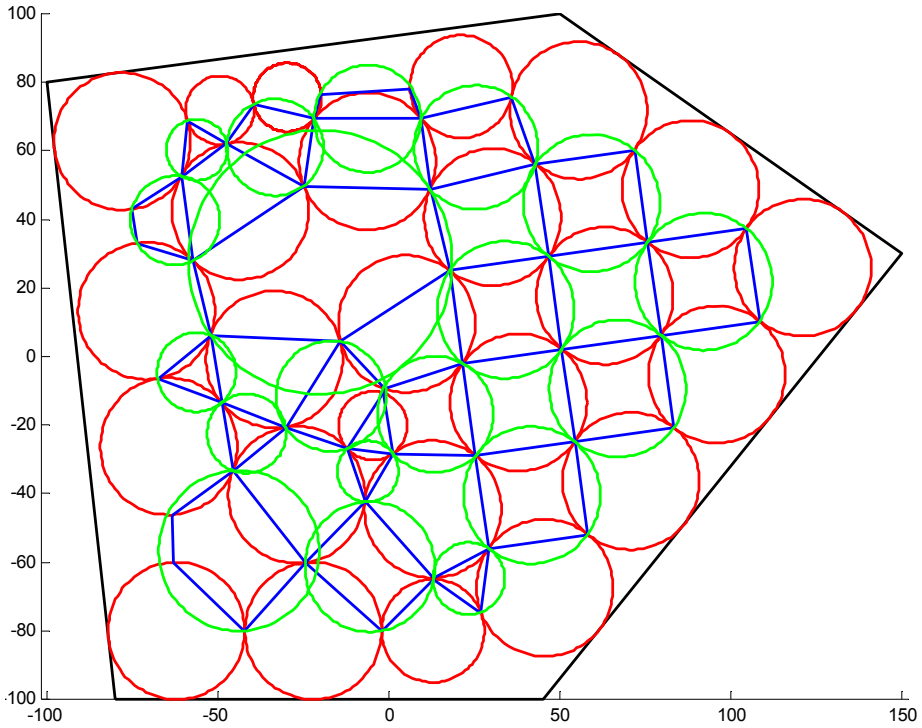

(b) Calculate the enclosing circles.

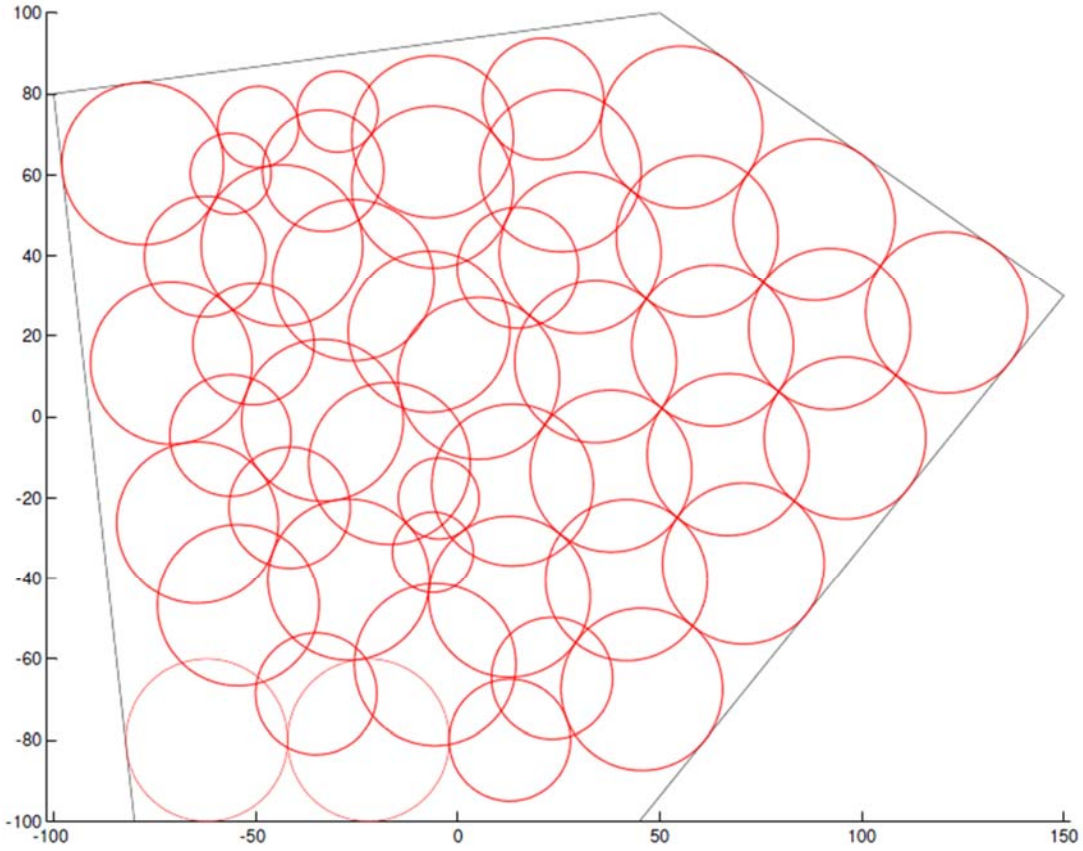

(c) Readjusting the enclosing circles.

Figure (4. 21). First case study.

Table (4. 3). First case study results.

Circle size	R_1=20 mm	R_2=15 mm	R_3=10 mm	Covered area
No. of circles	33	10	5	88.11 %

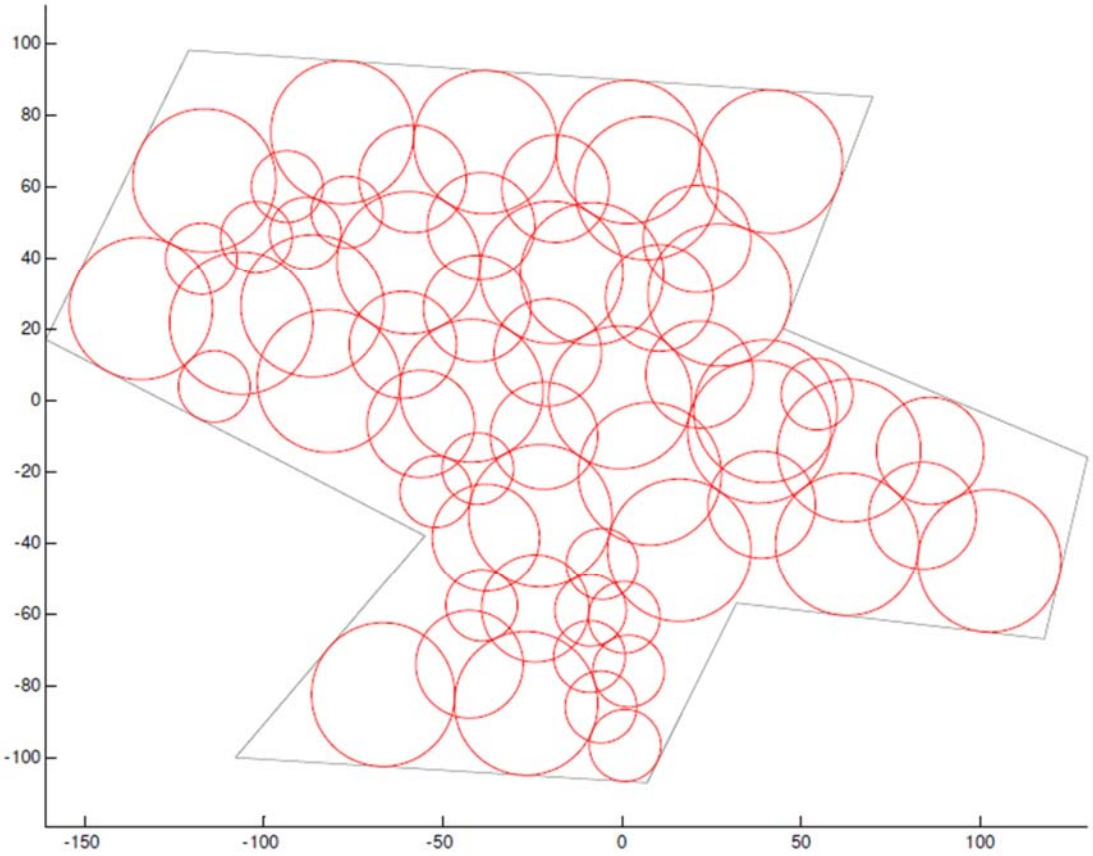

Figure (4. 22). Second case study.

Table (4. 4). Second case study results.

Circle size	R_1=20 mm	R_2=15 mm	R_3=10 mm	Covered area
No. of circles	26	17	17	84.95 %

4.3 Tool path optimization

After applying the circle packing algorithm, and covering the free area algorithm, the machining time is improved, specifically, the cutting time by finding the least number of plunging times. The coming step is to optimize the tool path which links these plunging places. By optimizing the tool path for each tool the non-cutting time will be improved.

The problem is to find the shortest path connecting the plunging places since the tool is required to visit each plunging place once, which can by formulated as a travelling sales man problem (TSP).

4.3.1 Solving travelling salesman problem (TSP) by using simulated annealing algorithm (SA)

Travelling sales man problem is represented mathematically as an optimization problem with the objective function:

$$\min \sum_{i \neq j} c_{ij} x_{ij} \tag{4.78}$$

Such that

$$\sum_{i=1, i \neq j}^{n} x_{ij} = 1 \qquad j = 1, ..., n \tag{4.79}$$

$$\sum_{j=1, i \neq j}^{n} x_{ij} = 1 \qquad i = 1, ..., n \tag{4.80}$$

According to many researchers Simulated Annealing (SA) has been successfully applied and adapted to give an approximate solution for the TSP. Simulated annealing is an optimization technique, analogous to the annealing process of metal atoms. The simulated annealing techniques were proposed by Kirkpatrick, et al, (1983). The system simulates the annealing process of metal atoms. Metal atoms at a high temperature will become unstable at their initial states, and therefore they are looking for other states. While cooling, the metal atoms will find an energy state that is lower than their initial state. The state changing procedure can be applied to solve real problems. The system generates a new state and then compares the energy of the new state with the energy of the current state. If

the energy of the new state is lower than the energy of the current state, then the system accepts this state. Otherwise, the system changes to this state according to the transition probability P, shown as follows:

$$P = e^{(-\frac{\Delta E}{kT})} \tag{4.81}$$

$$\Delta E = E(\mathrm{S}') - E(\mathrm{S}) \tag{4.82}$$

Where ‘k’ is the Boltzmann constant, ‘T’ is the current temperature of the system, ‘S’ is the current state, ‘S'’ is the new state, and ‘E’ is the energy function. If the system temperature is being cooled to a predefined temperature or the maximum number of iterations are met, the system prints out the best state, i.e., the near optimal solution. Fig. (4.23) shows the flowchart of the simulated annealing algorithm.

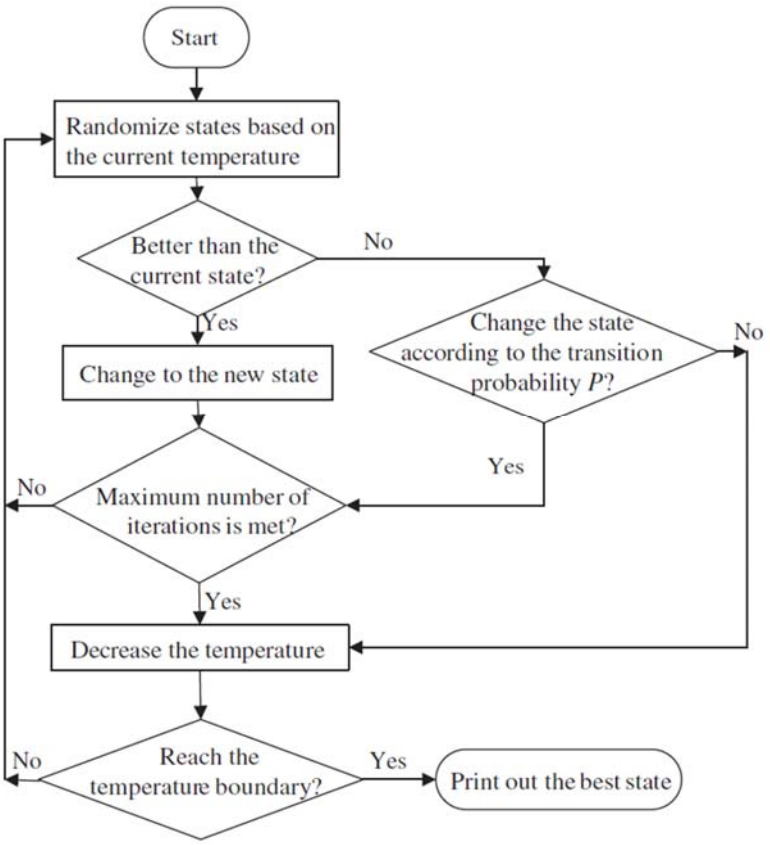

Figure (4. 23). Simulated annealing algorithm flow chart.

To find the optimum tool path for the plunging tools for the pre-described case studies; the circles are grouped according to their radii to different groups. The centers for the circles will be considered as the cities to be visited. For each group the SA algorithm will be applied on all the centers to find out the optimum tool path as shown in Fig. (4.24), and Fig. (4.25).

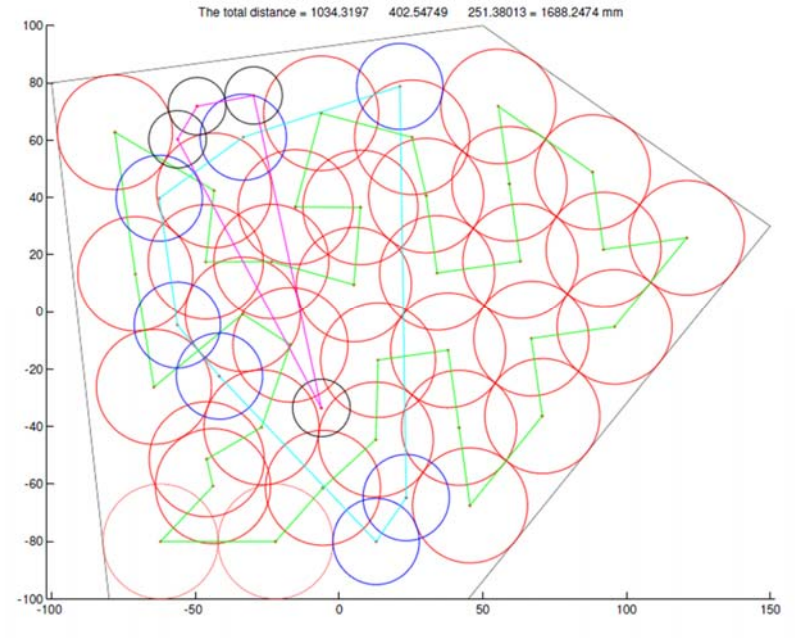

Figure (4. 24). Appling simulated annealing to optimize the tool path case study I for each group of circles have common radius.

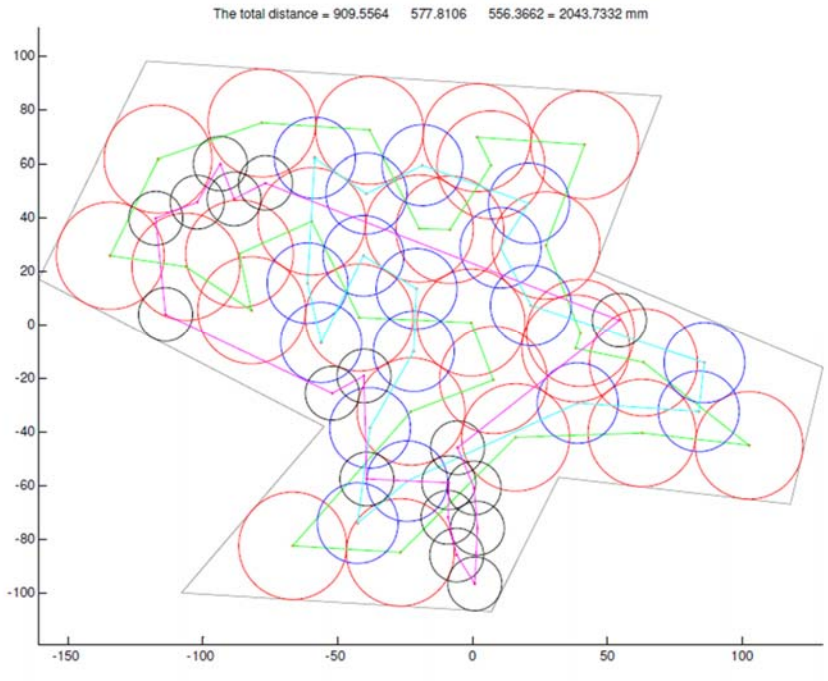

Figure (4. 25). Appling simulated annealing to optimize the tool path case study II for each group of circles have common radius.

4.3.2 Pocket with island

An island is an area in which the cutting tool will avoid when machining the selected pocket area. According to the design purposes, the parts may get one or more pockets with an island among its features. The more cases the algorithm can solve, the more power it has. To make our new approach suitable for the real manufacturing; another feature is added to the algorithms. This feature considers the island existence in the pocket during the calculation because pockets mostly represent die mold cavities or thin wall parts which might have islands. Fig. (4.26), and Fig. (4.27) show two case studies with islands. The results of applying our approach on the two case studies are shown in tables (4.5), and (4.6).

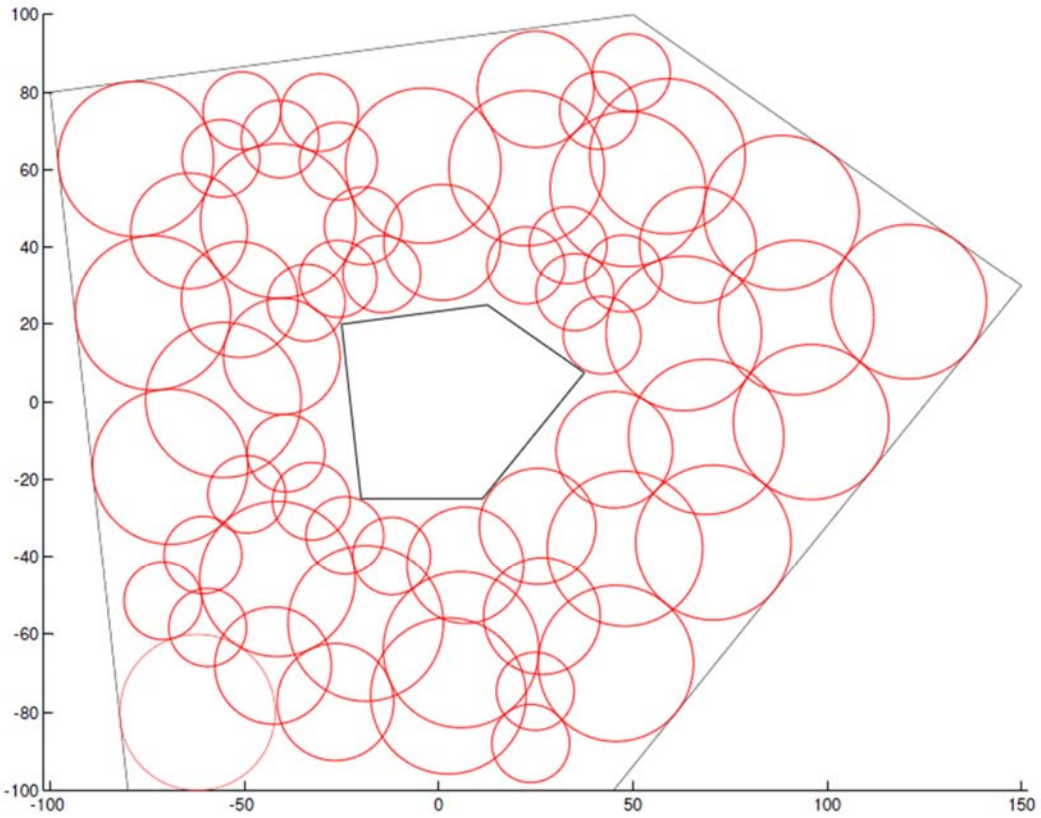

(a) Applying the CP algorithm

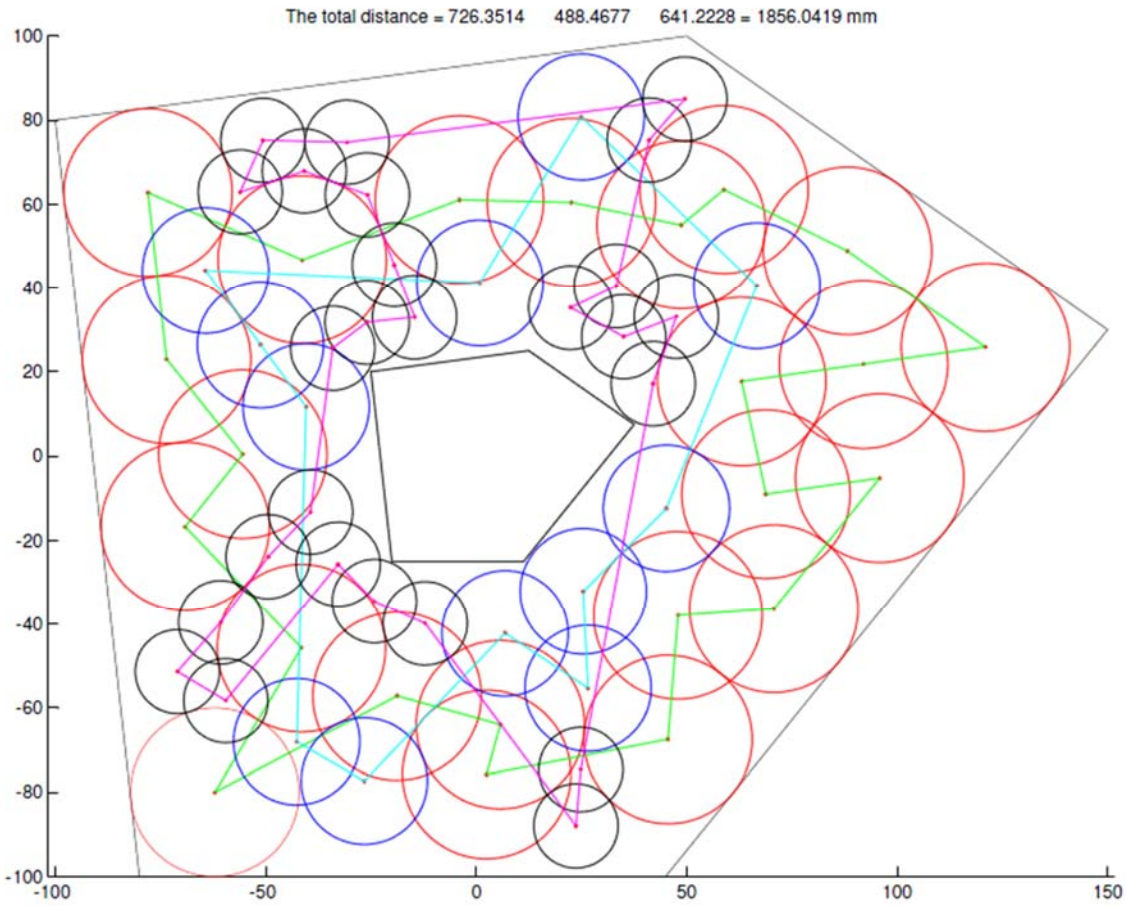

(b) Tool pass optimization by using SA

Figure (4. 26). Third case study for convex polygon with island.

Table (4. 5). Case study III results.

Circle size	R_1=20 mm	R_2=15 mm	R_3=10 mm	Covered area
No. of circles	23	12	26	84.04 %

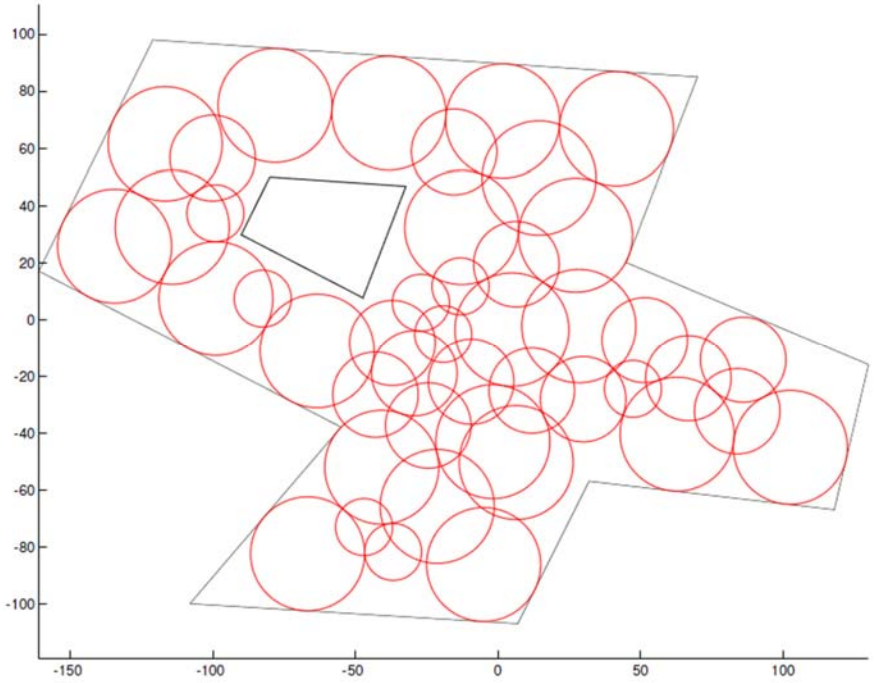

(a) Applying the CP algorithm

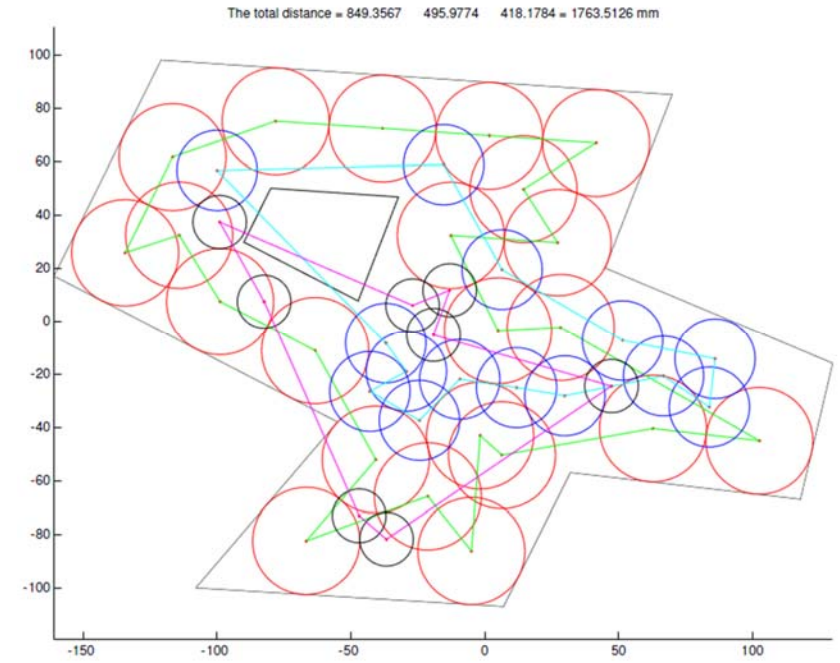

(b) Tool pass optimization by using SA

Figure (4. 27). Fourth case study for concave polygon with island.

Table (4. 6). Case study IV results.

Circle size	R_1=20 mm	R_2=15 mm	R_3=10 mm	Covered area
No. of circles	22	14	8	79.89 %

4.3.3 Free form boundary pocket with island

Due to the progress of the Computer Aided Design (CAD) techniques, the free form curves and surfaces have been widely adopted in the mechanical design. As a result, the pockets with free form boundaries became important features in mechanical parts which urged us to apply the algorithm on such types of features. Since the main idea of that approach is to fill a polygon with circles, the free form boundary is simplified to a polygon with many edges. By discretizing the free form boundary to very small segments, it becomes a polygon with many edges. The algorithm is tested on a more realistic case study; a pocket with island in which both have free form boundary. Fig. (4.28) shows a case study with free form boundaries for the pocket and the island designed by CATIA and machined to its final shape by using the CATIA contouring module. Fig. (4.29) shows the results of applying the proposed approach, and the validation of the result on the DMU 60T machining center.

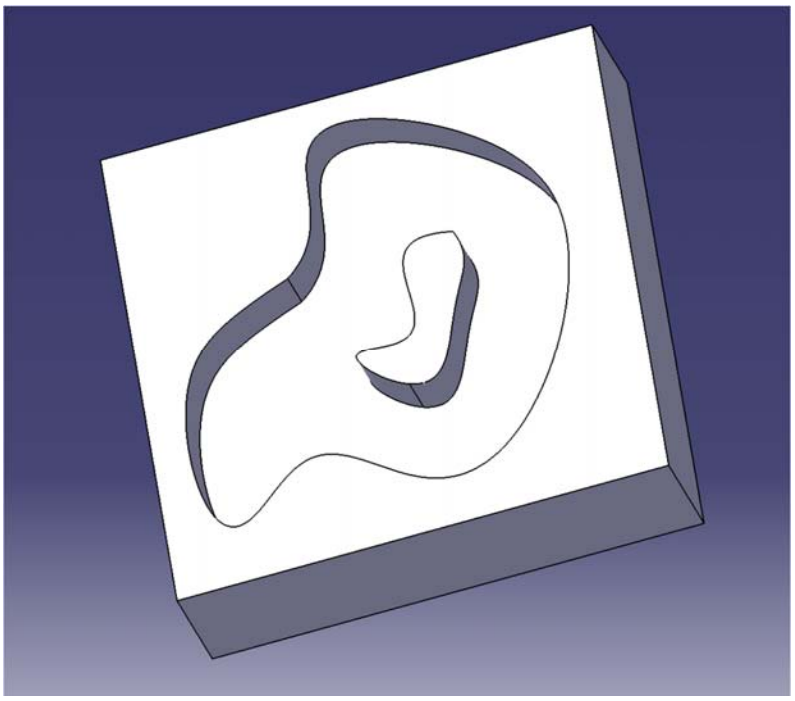

(a) CATIA model for pocket with island have free form boundary.

(b) The machined part by using CATIA contouring.

Figure (4. 28). Case study V, the pocket and island boundaries are free form curve.

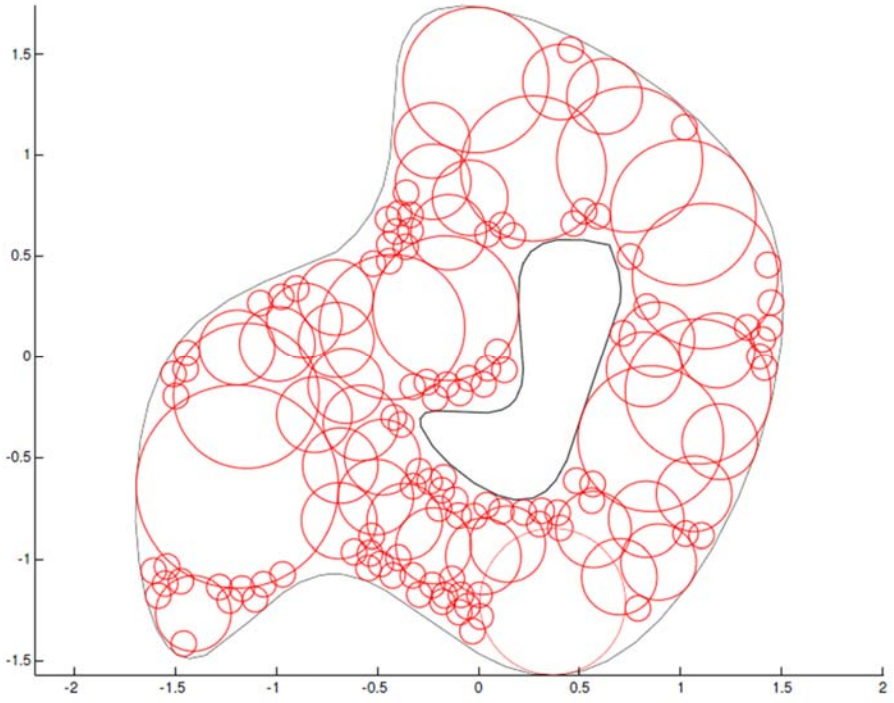

(a) Applying the CP algorithm

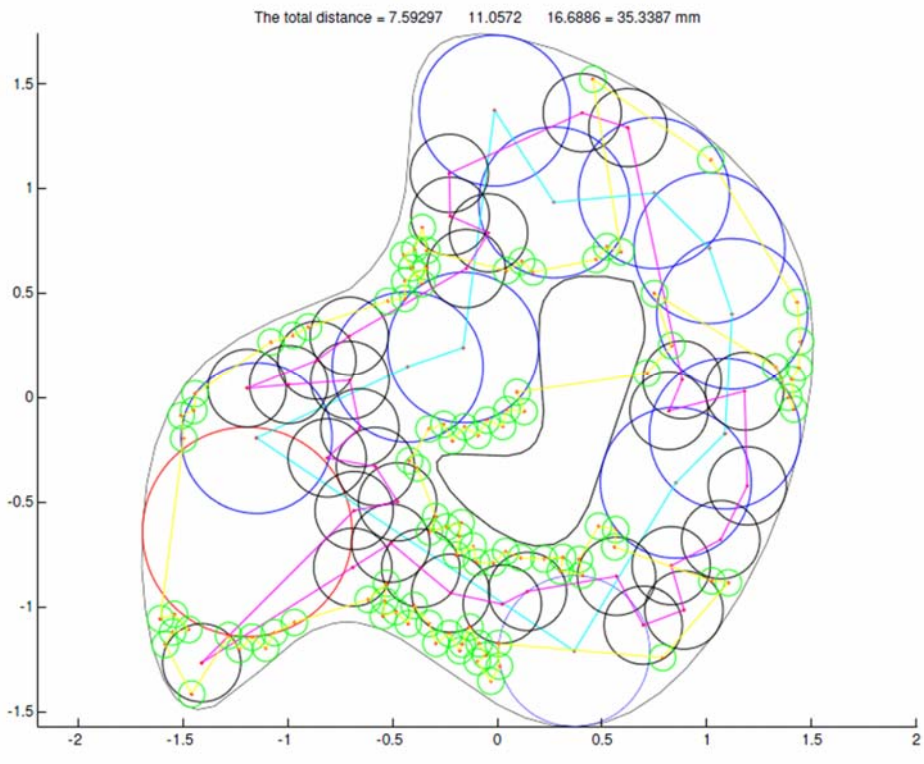

(b) Tool pass optimization by using SA on each group of circles

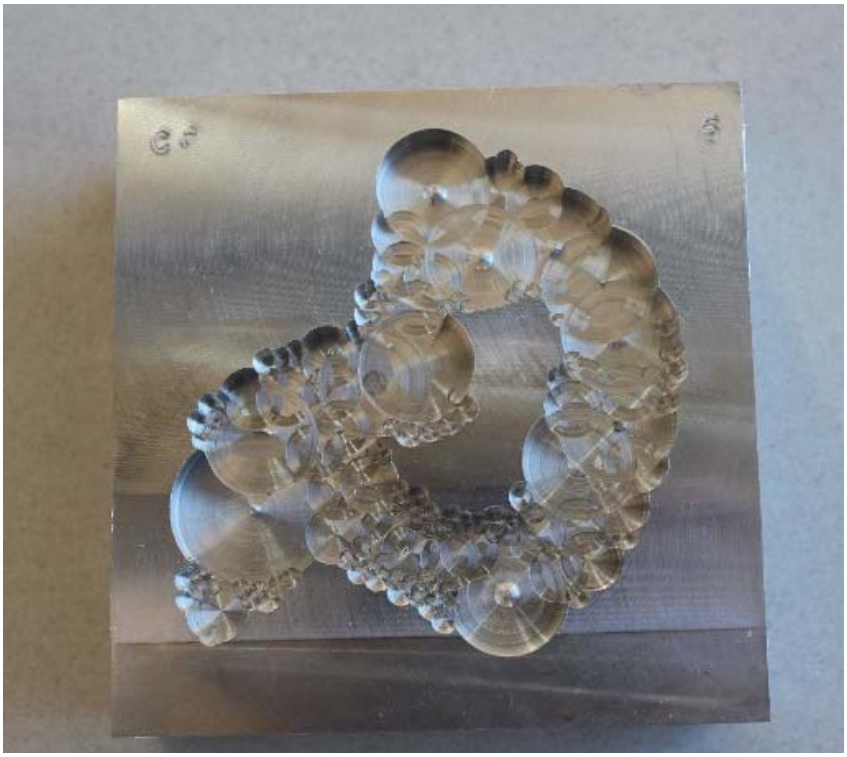

(c) The machined part

Figure (4. 29). Appling the CP algorithm on case study V.

4.3.4 Comparison between CP method and the current methods

In this section, we will compare our method with two existing methods: (1) OCfill method [7], and (2) Plunging module in CATIA. In the case study V, which is a pocket with an island both have free form boundaries. Fig. (4.29) showed the result obtained by using CP approach, Fig. (4.30) shows the result obtained by using the OCfill method, and Fig. (4.31) shows the result obtained by applying the plunge milling module in CATIA. The results of the comparison are illustrated in Table (4.7). The comparison was carried out on several parameters: (1) the number of plunging places, (2) the percentage of the accessible area, and (3) the reduction of the machining time comparing to the contour machining. The last row in the table (4.7) shows the total free tool pass after applying the SA technique.

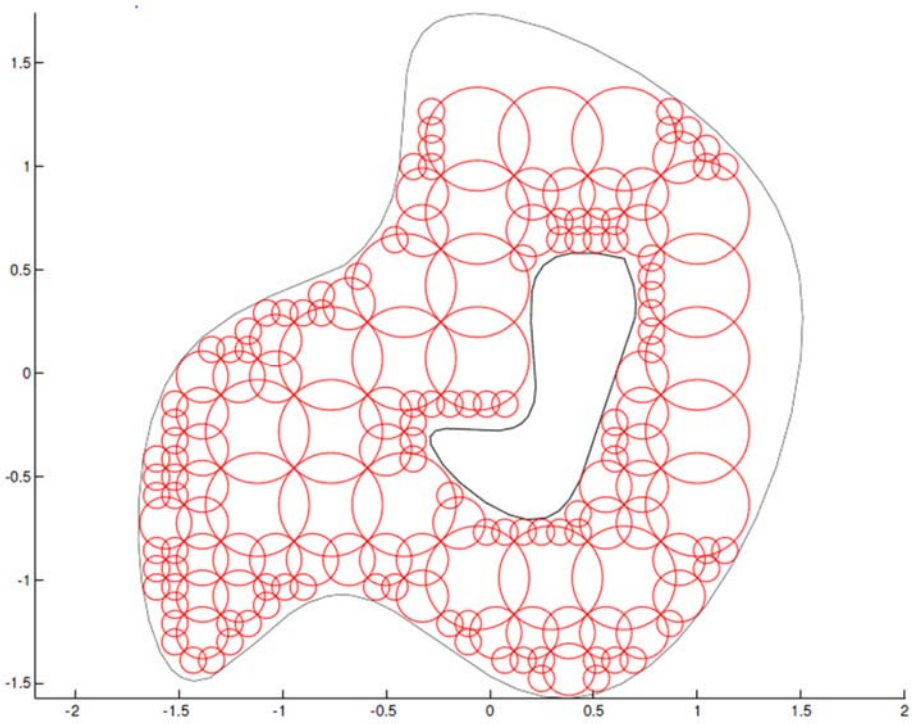

(a) Results by using the OCfill algorithm

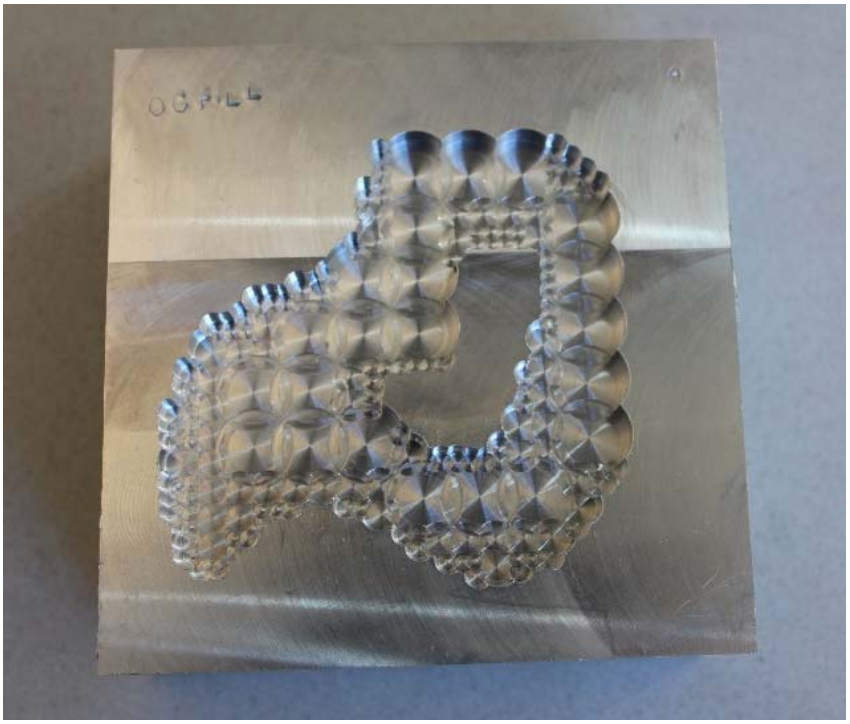

(b) The machined part

Figure (4. 30). Appling the OCfill method on case study V.

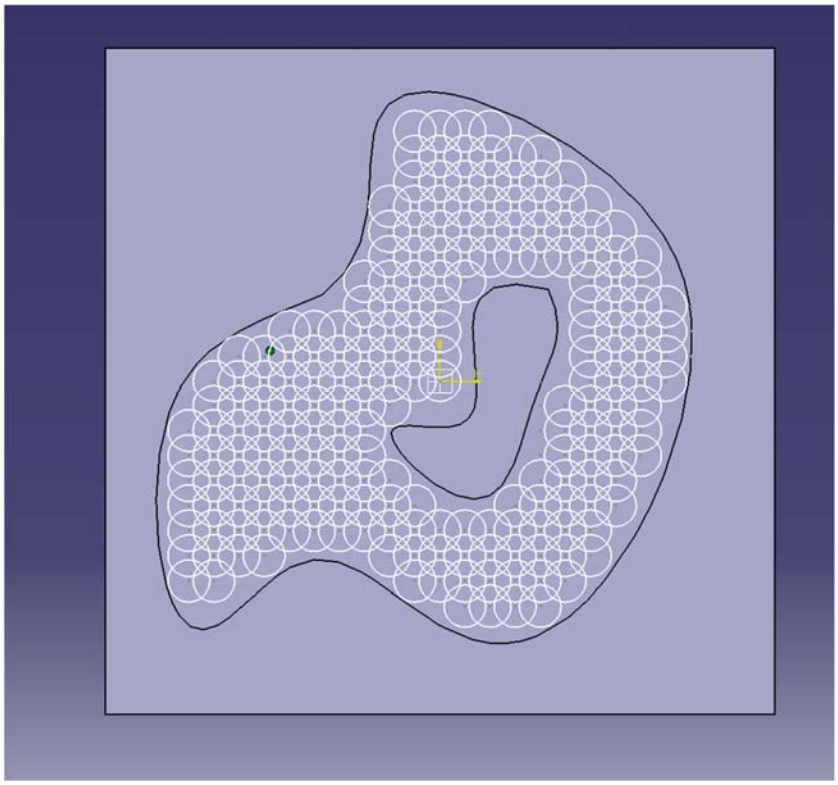

(a) Results by applying plunge milling feature in CATIA

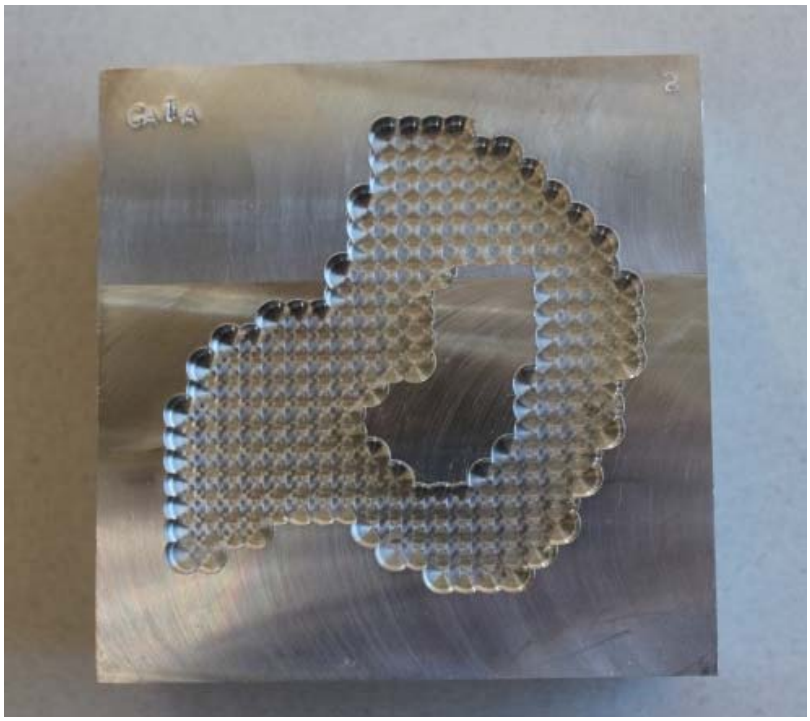

(b) The machined part

Figure (4. 31). Appling the Plunge milling feature in CATIA on case study V.

Table (4. 7). Comparison between CP algorithm, OCfill method, and CATIA

	CP		OCfill		Catia plunging	
Tool diameters (inch)	Dia.	No.	Dia.	No.	Dia.	No.
	1	1	0.5	22	0.25	149
	0.72	11	0.25	48	-	-
	0.373	32	0.125	101	-	-
	0.125	100	-	-	-	-
No. of plunging times	Total	144	Total	171	Total	149
Accessible area	91.298 %		83.34 %		77.27 %	
Machining time reduction Compared with CATIA countering	42.1 %		31.1 %		5.26 %	
Travelling path length (inch)	35.34		38.536		34.443	

4.3.5 Conclusion

Plunge milling has a high metal removal rate which is significantly reduces the rough machining time making it suitable for parts that need to loss high amount of the material during the roughing process like pockets. The proposed approach facilities finding the optimum tool path during plunging the pockets with islands. It also introduces a new feature to calculate the tool path when plunging the pockets that have free form boundary with an island. According to the cases studied, the approach is able to reduce the machining time by up to 42.1 %, and gives a significant improvement of the machining efficiency compared to the existing methods. The new approach has the ability to cover more area with less number of plunging places. As shown in the comparison, the area covered is about 91 % when the new approach is used with less number of plunging places compared to the other methods. One of the most efficient features in our approach is the ability to use any pre-specified diameters of the tools being used with any numbers of the plunging tools.

Also, the algorithm is applicable on the pockets with an island both have free form boundaries which have wide applications in the industry.

4.4 Pocket with sculpture bottom surface with polynomial function case study

In the previous case studies we discussed the pockets have flat bottom in which the depth of cut is constant for all the plunged places. In this section, we will widen the scope of our work to include the pockets with a sculptured surfaces bottoms. These types of pockets became widely used after the high progress in the CAD software which led to impressive development in the parts design, especially, in the field of dies' design. Dies can be described as pockets but with non-flat bottoms. Sheet metal, or plastic parts are produced using dies. Due to the complexity of the parts, the dies have a sculptured bottom surfaces. Some of the sculptured surfaces follow polynomial functions. Our focus will be on the sculptured surfaces which follow the polynomial functions. By using our optimization approach, we will be able to find the exact depth of cut for each plunged place in a fast manner to avoid gauging with the pocket bottom.

Finding the accurate depth of cut at each plunging place calculated by using the plunge milling approach is very important. To avoid the gauging, the tool at each plunging place must stop before reach the pocket bottom by the value of the finishing allowances. In case of the plan bottom the depth of cut is constant value for all the plunging places but for the sculpture surface the depth of cut will be at the highest point of the sculpture bottom surface within the cross section of the plunging tool. So if we are able to calculate the height of the maximum point of the sculpture bottom surface inside the circle represents

the plunger; that value plus the value of the finishing allowances (since plunge milling is a rough process) must be the depth of cut at which the tool should stop.

Therefore to achieve the task mentioned above; our new optimization algorithm will be applied to provide the desired accuracy in a proper calculation time. The working steps are summarized in: (1) Find the min no. of circles can cover the pocket area. (2) Calculate all the local maximum points for the bottom surface. (3) Calculate the global maximum point of the surface for each projected circle.

1. Find the circles which cover the pocket surface, and their optimum tool path by applying the algorithms for circle packing as shown in Fig. (4.32), and table (4.8).

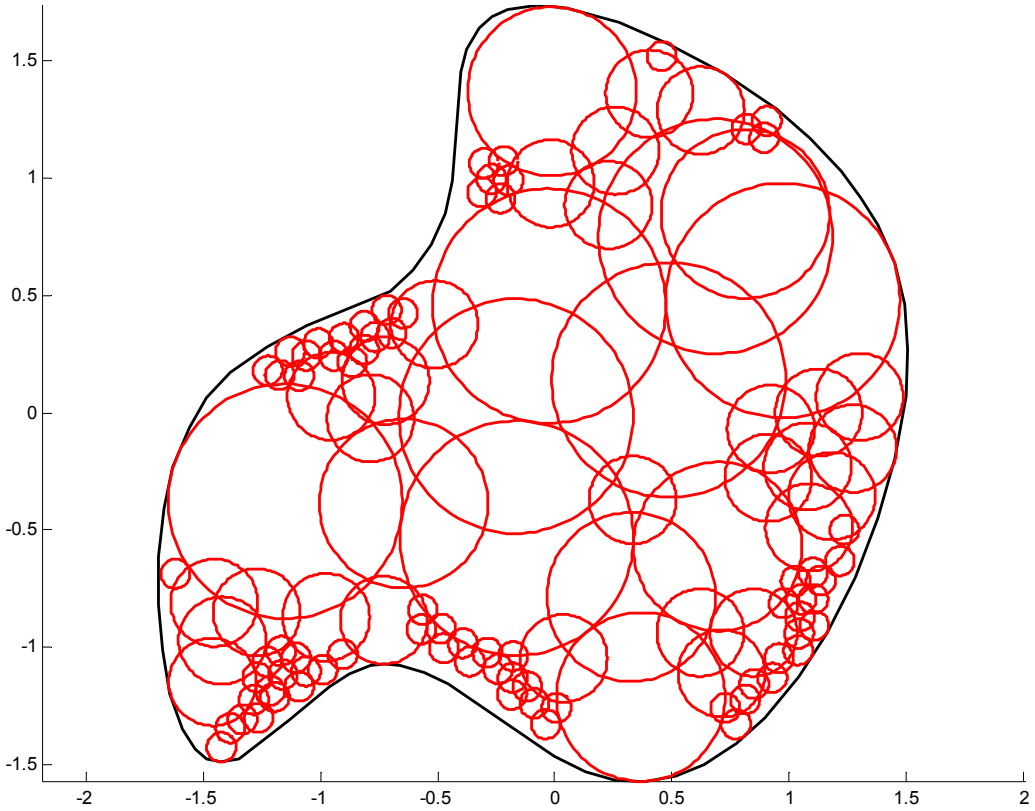

(a) Boundary covered by using CP algorithm

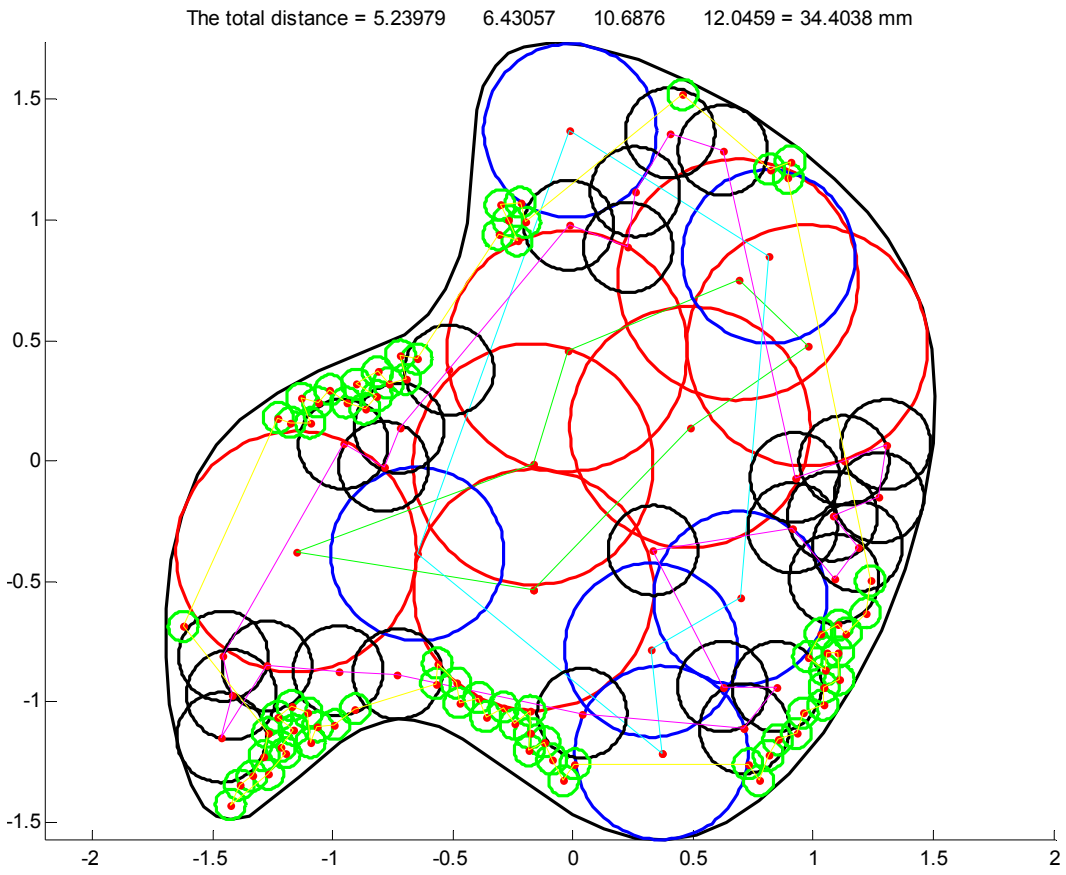

(b) Optimum tool path.

Figure (4. 32). Applying the CP algorithm on the free form boundary case study.

Table (4. 8). Case study results.

Circle size	D_1=1 in	D_2=0.72 in	D_3=0.373 in	D_4=0.125 in	Covered area
No. of circles	7	6	28	75	93.336 %

2. Calculate all the local maxima of the constrained objective function which is the surface equation. The pocket bottom is a sculpture surface represented by polynomial function as shown in Fig. (4.33) and equation (4.83).

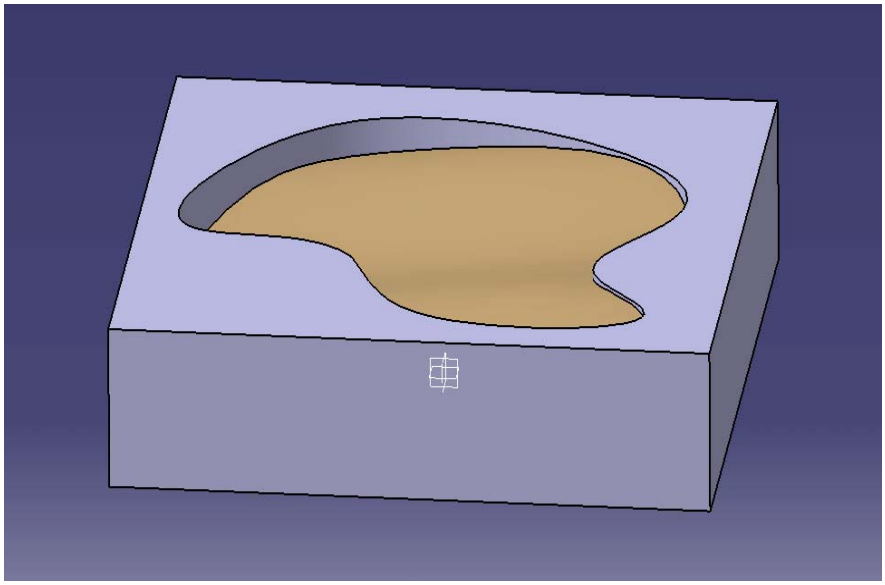

(a) Catia model.

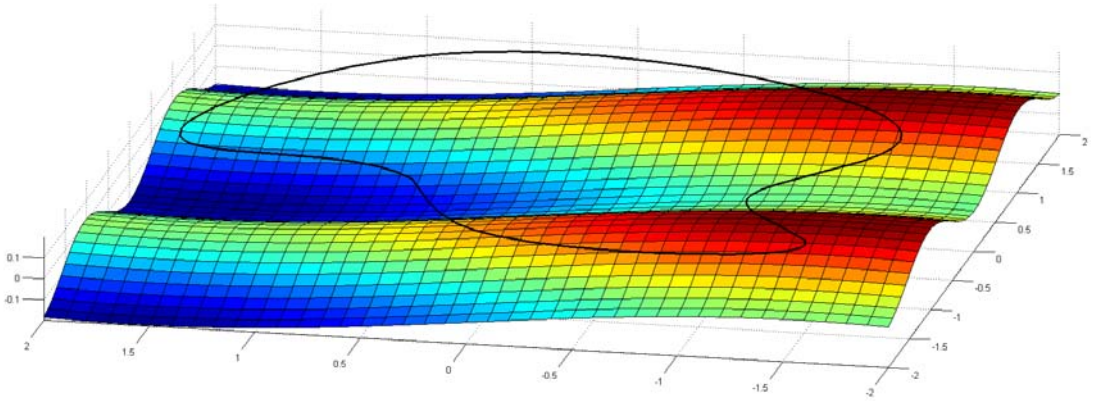

(b) Matlab model.

Figure (4. 33). Case study for pocket with sculpture bottom.

$$f(x, y) = \cos(3x + 3.15) + \sin(y + 3.15) \qquad (4.83.a)$$

Such that

$$-2 \leq x \leq 2$$
$$-2 \leq y \leq 2 \qquad (4.83.b)$$

The local maxima can be calculated according to our optimization algorithm as follow:

a. Find the grid mesh of the surface.

b. Calculate the curvature at each data (grid) point as shown in Fig. (4.34) and group according to the type of curvature.

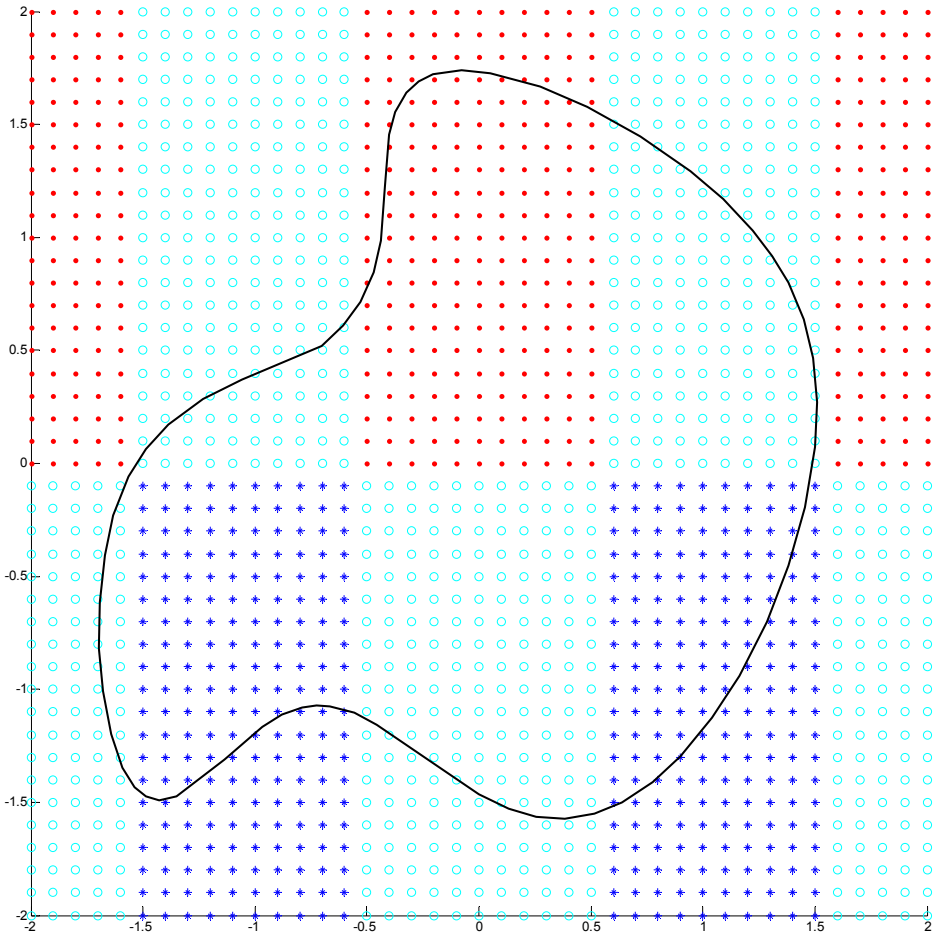

Figure (4. 34). Data points groups (Convex group " . ", Concave group " * ", hyperbolic group " o ", and plane group " x ").

c. As shown in Fig. (4.35), for the maximum optimization problem the concave group is under study. By applying the subtractive clustering we have two clusters with cluster centers as shown in table (4.9) which are the initial points. By applying the Quasi Newton method we have the exact local maxima as shown in table (4.10)

Table (4. 9). Case study clusters centers.

	x	y
1	-1	-1
2	1	-1

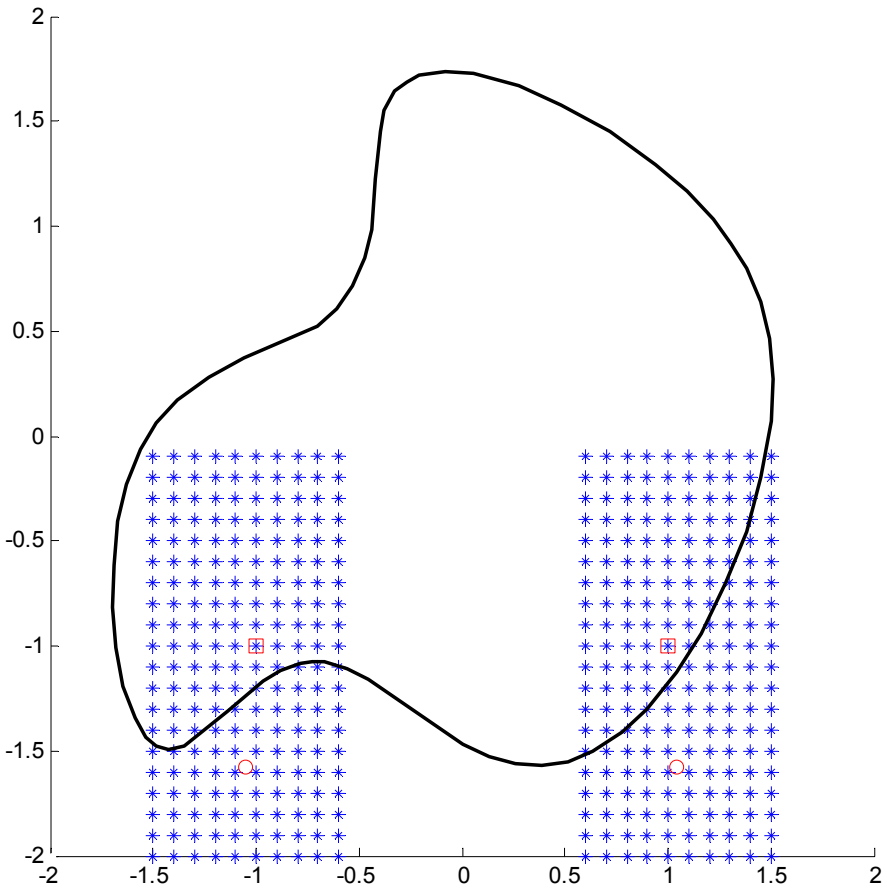

Figure (4. 35). Concave data points clusters "*" with the clusters centers "□" and the exact local maximum point "O"

Table (4. 10). Case study exact local maxima.

	x	y	f(x,y)
1	-1.05	-1.579	0.2
2	1.044	-1.579	0.2

3. From the previous two steps we calculated the loci of the circles cover the pocket area and all the local maximum points for the constrained objective function as shown in Fig. (4.36).

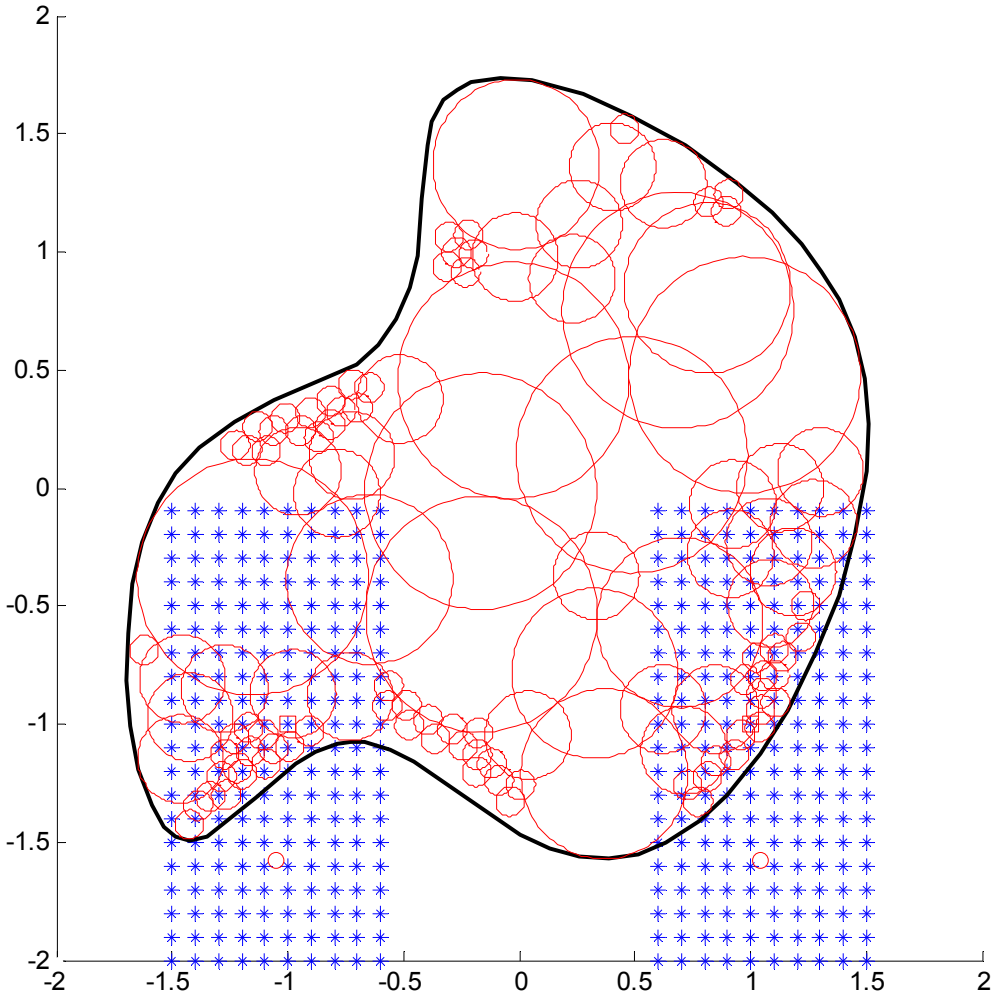

Figure (4. 36). The cover circles and all the local maximum points "o".

From these information for each circle the local maximum points will be checked if one or more of them are inside the circle or not. If yes the maximum between them will be the stop point. If not the maximum point will be on the projected boundary of this circle on the bottom surface as shown in Fig. (4.37).

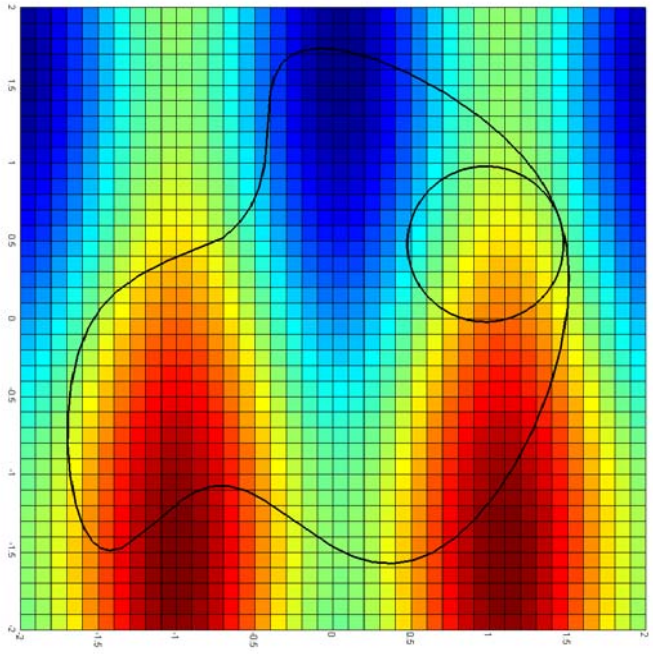

(a)

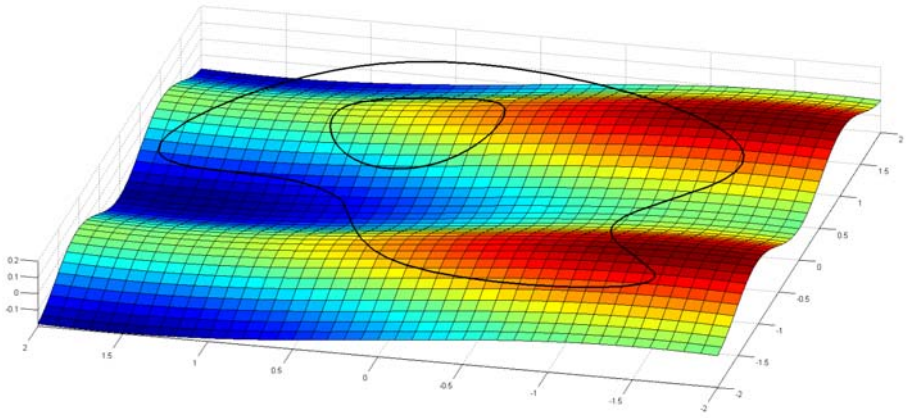

(b)

Figure (4. 37). The projected boundary of the circle on the bottom surface.

By substituting with:

$$x = x_c + R\cos(\theta)$$
$$y = y_c + R\ \sin(\theta) \tag{4.83}$$

In the surface equation:

$$f(\theta) = \cos\ (3x_c + 3R\ \sin\ (\theta) + 3.15) + \sin\ (y_c + R\ \sin\ (\theta) + 3.15) \tag{4.84}$$
$$0 \le \theta \le 2\pi$$

x_c ... x cordinate of the circle center.

y_c ... y cordinate of the circle center.

R ... the raduis of the circle.

Equation (4.84) represents the projected boundary of the circle which contains the maximum point in this case. By applying the new optimization technique the projected circle boundary is gridded to several data points. The data points grouped to convex, concave, and plan points as shown in Fig (4.38).

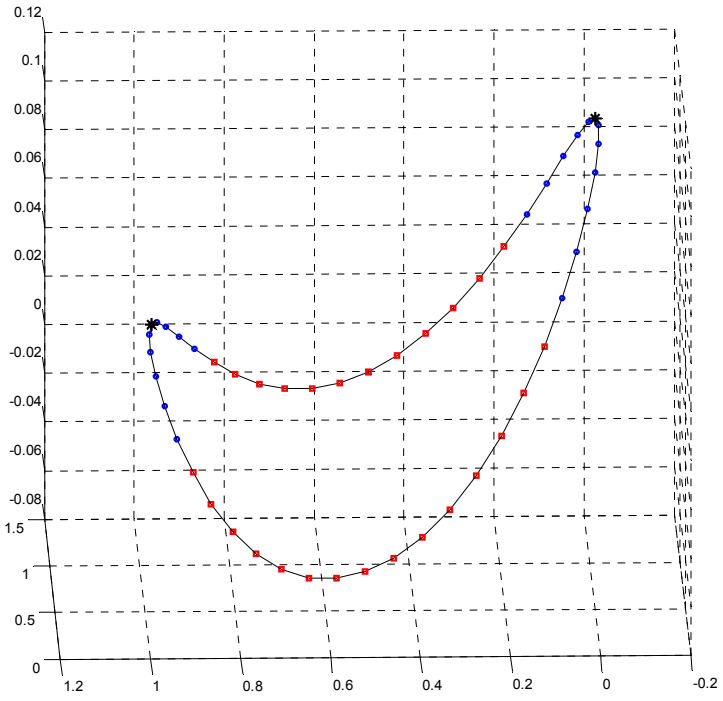

Figure (4. 38). Data points groups (Convex group " □ ", Concave group "o"), and Cluster center "*".

For the concave group, it is clustered and the clusters centers are calculated. By using the clusters centers as initial points the global maximum point will be calculated as shown in Fig. (4.39).

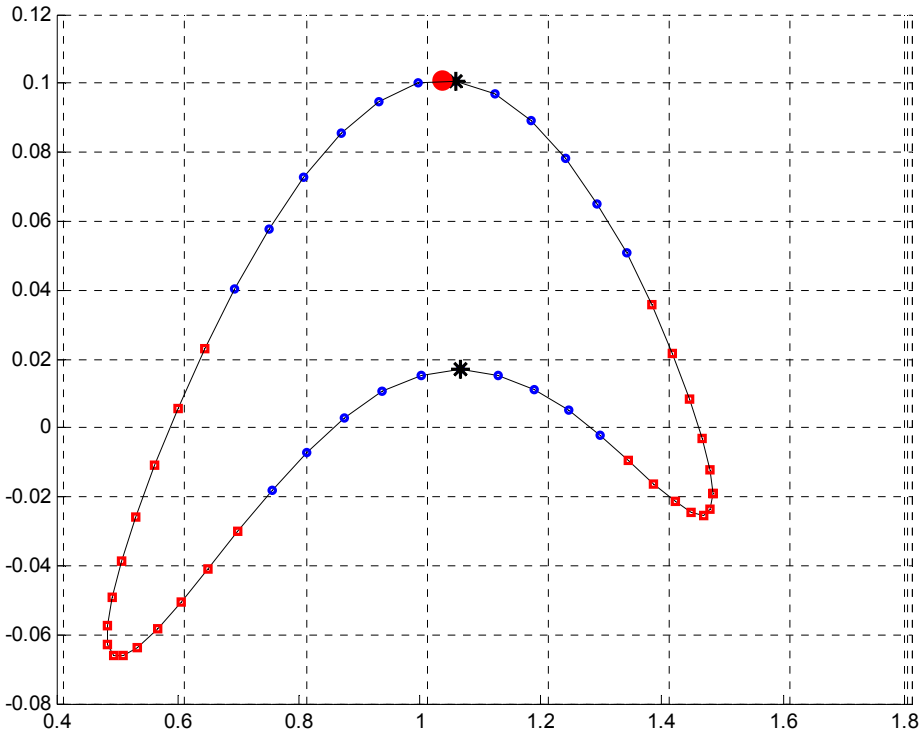

Figure (4. 39). The global maximum point "●"

Fig. (4.40) shows the case study on a CNC milling machine by using CATIA roughing module and plunge milling roughing by applying the CP algorithm and our global optimization algorithm.

(a) CATIA roughing.

(b) Plunge milling roughing by CP algorithm with considering the depth of cut.

Figure (4. 40). Case study of pocket with free form boundary and sculpture bottom.

4.4.1 Conclusion

By applying the new two approaches for CP algorithm and our global optimization algorithm on the case study of pocket with free form boundary and sculpture surface bottom; The rough plunge milling reduces about 62.8% of the rough machining time compared with applying CATIA roughing.

Chapter 5

Conclusion and future work

In this research, new methods have been developed for optimize the total machining time of the plunge milling process during the rough machining of the pockets. Also a new method to find out the polynomial function global optimization by using subtractive clustering technique. The major contributions of this research are summarized as follows:

- A new approach to optimize the total machining time of the rough machining of the pockets by using the plunge milling is established. This approach consists of three main algorithms. (1) Algorithm to packing the pocket area with the minimum number of specified radii circles without overlapping by using the maximum hole degree (MHD) theory in solving the circles packing problem. (2) Algorithm to accurately cover the areas left the non-overlapped circles by the same used specified radii. (3) Algorithm to solve the travelling sales man problem which represents the free tool path between the plunging places by using the simulated annealing optimization (SA) technique. This algorithm reduces the total machining time by reducing both the cutting time and the non-cutting time. The cutting time is reduced by finding the lowest number of plunging places by using a specified tools radii to cover the same pocket area, and reduces the non-cutting time by reduce the free traveling time between the plunging places. The most important feature of this approach are its applicability on the types of pockets even they have a polygon boundary or free form boundary, also if the

pocket has an island or not, and its ability of use any number of the available tools with the standard radii. The case studies showed that using the approach reduces the total machining time by about 40%, also the accessible area reached 90%.

- A new approach to calculate the global optimal solution of the constrained polynomial function to reduce the computing time, improve the accuracy, and avoid stuck in the local minimum. Our focus is on the one variable and two variables constrained polynomial functions because they represent curves and surfaces which are the most used in the industrial field. This approach help a lot to find accurately the depth of cut at each plunging place when plunging a pockets with sculpture bottom represented by polynomial function, which increases the efficiency of the plunging process. The comparison with another optimization techniques showed that this approach reduces about 55% of the calculating time and increases the accuracy in the same time, with no possibility to stick in the local minimum.

The future work

For the future research, the following topics are suggested to expand the present research work:

- Develop the plunging approach to use the hollow plungers.
- Develop the plunging approach to be used on the complex pockets with the 5 axis CNC milling machine.

REFERANCES

1. Li, Y., Liang, S., Petrof, R., and Seth, B., 2000, “Force modeling for cylindrical plunge cutting,” The International Journal of Advanced Manufacturing Technology, Vol. 16, pp. 863 - 870.
2. Wakaokaa, S., Yamane, Y., Sekiya, K., and Narutaki, N., 2002, “High-speed and high-accuracy plunge cutting for vertical walls,” Journal of Materials Processing Technology, Vol. 127, pp. 246 - 250.
3. Ko, J., and Altintas, Y., 2007, “Time domain model of plunge milling operation,” International Journal of Machine Tools and Manufacture, Vol. 47, pp. 1351 - 1361.
4. Damir, A., Ng, E., and Elbestawi, M., 2011, “Forces prediction and stability analysis of plunge milling of systems with rigid and flexible workpiece,” International Journal of Manufacturing Technology, Vol. 54, pp. 853 - 877.
5. Al-Ahmad, M., Acunto, A., and Martin, P., 2007, “Identification of plunge milling parameters to compare with conventional milling,” Advances in Integrated Design and Manufacturing in Mechanical Engineering, Vol. 2, pp. 461 - 474.
6. Ren, J., Yao, C., Zhang, D., Xue, Y., and Liang, Y., 2009, “Research on tool path planning method of four-axis high-efficiency slot plunge milling for open blisk,” International Journal of Manufacturing Technology, Vol. 45, pp. 101 - 109.
7. El-Midany, T., and Elkeran, A., 2006, “Optimal CNC plunger selection and tool point generation for roughing sculptured surfaces cavity,” Journal of Manufacturing Science and Engineering, Vol. 128, pp. 1025 - 1029.
8. Tawfik, H., 2006, “A new algorithm to calculate the optimal inclination angle for filling of plunge milling,” International Journal of CAD/CAM, Vol. 6, pp. 801 - 809.

9. Wenfeng, G., Jianzhong, F., Zhiwei, L., and Yuchun, L., 2010, “Tool-path planning based on iso-scallop for plunge milling in pocket walls manufacture,” Mechanic Automation and Control Engineering (MACE), Vol. 3, pp. 3434 - 3437.
10. George, J., George, J., and Lamar, B., 1995, “Packing different sized circles into a rectangular container,” European Journal of Operational Research, Vol. 84, pp. 693 - 712.
11. Castillo, I., Kampas, F., and Pinter, J., 2008, “Solving circle packing problems by global optimization: Numerical results and industrial applications,” European Journal of Operational Research, Vol. 191, pp. 786 - 802.
12. Huang, W., Li, Y., Li, C., and Xu, R., 2006, “New heuristics for packing unequal circles into a circular container,” Computers and Operations Research, Vol. 33, pp. 2125 - 2142.
13. Huang, W., Li, Y., Akeb, H., and Li, C., 2005, “Greedy algorithms for packing unequal circles into a rectangular container,” Journal of The Operational Research Society, Vol. 56, pp. 539 - 548.
14. Lü, Z., and Huang, W., 2008, “PERM for solving circle packing problem”, Computer and Operation Research, Vol. 35, pp. 1742 - 1755.
15. Kubach, T., Bortfeldt, A., and Gehring, H., 2009, “Parallel greedy algorithms for packing unequal circles into a strip or a rectangle,” Central European Journal of Operation Research (CEJOR), Vol. 17, pp. 461- 477.
16. Akeb, H., Hifi, M., and Hallahd, R., 2009, “A beam search algorithm for the circular packing problem,” Computer and Operation Research, Vol. 36, pp. 1513 - 1528.

17. Akeb, H., Hifi, M., and Negre, S., 2011, “An augmented beam search-based algorithm for the circular open dimension problem”, Computers and Industrial Engineering, Vol. 61, pp. 373 - 381.

18. Visweswaran, and V., Floudas, C., 1992, “Unconstrained and constrained global optimization of polynomial functions in one variable”, Journal of global optimization, Vol. 2, pp. 73 - 99.

19. Lasserre, J., 2001, “Global optimization with polynomial and the problem of moments”, SIAM Journal on optimization, Vol. 11, pp. 796 - 817.

20. Hanzon, B., and Jibetean, D., 2003, “Global minimization of a multivariate polynomial using matrix methods”, Journal of global optimization, Vol. 27, pp. 1-23.

21. Nataraj, P., and Arounassalame, M., 2007, “A new subdivision algorithm for the bernstein polynomial approach to global optimization”, International journal of automation and computing, Vol. 4, pp. 342 - 352.

22. Nataraj, P., and Arounassalame, M., 2011, “Constrained global optimization of multivariate polynomials using Bernstein branch and prune algorithm”, Journal of global optimization, Vol. 49, pp. 185 - 212.

23. Yager, R., and Filev, D., 1992, “Approximate clustering via the Mountain method”, IEEE transactions on, systems, man, and cybernetic, Vol. 24, pp. 1279 - 1284.

24. Chiu, S., 1994, “Fuzzy model identification based on cluster estimation”, Journal of intelligent and fuzzy systems, Vol. 2, pp. 267 - 278.

25. Bataineh, K., Naji, M., Saqer M., 2011, “A comparison study between various fuzzy clustering algorithms”, Jordan journal of mechanical and industrial engineering, Vol. 5, pp. 335 - 343.